

# **Caveolin1 Tyr14 phosphorylation: Regulation and role in adhesion-dependent cellular responsiveness of normal and cancer cells**

A thesis

Submitted in partial fulfillment of the requirements

Of the degree of

**Doctor of Philosophy**

By

**Natasha Nandkishore Buwa**

20133255



**INDIAN INSTITUTE OF SCIENCE EDUCATION AND RESEARCH PUNE**

**2021**

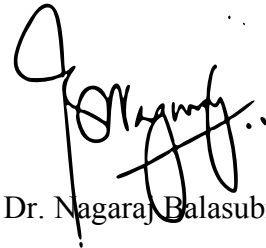
*This Thesis is dedicated to my grandfather*

*Pundalik Patkotwar*

*Who patiently yet ardently waited for this*

## CERTIFICATE

Certified that the work incorporated in the thesis entitled “**Caveolin1 Tyr14 phosphorylation: Regulation and role in adhesion-dependent cellular responsiveness of normal and cancer cells**” submitted by Natasha Buwa was carried out by the candidate, under my supervision. The work presented here or any part of it has not been included in any other thesis submitted previously for the award of any degree or diploma from any other University or institution.



Dr. Nagaraj Balasubramanian

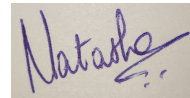
Associate Professor,

IISER, Pune, India.

Date: March 22, 2021

## DECLARATION

I declare that this written submission represents my ideas in my own words and where others' ideas have been included, I have adequately cited and referenced the original sources. I also declare that I have adhered to all principles of academic honesty and integrity and have not misrepresented or fabricated or falsified any idea/data/fact/source in my submission. I understand that violation of the above will be cause for disciplinary action by the Institute and can also evoke penal action from the sources which have thus not been properly cited or from whom proper permission has not been taken when needed.

A rectangular box containing a handwritten signature in blue ink that reads "Natasha".

Natasha Buwa

Roll No. 20133255

Date: March 22, 2021

## Acknowledgements

At the outset I sincerely thank my PhD advisor Dr. Nagaraj Balasubramanian. The meticulous training I received from him has been one of the most significant learning experiences in my nascent research career. Nagaraj not only guided me academically through this journey, but also believed in me, and taught me through example, things too numerous to be enlisted here. His unstinting support and understanding all through will remain unparalleled.

I would also like to thank the wonderful group of scientists Dr. Girish Ratnaparkhi, Dr. Deepa Subramanyam and Dr. Thomas Pucadyil to have helped oversee my training as my committee. I am indebted to all of them for the critique and encouragement, and their advice, inputs and interactions. I thank them all, especially Dr. Ratnaparkhi for always making time to talk when I needed to, and for making it seem so effortless. I am also most grateful for the excellent environment at the Biology department and thank its members for the fantastic interactions that have played a huge part in indulging my scientific temper. I acknowledge the financial support from IISER Pune and CSIR without which tranquility would have been scarce. I also thank all the tireless staff seemingly behind the scenes, but actually at the fore. I thank the delightful lab group who I had the opportunity to work with and share my woes and laughs alike. I especially thank Nivedhika, Shaunak and all those who worked with me and taught me mentorship. I thank my friends Keerthi, Devika, Indu and Neha at IISER who were a constant source of support, encouragement and like family at work. I am grateful to have a friend in a colleague in Keerthi, who helped me stay sane through some trying times.

And I am thoroughly and utterly indebted to the global scientific community for fueling my love and pursuit of the unknown.

All this – literally, figuratively, physically and in all senses – would have been impossible without my parents Dr. N. K. Buwa and Dr. Neelima Buwa, my grandmother Prabha Patkotwar and my brother Nikhil. My grandmother and father inculcated in me curiosity, and a pursuit for knowledge for the sake of it: all now an indispensable part of me. All their love, support, teachings, inspiration, and the utter unconditionality, I cannot even begin to enlist in its entirety. Words too inadequate, pages too few, but I am glad they know and knew.

*The roads were rough, and I did take many,  
Albeit, it was a thoroughly enjoyable journey..*

-Natasha Buwa

# CONTENTS

	<b>Page no.</b>
<b>SYNOPSIS</b>	<b>1-4</b>
<b>CHAPTER 1: Cav1 phosphorylation: Adhesion-dependent regulation</b>	<b>5-44</b>
<b>Abstract</b>	<b>6</b>
<b>Introduction</b>	<b>7-16</b>
Caveolins and caveolae formation	7-12
Non-caveolar caveolins	12-13
Caveolin1 phosphorylation (pY14Cav1) – regulation and functions	13-15
Adhesion-dependent cellular responsiveness – role and regulation of pY14Cav1	15-16
<b>Materials and Methods</b>	<b>17-25</b>
Cell culture	17
Antibodies and Reagents	17-18
Suspension and re-adhesion of cells	18-19
Surface labelling and endocytosis of GM1	19
Detergent-free caveolae isolation	19-21
Cav1 immunoprecipitation	21
Focal adhesion (FA) isolation	22
Western Blotting	23
Two-dimensional gel electrophoresis (2D-GE)	23
Sample preparation and immunogold labelling for FESEM imaging	23-24
Electron microscopy	25
Fluorescence and confocal microscopy imaging	25
Statistical analysis	25
<b>Results</b>	<b>26-41</b>
pY14Cav1 regulates GM1 endocytosis upon loss of adhesion	26-27
Cav1 phosphorylation is regulated upon loss of adhesion in mouse Fibroblasts	28-29

Cav1 phosphorylation is restored on re-adhesion to fibronectin in MEFs	28-30
pY14Cav1 is detected in isolated caveolae in MEFs	31-36
pY14Cav1 is detected in isolated focal adhesions (FA) in MEFs	37-39
Re-adhesion mediated recovery of pY14Cav1 is dependent on FAK activation in MEFs	40-41
<b>Discussion</b>	<b>42-44</b>
<b>CHAPTER 2: Cav1 phosphorylation: Matrix stiffness-dependent regulation in 3D and 2D microenvironments</b>	<b>45-72</b>
<b>Abstract</b>	<b>46</b>
<b>Introduction</b>	<b>47-50</b>
Mechanical forces in cells	47
Mechanosensing through Caveolae, Cav1 and pY14Cav1	48-50
<b>Materials and Methods</b>	<b>51-56</b>
Cell culture	51
Antibodies and Reagents	51-52
2D polyacrylamide gels of varying stiffness	52-54
Embedding cells in 3D collagen gels	54-55
Western Blotting	55
Microscopy imaging	55-56
Statistical analysis	56
<b>Results</b>	<b>57-68</b>
Cav1 phosphorylation is regulated by matrix stiffness	57-58
Matrix-stiffness dependent regulation of Cav1 phosphorylation is FAK-dependent	59-61
Cav1 phosphorylation regulates differential spreading of WTMEFs on 2D gels of varying stiffness	62-64
Regulation and Role of Cav1 phosphorylation in 3D collagen gels	65-68
<b>Discussion</b>	<b>69-72</b>

<b>CHAPTER 3: Cav1 phosphorylation in cancers: PTP-mediated regulation and role in anchorage-independence</b>	<b>73-100</b>
<b>Abstract</b>	<b>74</b>
<b>Introduction</b>	<b>75-78</b>
pY14Cav1: Role in migration and invasion in cancers	75-76
pY14Cav1: Role in caveolar endocytosis in cancers	76-77
pY14Cav1 regulation by protein tyrosine phosphatases (PTPs) in cancers	77-78
<b>Materials and Methods</b>	<b>79-84</b>
Cell culture	79
Antibodies and Reagents	79-80
Suspension and re-adhesion of cells	80
Surface GM1 labelling	80-81
Pervanadate treatment	81
RNA isolation	81
cDNA preparation and Quantitative RTPCR	81-82
Generation of stable shCav1 SKOV3 clones	82
Statistical analysis	82
SMARTPool and shRNA oligos and Primer sequences	83-84
<b>Results</b>	<b>85-97</b>
pY14Cav1 in Cav1-expressing cancers	85-86
Adhesion-dependent regulation of Cav1 phosphorylation in cancers	87-88
Active regulation of adhesion-dependent Cav1 phosphorylation by protein tyrosine phosphatases (PTPs) in cancer cells	89-94
Role of PTP-mediated Cav1 phosphorylation in cancer cells	95-97
<b>Discussion</b>	<b>98-100</b>



<b>APPENDIX</b>	<b>101-105</b>
Appendix Figure 1. Electron Microscopy (FESEM and TEM) of caveolae isolated from WTMEFs	102
Appendix Figure 2. Standardization of Cav1 IP to isolate Cav1-binding proteins from caveolae with minimal IgG elution	103
Appendix Figure 3. Cloning of Cav1 shRNA oligos into stable expression vector pLKO.1	104
Appendix Figure 4. shRNA-mediated stable Cav1 knockdown in SKOV3 cells – Screening of positive colonies	105
<b>REFERENCES</b>	<b>106-132</b>

# **SYNOPSIS**

The extracellular matrix (ECM) is a vital regulatory player in the cellular microenvironment. Cell-matrix adhesion, mediated by integrin receptors, regulates cellular responses to the dynamic biochemical and mechanical properties of the extracellular matrix (ECM). Cell-matrix adhesion triggers rapid and sustained downstream signalling to support survival and proliferation. This is mediated in part by regulation of membrane trafficking through caveolae to control anchorage-dependent signaling. Caveolae are plasma membrane invaginations with a diameter of 60-80nm, typical inverted omega-shaped morphology, and stable structures easily identifiable by electron microscopy. Caveolae are also mechanosensitive, and known to support signaling and endocytosis. They are characterized by presence of structural membrane proteins caveolins (Cav1,2,3) and cavins, Cav1 and Cavin1 both being indispensable for caveolae formation. Cav1 undergoes various post-translational modifications, one of the most important ones being phosphorylation on its Tyr14 (pY14Cav1). Adhesion-dependent caveolar endocytosis of membrane raft microdomains requires this phosphorylation (del Pozo *et al*, 2005). Cav1 Tyr14 phosphorylation is also crucial for its role at non-caveolar sites like focal adhesions (Joshi *et al*, 2008), but not much else is known as to how adhesion could regulate the same. We find that total cellular pY14Cav1 levels are stimulated by cell-matrix adhesion, similar to integrin-dependent FAK activation (Buwa *et al*, 2020a). Despite its known role at both caveolae and focal adhesions, the exact localisation of pY14Cav1 is not known. This is partly due to non-specificity of reagents to study the same, pY14Cav1 immunostaining is limited by the cross-reactivity of the antibody with phosphorylated Paxillin (Hill *et al*, 2007). Furthermore, Cav1 overexpression and fluorescent tagging has been reported to affect its differential localization and function in cells (Han *et al*, 2015; Hanson *et al*, 2013; Parton & Howes, 2010; Pol *et al*, 2020; Payne-Tobin Jost & Waters, 2019). Our studies, using biochemical fractionations, reveal endogenous pY14Cav1 to localize to both caveolae and focal adhesions in mouse fibroblasts (Buwa *et al*, 2020a). pY14Cav1 levels in caveolae isolated from adherent and suspended cells are comparable, suggesting cell-matrix adhesion to not regulate caveolar pY14Cav1. This further suggests the focal adhesion-associated pY14Cav1 to be regulated by adhesion. Interestingly, inhibition of FAK activation using a small molecule inhibitor abrogates re-adhesion-mediated recovery of pY14Cav1 (Buwa *et al*, 2020a). These studies establish the FAK-pY14Cav1 crosstalk at focal adhesions and its regulation by cell-matrix adhesion.

One of the initial consequences of cell-matrix adhesion entails formation of focal adhesions (FA) (Schwartz, 2010; Levental *et al*, 2009; Friedland *et al*, 2009; Gehler *et al*, 2009). These

large macromolecular complexes form at integrin-ECM engagement sites, are dynamic and capable of transmitting mechanical signals from the ECM through the cytoskeleton. Mechanical cues like matrix stiffness regulate both FA number and FA size (Riveline *et al*, 2001; Schiller & Fässler, 2013; Yeh *et al*, 2017), allowing for more subtle changes in FA-dependent signaling. We find that fibroblasts adherent on 2D polyacrylamide gels of increasing matrix stiffness show a steady increase in FAK activation and a concomitant increase in Cav1 phosphorylation (Buwa *et al*, 2020a). PF-228 mediated inhibition of FAK, though comparable across increasing matrix stiffness, regulates Cav1 phosphorylation more prominently at higher stiffness (Buwa *et al*, 2020a). Taken together, loss of adhesion and fibroblast adhesion on 2D matrices not only establishes the FAK-pY14Cav1 crosstalk, but also reveals how it could be regulated downstream of adhesion. These findings are summarized in the cartoon in Fig. A.

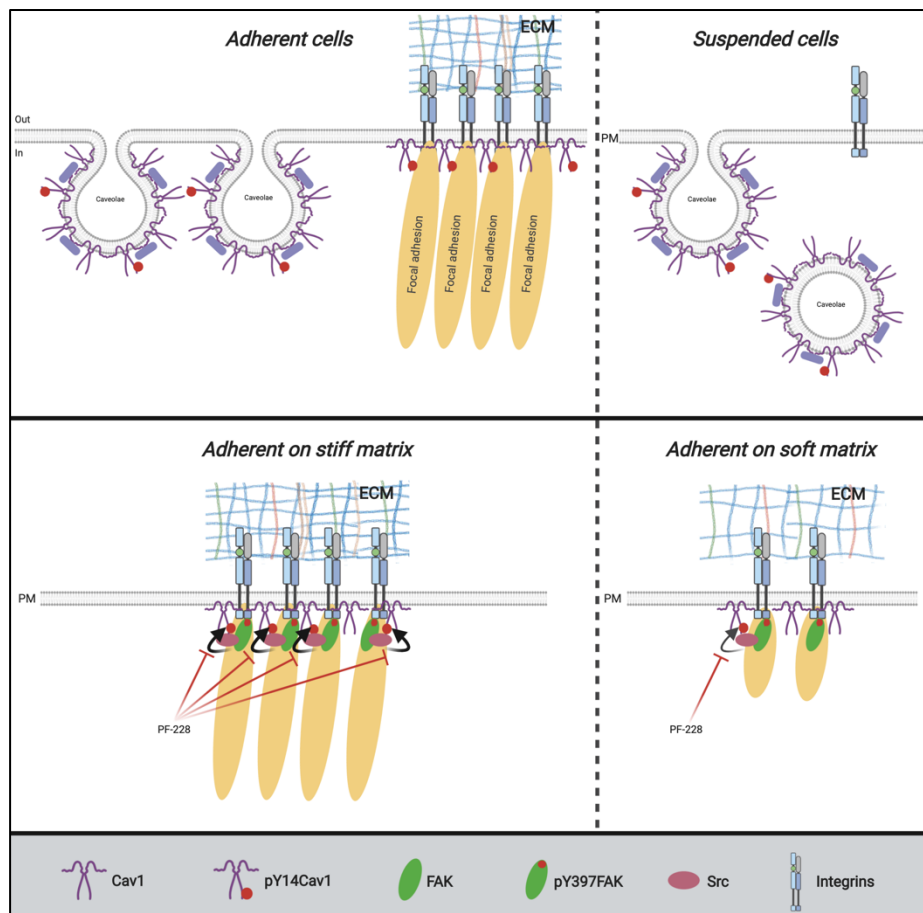


**Figure A. Adhesion-dependent regulation of pY14Cav1.** Endogenous pY14Cav1 (red dot) is localised to both caveolae and focal adhesions, and is regulated by cell-matrix adhesion in mouse fibroblasts. Caveolar pY14Cav1 levels are not affected upon loss of adhesion, suggesting the adhesion-mediated change to happen at focal adhesions. Cells adherent on stiff matrices have more active FAK and also higher Cav1 phosphorylation compared to soft matrices. FAK inhibition (PF-228) inhibits Cav1 phosphorylation differentially on changing matrix stiffness. FAK-dependent regulation of pY14Cav1 could be mediated by FA-associated Src kinase. Figure is adapted from (Buwa *et al*, 2020a).

Apart from their role in caveolar endocytosis and focal adhesion functions in non-transformed cells, pY14Cav1 also has a regulatory role in cancers. Cav1 was initially thought to be a tumour suppressor (Williams, 2004), but some reports have correlated its expression with cancer progression. Cav1 expression is associated with poor prognosis in prostate and breast cancer patients and reduced survival in rectal cancer patients (Joshi *et al*, 2008; Parton, 2018). The role of Cav1 as a tumour suppressor or promoter in cancers is hence still contentious, and could in part be dependent on its Tyr14 phosphorylation (Wong *et al*, 2020; Buwa *et al*, 2020b). Studies have linked pY14Cav1 as an effector of Src and Rho/ROCK-dependent signalling to promote tumour cell motility and invasiveness (Joshi *et al*, 2008). This is likely due to the ability of pY14Cav1 to act as a Rho activator and regulator of directional migration in MEFs (Grande-García *et al*, 2007). Anchorage independence in cancers is achieved *via* bypassing the requirement of cells to attach to a substrate for survival and growth. Since raft microdomains harbour many known players of growth and survival signalling pathways, cancer cells orchestrate this phenomenon partly through deregulation of adhesion-dependent membrane raft trafficking by disruption of caveolar endocytosis (Bourseau-Guilmain *et al*, 2016; Chandran *et al*, 2020). This could happen by loss of Cav1 in some cancer types, or *via* deregulation of Cav1 phosphorylation in Cav1-expressing cancers (Martínez-Meza *et al*, 2019; Díaz-Valdivia *et al*, 2020). The objective of our study is hence to explore the role of pY14Cav1 and its possible regulators in anchorage independence in Cav1-expressing cancers.

We find that adhesion regulates pY14Cav1 levels in some, but not all, Cav1-expressing cancer cell lines, suggesting different regulatory pathways for the Tyr14 phosphorylation. We find Cav1 phosphorylation to be actively regulated by protein tyrosine phosphatases (PTP) in T24 bladder cancer and DU145 prostate cancer cells. siRNA-mediated targeting of PTPs increases pY14Cav1 levels in T24 bladder cancer cells to support anchorage-independent signalling, and in DU145 cells to support adhesion-dependent caveolar endocytosis. Taken together, our studies reveal a distinct adhesion-dependent regulation and role for Cav1 Tyr14 phosphorylation in normal and cancer cells, and emphasize the need to study its role depending on its sub-cellular localisation.

## **CHAPTER 1:**

**Cav1 phosphorylation:**

**Adhesion-dependent regulation**

## ABSTRACT

---

Cell-matrix adhesion regulates cellular responses to changing mechanical and biochemical properties of the extracellular matrix. Cell matrix-adhesion regulates membrane raft trafficking through caveolae to control anchorage-dependent signaling. Caveolae are distinct, mechanosensitive plasma membrane invaginations lined by the transmembrane protein Caveolin1 (Cav1), that support signaling and endocytosis. Caveolar endocytosis is dependent on the phosphorylation of Cav1 on its Tyr14 residue (pY14Cav1), which also regulates functions at focal adhesions. Contrary to earlier reports, we find total pY14Cav1 levels to be regulated by cell-matrix adhesion in mouse fibroblasts. On loss of adhesion pY14Cav1 levels drop significantly and are restored rapidly upon re-adhesion, comparable to the regulation of focal adhesion kinase (FAK). Biochemical fractionation studies reveal endogenous pY14Cav1 to be present in both caveolae and focal adhesions isolated from fibroblasts. Caveolae isolated by detergent-free fractionation from adherent and suspended cells show comparable levels of endogenous pY14Cav1, suggesting caveolar pY14Cav1 to not be regulated by adhesion. Focal adhesions (FA) isolated from re-adherent cells show the presence of endogenous pY14Cav1, which could be the pool regulated by adhesion. Indeed, FAK inhibition using PF-228 also disrupts the re-adhesion mediated recovery of pY14Cav1, suggesting FA-dependent regulation. Taken together, these studies help establish the FAK-pY14Cav1 crosstalk at focal adhesions, and suggest the caveolar and focal adhesion pools of pY14Cav1 to be regulated differentially by cell-matrix adhesion.

## INTRODUCTION

---

An enclosure of a mere 30-40 Angstrom hydrophobic plasma membrane (PM) delimits cells from the external environment, helping them retain their contents and compartmentalise biochemical processes (Mitra *et al*, 2004; Mouritsen, 2005; Mouritsen & Bagatolli, 2015). One of the most striking features of PM in mammalian cells is presence of invaginations that allow endocytosis, membrane trafficking, compartmentalization and signaling. The most common PM invaginations found in mammalian cells are clathrin-coated pits, caveolae and clathrin- and caveolae-independent structures. Caveolae have several distinct features that set them apart from clathrin-coated pits. They do not have an obvious electron-dense coat, and unlike clathrin-coated pits, caveolae do not show different stages of neck closure during endocytosis (Root *et al*, 2019). Density and presence of caveolae also varies across different tissues, with some cell types like hepatocytes and nerve cells lacking caveolae altogether (Parton, 2018; Parton *et al*, 2020b). Abundance of caveolae is distinctive in cells exposed to frequent mechanical stress, such as fibroblasts, endothelial cells, muscle cells and adipocytes (Nassoy & Lamaze, 2012; Parton & Del Pozo, 2013). Caveolae have a uniform diameter of 60-80nm, a typical inverted omega-shaped morphology and are easily identifiable by electron microscopy (EM). Proteins of the caveolin and cavin family are the major structural proteins that form caveolae (Monier *et al*, 1995; Hill *et al*, 2008), and insights into the function of caveolae have been majorly contributed to by knockout mice.

### ***Caveolins and caveolae formation***

Caveolins are small proteins with molecular weights ranging from 17-24 kD, with 3 isoforms Caveolin1, -2 and -3 having a tissue-specific expression. Caveolin1 (Cav1) expressed in most cell types is indispensable for caveolar biogenesis, with Cav3 expressed exclusively in skeletal, smooth, and cardiac muscle cells (Way & Parton, 1995). Cav2 has an expression profile similar to Cav1 but is dispensable for caveolae formation. Caveolins contain 4 distinctly defined domains, an N-terminal, a scaffolding domain, an intramembrane domain, and a C-terminal domain. Cav1 forms a hairpin structure with both N- and C- termini jutting out into the cytoplasm, and the bent hairpin membrane domain inserted within the membrane bilayer (Lee & Glover, 2012; Aoki *et al*, 2010). The transmembrane domain has a stretch of hydrophobic residues that are known to form loop/wedge-shaped insertions in the membrane (Suetsugu *et al*, 2014), thus inducing membrane deformation. Cav1 is thought to undergo oligomerization upon membrane interaction, which further generates curvature to invaginate the membrane (Parton *et al*, 2006). A large portion of the protein, including the scaffolding domain region,



could be tightly membrane associated (Ariotti *et al*, 2015). The C-terminal region of Cav1 has palmitoylation sites that could stabilize its interaction with lipids in the bilayer and other proteins, but the exact membrane embedded sites are not known (Ariotti *et al*, 2015). The domain organization of Cav1 protein is represented in Fig. 1. Cav2 interacts with Cav1 to form a stable high-molecular-mass heterooligomer which localizes to caveolae. Cav2 does not form homo-oligomers, remains in a monomer-dimer form in the absence of Cav1 (Scherer *et al*, 1996), and in absence of Cav1 gets entrapped in the Golgi (Parolini *et al*, 1999; Mora *et al*, 1999). Cav3 is 151 amino acids long and consists of four domains like Cav1, with the scaffolding domain essential for homo-oligomerization and transmembrane domain forming a hairpin loop in the sarcolemmal membrane (Gazzerro *et al*, 2010). Although caveolae formation in mammalian cells requires multiple other structural and accessory proteins, Cav1 alone has been shown to give rise to invaginations in more basic model systems like bacterial cells (Walser *et al*, 2012).

Cav1 knockout mice survive but have shorter lifespans, are afflicted by cardiovascular diseases like pulmonary hypertension and cardiomyopathy, lipodystrophy; and a propensity to develop tumors and aggravation of certain cancer phenotypes has been linked to lack of Cav1 (Razani *et al*, 2001; Drab *et al*, 2001; Razani *et al*, 2002a; Zhao *et al*, 2002; Capozza *et al*, 2003). Lack of Cav2, being dispensable for caveolae formation, does not affect normal caveolae formation, morphology and cellular distribution (Razani *et al*, 2002b). Cav3 knockout mice lack caveolae in muscle cells, but show normal Cav1 expression and caveolae formation in non-muscle cells (Galbiati *et al*, 2001; Minetti *et al*, 1998). At the cellular level, cells lacking Cav1 and caveolae manifest aberrations in various cellular processes including lack of PM mechano-protection against mechanical stress, lack of caveolar trafficking (Sinha *et al*, 2011; del Pozo *et al*, 2005); polarisation, migration, Rho GTPase activation, focal adhesion dynamics (Grande-García *et al*, 2007; Joshi *et al*, 2008), and in general display aberrant signaling especially in response to extracellular cues.

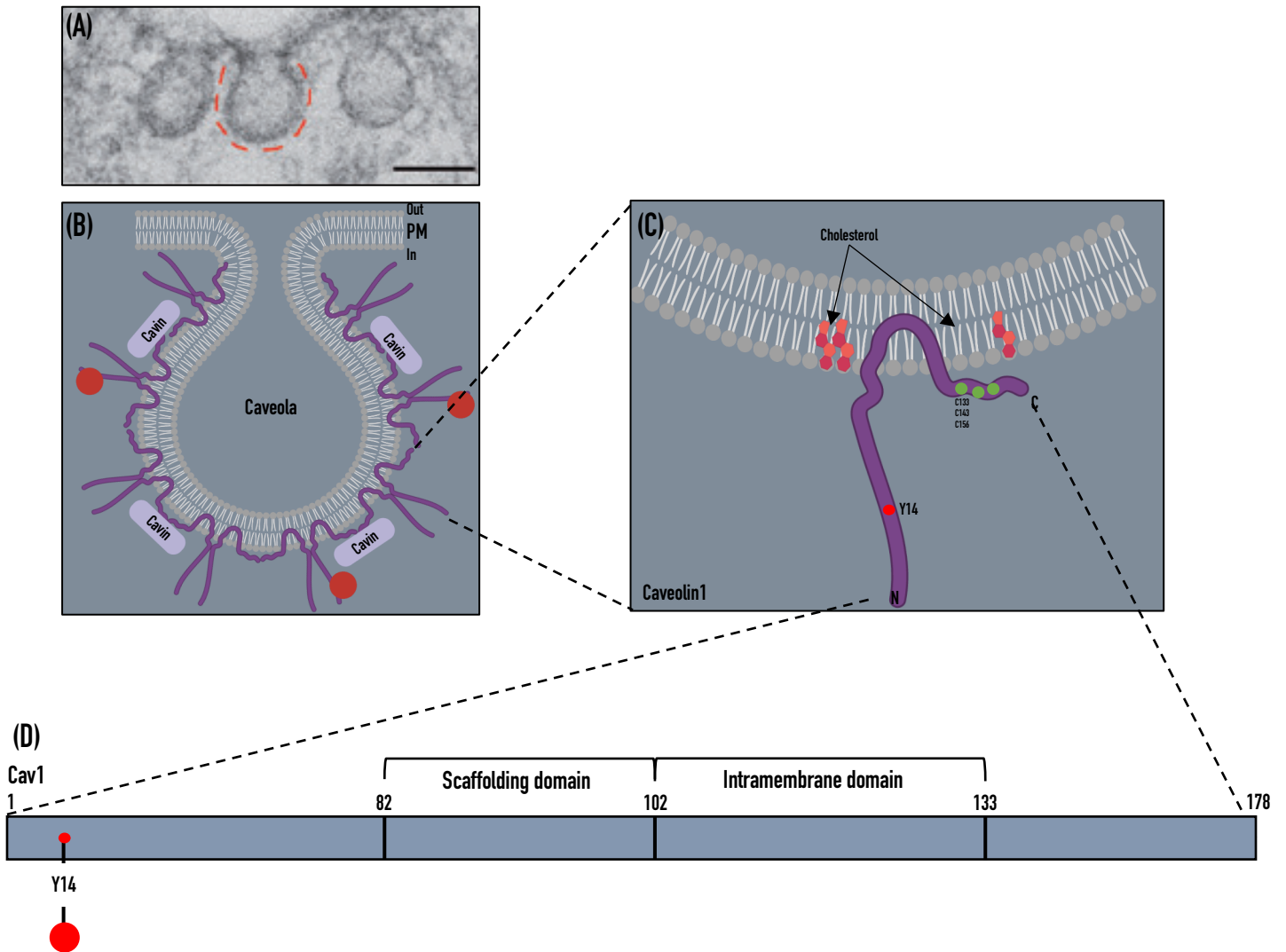


**Figure 1. Caveolae and Caveolin1.** (A) Electron microscopy image (high magnification) of caveola in fibroblasts. Adapted from Parton et. al. *Nat. Rev. Mol. Cell. Biol.* (2013). (B) Schematic representation showing a typical plasma membrane caveola with Caveolin1 (Cav1) and Cavin1 as indicated. (C) Cav1 topology in the membrane. N and C termini of Cav1 face the cytoplasm. Y14 phosphorylation of Cav1 is one of the most important post-translational modifications. Cav1 interacts with cholesterol in the plasma membrane. B, C are created using BioRender.com. (D) Domain organization of Cav1. Cav1 is a 178 amino acid protein with distinct domains for oligomerisation, interaction with other proteins and membrane insertion. The Tyr14 phosphorylation site is indicated in red.

Another important family of cytoplasmic proteins called cavins work cooperatively with caveolins, and are indispensable to caveolae formation in mammalian cells. This family includes Cavin1 (PTRF), SDPR (serum deprivation response protein), Cavin3 (SRBC) and Cavin4 (MURC). Cavin1/PTRF was originally discovered as a nuclear protein which can dissociate paused ternary transcription complexes (Jansa *et al*, 1998). Cavins 2 and 3 were identified as protein kinase C (PKC) substrates and hypothesized to target PKC to caveolae (Gustincich *et al*, 1999; Mineo *et al*, 1998). Their roles in caveolae formation include generation of membrane curvature and formation of caveolar endocytic carriers (Hansen *et al*, 2009; McMahon *et al*, 2009). Cavin4, like Cav3, is predominantly expressed in cardiac and skeletal muscle (Bastiani *et al*, 2009). Presence of Cavin1 is indispensable for the formation of caveolae in cells containing caveolins (Hill *et al*, 2008). In Cavin1 knockout mice, Cav1 is endocytosed and lysosomally degraded (Hill *et al*, 2008). Apart from caveolins and cavins, Pacsin2, EHD2 and ROR1 are also shown to play important roles in maintaining the stability of caveolae at the plasma membrane (Torrino *et al*, 2018; Krawczyk *et al*, 2015; Yamaguchi *et al*, 2016). Pacsin2 and EHD2 recruited to caveolin complexes facilitate caveolae formation and assist in sculpting caveolar membranes as well as regulate caveolae dynamics (Aboulaich *et al*, 2004; Hill *et al*, 2008; Hansen & Nichols, 2010; Hansen *et al*, 2011; Morén *et al*, 2012; Stoeber *et al*, 2012; Ariotti & Parton, 2013; Ludwig *et al*, 2013; Kovtun *et al*, 2014, 2015). EHD proteins associate with the caveolar neck, and loss of EHD2 alters neck morphology and caveolae residence time on PM (Matthaeus *et al*, 2020). Pacsins have also been proposed to recruit dynamin II to caveolae necks, hence regulating their scission (Senju *et al*, 2015). ROR1 has been implicated in caveolae formation by independently binding caveolin and Cavin1 and Cavin3 through the cytoplasmic domains, and preventing their degradation (Yamaguchi *et al*, 2016, 2019).

Caveolae assembly is a progressive process starting in the ER, and involves caveolin oligomerization, binding and ordering of different proteins and lipid species in different compartments: ER, Golgi and PM (Hayer *et al*, 2010). The caveolae assembly process is represented in Fig. 2. A single caveola at the PM is estimated to contain ~140 Cav1 molecules, ~29 Cav2 molecules, ~40-50 Cavin1 molecules, ~20 Cavin2,-3 molecules and ~40 EHD2 molecules (Pelkmans & Zerial, 2005; Ludwig *et al*, 2016; Parton *et al*, 2020a; Gambin *et al*, 2014).

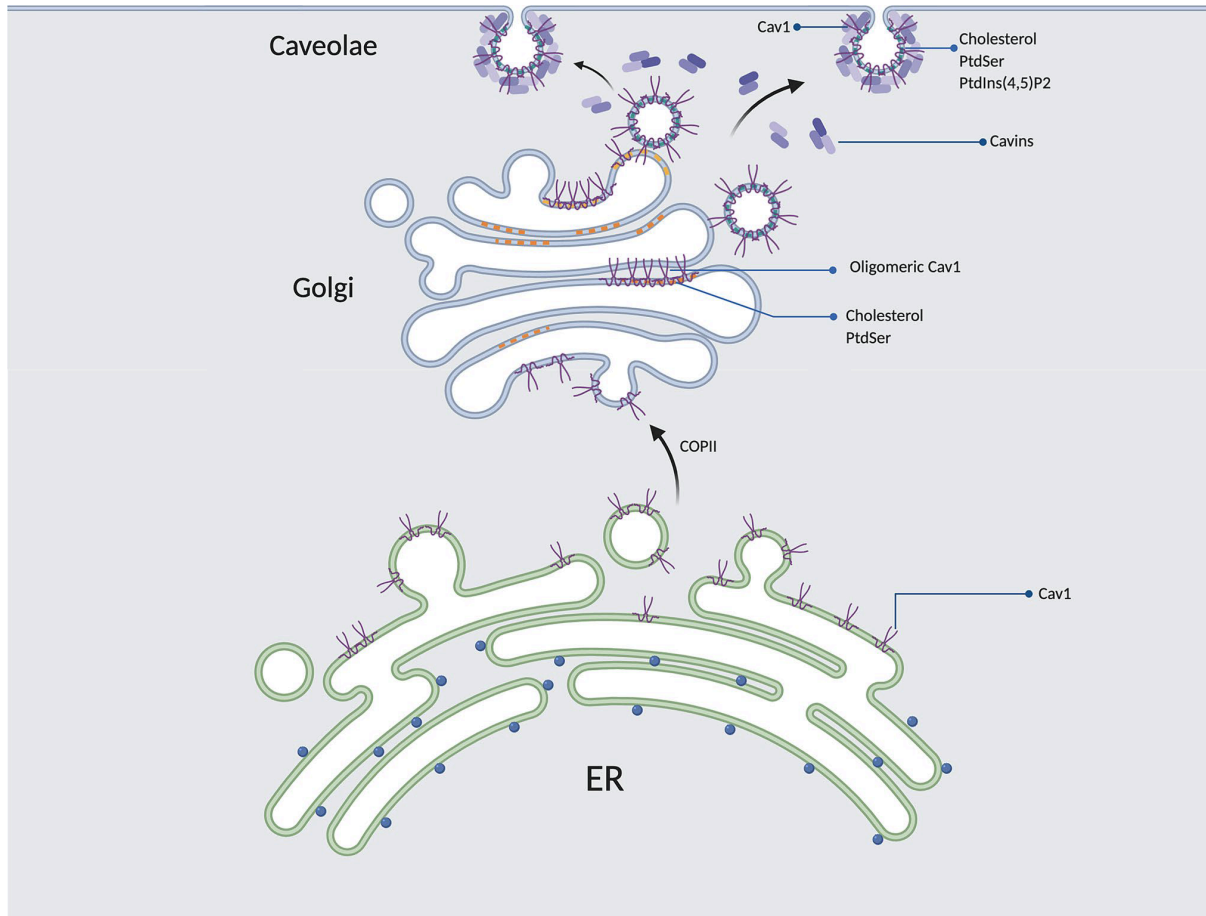


**Fig. 2. Caveolae assembly.** Cav1 synthesized in the ER is transported to Golgi in a COPII-dependent manner. Cav1 associates with cholesterol in the Golgi supporting its oligomerization. Exit of Cav1-containing vesicles from the Golgi is followed by binding of Cavin1, -2 and -3 at the PM to create complete caveolae, enriched in PtdSer and PtdIns(4,5)P<sub>2</sub>. Figure is adapted from (Buwa *et al*, 2020b).

In addition to its protein components, lipids play an equally important role in caveolae formation. Cholesterol in particular is an essential component of caveolar membranes which also binds Cav1 (Murata *et al*, 1995). Treatment of cells with methyl- $\beta$ -cyclodextrin that sequesters cholesterol is known to disrupt caveolae leading to the disassociation of Cavin2 (Breen *et al*, 2012). The high affinity of Cav1 for cholesterol could cluster cholesterol and induce membrane curvature (Wanaski *et al*, 2003; Epand *et al*, 2005; Krishna & Sengupta, 2019). Binding of EHD2 to caveolar structures is possible only in the presence of cholesterol (Morén *et al*, 2012) and PtdIns(4,5)P<sub>2</sub> which is enriched around caveolar necks (Fujita *et al*, 2009; Morén *et al*, 2012; Stoeber *et al*, 2012; Hubert *et al*, 2020a). PtdSer, glycosphingolipid, ganglioside GM3, sphingomyelin and PtdIns(4,5)P<sub>2</sub> are also abundant in caveolae (Fujita *et al*, 2009; Örtengren *et al*, 2004; Singh *et al*, 2010; Hirama *et al*, 2017). Cav1 peptide corresponding to its scaffolding domain (aa 82-101) when added to liposomes induces the formation of

membrane domains enriched in acidic lipids PtdSer, PtdIns(4,5)P<sub>2</sub> and cholesterol (Wanaski *et al*, 2003). PtdSer and sphingomyelin have been shown to be required for caveola formation and stability (Hirama *et al*, 2017; Hubert *et al*, 2020b). Cavins bind PtdSer *in vitro* (Hill *et al*, 2008; Bastiani *et al*, 2009; Izumi *et al*, 1997; Burgener *et al*, 1990; Gustincich *et al*, 1999), and a combination of membrane curvature, order, presence of Cav1 and specific lipids all could be needed for cavin recruitment to caveolae. Presence of cholesterol, sphingomyelin, PtdSer and gangliosides thus gives caveolae their distinct shape, biochemical composition and characteristics.

Abundance of caveolae is a striking feature of PM in mammalian cells experiencing frequent mechanical strain, like endothelial cells, adipocytes, fibroblasts and smooth muscle cells (Nassoy & Lamaze, 2012; Parton & Del Pozo, 2013). Not surprisingly one of the major caveolar functions includes mechano-protection, as caveolae are seen to flatten in response to mechanical stresses like shear, uniaxial stretch and osmotic swelling in a multitude of systems including endothelial cells, fibroblasts, skeletal muscle cells and zebrafish notochord (Cheng *et al*, 2015; Lim *et al*, 2017; Lo *et al*, 2016; Sinha *et al*, 2011; Yeow *et al*, 2017; Gervásio *et al*, 2011). Caveolar flattening due to mechanical stretch leads to release of associated cavins, to further regulate effector interaction (McMahon *et al*, 2019) and gene expression (Joshi *et al*, 2012). Hepatocytes, lymphocytes, neurons, some cancer cells, and even *C. elegans* express Cav1 but lack caveolae (Calvo *et al*, 2001; Parton *et al*, 2018; Fiala & Minguet, 2018; Hill *et al*, 2008; Moon *et al*, 2014; Kirkham *et al*, 2008; Jung *et al*, 2018; Walser *et al*, 2012). Interestingly, caveolins can exist as non-caveolar domains or scaffolds at the PM (Khater *et al*, 2019) which could regulate cellular functions (Pol *et al*, 2020).

### ***Non-caveolar Caveolins***

Although indispensable components of caveolae, caveolins have non-canonical roles in cells. Caveolins are reported to be expressed without forming detectable caveolae in many cell types including hepatocytes, lymphocytes, neurons and some tumour cells, as well as *Caenorhabditis elegans*. In addition, given their functions outside of caveolae, the non-caveolar roles and localisation of caveolins are only recently starting to be appreciated (Nassar *et al*, 2015; Pol *et al*, 2020). As outlined above, the membrane-binding and organising properties of caveolins could be a major contributor to these non-canonical roles. In the absence of Cavin1, Cav1 can exist on the PM as oligomeric structures. These are initially delivered to the PM as smaller complexes of ~5-8 molecules as deemed by super-resolution microscopic analysis (Khater *et al*, 2019). These complexes have been termed scaffolds, and could dimerize to form bigger

scaffolds, which further co-assemble into curved domains. These scaffolds are known to diffuse rapidly, internalized relatively quickly through non-caveolar pathways, and are then degraded (Hill *et al*, 2008). Caveolae disassembly or flattening leads to release of cavins, leading to increased lateral mobility of caveolins (Sinha *et al*, 2011), and could potentially manifest a behaviour similar to caveolin scaffolds. One of the major functions of Cav1 scaffolds is thought to be transport and homeostasis of lipids like cholesterol, PtdSer and PtdIns(4,5)P2 (Pol *et al*, 2020). Caveolin scaffolds can also regulate actin cytoskeleton at the PM (Rangel *et al*, 2019; Tomassian *et al*, 2011), to regulate endocytosis. Some of the potential non-caveolar functions of Cav1 are its regulation of focal adhesion dynamics, migration and invasion (Grande-García *et al*, 2007; Joshi *et al*, 2008; Moon *et al*, 2014). Although the importance of Cav1 in regulating this pathway is widely established, how Cav1 exists at or near these structures is not known. Caveolin functions at caveolae and non-caveolar localisations are likely interrelated, and could explain the apparently disconnected phenotypes described in caveolin-deficient cells and animals.

### ***Caveolin1 phosphorylation (pY14Cav1) – regulation and functions***

Caveolin1 was identified as a major tyrosine-phosphorylated protein in a v-Src screen in Rous sarcoma virus-transformed chicken cells (Glenney, 1989). Cav1 is phosphorylated at Ser80 by PKC (Garver *et al*, 1999; Rybin *et al*, 1999). Ser80 phosphorylation is implicated in cholesterol transport and regulates the ER retention and secretion of Cav1 (Schlegel *et al*, 2001; Fielding *et al*, 2004; Yang *et al*, 2014), but its Tyr14 phosphorylation seems to mediate majority of Cav1 functions (Wong *et al*, 2020; Buwa *et al*, 2020b). Tyr14 phosphorylation of Cav1 is mediated primarily by Src family kinases in response to various cues, but can also be phosphorylated by Fyn and Abl kinases (Mastick & Saltiel, 1997; Mastick *et al*, 2001). Src-mediated Tyr14 phosphorylation of Cav1 is thought to require palmitoylation of Cav1 on the C156 residue (Lee *et al*, 2001) suggesting this phosphorylation to occur prominently at the PM. Tyr14 phosphorylation of Cav1 is regulated by various extracellular cues, including biochemical stimuli like growth factor treatment, oxidative stress and adhesion; and mechanical stimuli like laminar shear, stretch and osmotic stress (Kim *et al*, 2000; Volonté *et al*, 2001; Ortiz *et al*, 2016; Radel & Rizzo, 2005; Zhang *et al*, 2007).

A fair proportion of the functions mediated by Cav1 have been attributed to phosphorylation of Tyr14 in the protein, and include functions at caveolae as well as non-caveolar localisations like focal adhesions. pY14Cav1 is required for caveolar endocytosis (del Pozo *et al*, 2005; Zimmnicka *et al*, 2016, 2015), and regulates caveolae formation in response to extracellular cues

like growth factor treatment (Orlichenko *et al*, 2006a) and mechanical stress (Joshi *et al*, 2012). In response to membrane stretch, pY14Cav1 leads to transcriptional regulation of both Cav1 and Cavin1 genes *via* the transcription factor early growth response protein 1 (Egr1) (Joshi *et al*, 2012). This feedback loop could promote caveola biogenesis in response to stretch (Joshi *et al*, 2012; Boyd *et al*, 2003). In addition to these caveolar functions, pY14Cav1 also regulates non-caveolar functions at focal adhesions (FA), that include regulating FA dynamics, turnover, migration and invasion (Joshi *et al*, 2008; Meng *et al*, 2017). Studies using pY14Cav1 mutants (Y14F-Cav1 and Y14D-Cav1) show that it stabilizes FAK exchange in FAs, to promote FA turnover and drive cancer cell migration (Joshi *et al*, 2008; Goetz *et al*, 2008a). Phosphomimetic Cav1 also enhances Vinculin tension at FAs, dampening force fluctuations and promoting FA stability (Meng *et al*, 2017). Concomitantly, pY14Cav1 is crucial in formation and maintenance of highly ordered membrane at FAs (Gaus *et al*, 2006). pY14Cav1 is known to bind and recruit several proteins, including SH2-domain containing proteins like Src, c-Src tyrosine kinase (Csk) and Grb7 at FAs (Lee *et al*, 2000; Cao *et al*, 2002; Gottlieb-Abraham *et al*, 2013), to mediate pY14Cav1-dependent FA dynamics (Joshi *et al*, 2008), RhoA activation (Grande-García *et al*, 2007), myosin light chain phosphorylation (Radel & Rizzo, 2005; Radel *et al*, 2007) and RhoA-mediated cytoskeletal rearrangements (Boettcher *et al*, 2010).

Given the known roles at spatially distinct caveolae and focal adhesions in cells, it is likely that pY14Cav1 could be present outside of caveolae and associated with non-caveolar regions (though still membrane-associated), but its exact cellular localisation is not known. This could be primarily attributed to non-availability of specific reagents, *viz.*, pY14Cav1-specific antibody, Cav1-specific small molecule inhibitors, as well as caveats associated with exogenous expression of Cav1 in various systems. Studying the localization and dynamics of endogenous pY14Cav1 by immunostaining has been limited by the cross-reactivity of a widely used mouse monoclonal anti-pY14Cav1 antibody (BD Transduction, Clone 56), with phosphorylated Paxillin (Hill *et al*, 2007). Furthermore, overexpression of fluorescently tagged Cav1 constructs can also affect its cellular localization and function (Han *et al*, 2015; Hanson *et al*, 2013; Parton & Howes, 2010; Pol *et al*, 2020). pY14Cav1 has been hypothesized to colocalize with Vinculin at FAs and be almost absent from caveolae (del Pozo *et al*, 2005), but this was determined by immunostaining with the non-specific pY14Cav1 antibody. A more recent study showed increased association of FA proteins Vinculin,  $\alpha$ -actinin, talin and filamin with phosphomimetic (Y14D-Cav1) peptides compared to non-phosphorylatable ones (Y14F-

Cav1) (Meng *et al*, 2017). pY14Cav1 has been shown to be enriched in pseudopodia of migrating cells (Joshi *et al*, 2008), although endogenous pY14Cav1 has not been distinctly shown to localize to FAs.

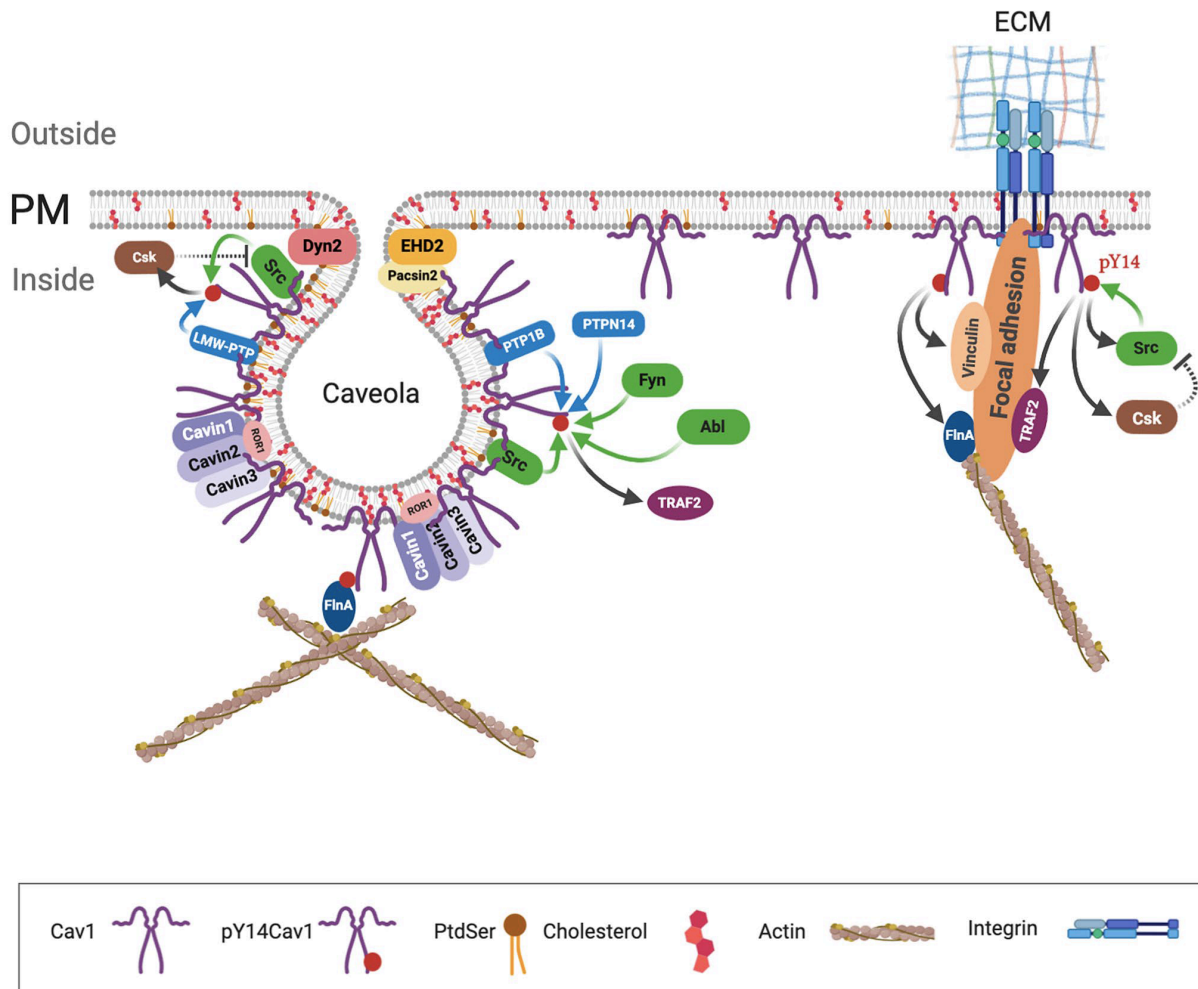


**Figure 3. Regulation of pY14Cav1 functions in caveolae and focal adhesions.** Cav1, an integral membrane protein associates with PM enriched in cholesterol and PtdSer to form caveolae with the help of Cavin1, Cavin2, Cavin3, EHD2, Pacsin2, ROR1 and supported by the actin cytoskeleton. The caveolar neck associates with EHD2 that maintains caveolae at the PM, and Dynamin2 that drives caveolar fission dependent on the actin cytoskeleton. Cav1 phosphorylation on the tyrosine-14 residue (pY14Cav1) is prominently mediated by Src kinase in caveolae and focal adhesions. Fyn and Abl kinases can also phosphorylate Cav1 at tyrosine-14. Protein tyrosine phosphatases localized in caveolae, PTP1B and LMW-PTP, regulate pY14Cav1 along with cytosolic PTPN14. pY14Cav1 binds and regulates Src, Csk, TRAF2 to regulate caveolar and focal adhesion function. The binding of Y14D-Cav1 peptides to Filamin A and Vinculin could support their role in caveolae and FAs. Filamin A links Cav1 to the actin cytoskeleton to regulate caveolar organization and trafficking. Y14D-Cav1 by its ability to enhance Vinculin tension in FAs dampens force fluctuations, promoting FA stability. Figure is adapted from (Buwa *et al*, 2020b).



### ***Adhesion-dependent cellular responsiveness – role and regulation of pY14Cav1***

Proteins associated with the PM actively liaise with the extracellular matrix (ECM), a vital regulatory player of the cellular microenvironment. Integrins are the most prominent PM receptors that actively sense changes in the biochemical and biophysical characteristics of the ECM and communicate these signals inside cells. Integrin-mediated cell-ECM adhesion triggers rapid and sustained downstream signaling and function. This is mediated by adhesion-dependent regulation of membrane trafficking, cytoskeletal organization and organellar dynamics and function (Schwartz, 1997; Del Pozo *et al*, 2004; Parsons *et al*, 2010; Singh *et al*, 2018).

Adhesion-dependent membrane trafficking is regulated by caveolar endocytosis and exocyst-dependent exocytosis, and plays a vital role in driving integrin-dependent signaling (del Pozo *et al*, 2005; Balasubramanian *et al*, 2010). Adhesion-dependent caveolar endocytosis is dependent on Cav1 phosphorylation, though adhesion is reported to not regulate pY14Cav1 levels (del Pozo *et al*, 2005).

Caveolar responsiveness to extracellular stimuli is mediated, among others, by changes in the regulatory phosphorylation of Cav1 (pY14Cav1) in response to biochemical and mechanical stimuli (Grande-García *et al*, 2007; Joshi *et al*, 2008; Goetz *et al*, 2008a; Joshi *et al*, 2012). This phosphorylation of Cav1 plays a role in caveolar trafficking (del Pozo *et al*, 2005), growth factor signaling (Zhang *et al*, 2007), integrin mechanotransduction (Radel & Rizzo, 2005), focal adhesion dynamics (Goetz *et al*, 2008a), actomyosin contractility through Rho GTPase dynamics (Joshi *et al*, 2008; Boettcher *et al*, 2010), cell migration (Grande-García *et al*, 2007), and remodeling of the ECM (Goetz *et al*, 2011).

We examine the spatial localization and regulation of endogenous pY14Cav1 in caveolae and FA in response to adhesion in this study. We find endogenous pY14Cav1 to be detected in purified caveolae and FAs. Adhesion interestingly regulates total cellular pY14Cav1 levels, without affecting caveolar pY14Cav1 on loss of adhesion. This adhesion-dependent regulation of pY14Cav1 is dependent on FAK activation, supporting the presence of an integrin-FAK-pY14Cav1 axis in mouse fibroblasts (Buwa *et al*, 2020a).

## MATERIALS AND METHODS

---

### Cell culture

Wild-type (WT) and Cav1-knockout (Cav1<sup>-/-</sup>) mouse embryonic fibroblasts (MEFs) (from Dr. Richard Anderson's lab, University of Texas Health Sciences Center, Dallas TX), NIH3T3 cells and IP6K<sup>+/+</sup>MEFs (from Dr. Rashana Bhandari, CDFD, India) were cultured in high glucose DMEM medium with 5% foetal bovine serum (FBS), penicillin and streptomycin (Invitrogen) (hereby referred to as complete DMEM). Cells were regularly checked for and found to be devoid of bacterial or mycoplasma contamination. Serum starvation of cells, where mentioned, was done for 14 h using DMEM medium with 0.2% FBS, penicillin and streptomycin (low-serum DMEM).

### Antibodies and Reagents

Primary antibodies used for Western blotting were diluted in 5% BSA made in TBST at following dilutions: Cav1 (Santa Cruz Biotech SC-894) at a dilution of 1:2000, pY14Cav1 (BD 611338) at 1:500, FAK (Cell Signaling Technology (CST) 3285) at 1:1000, pY397FAK (CST 3283) at 1:1000, Cavin1 (BD 611258) at 1:500, Flotillin (BD 610820) at 1:1000, pY118Paxillin (BD 611725) and Paxillin (BD 610052) at 1:2000, GM130 (BD 610822) at 1:500, RhoGDI (Millipore 06-730) at 1:2000, Actin (DSHB JLA20) at 1:2000 and  $\beta$ -tubulin (DSHB Clone E7) at 1:2000. HRP-conjugated secondary antibodies (anti-rabbit and anti-mouse) were purchased from Jackson Immuno Research Laboratories and used at a dilution of 1:10000. Methylcellulose for suspension assay was purchased from Sigma (Cat. no. M0262). Fibronectin (FN) was purchased from Sigma (Cat. no. F2006). FAK inhibitor PF-228 (Slack-Davis *et al*, 2007) was purchased from Sigma (Cat. no. PZ0117). Protease inhibitor cocktail PIC was purchased from Roche (04693132001), and phenylmethanesulfonyl fluoride (PMSF), sodium orthovanadate and sodium fluoride from Sigma. BCA assay kit used for protein estimation was purchased from Thermo Fisher (Cat. no. 23225). RIPA buffer composition: 50mM Tris-HCl at pH 8.0 + 150mM NaCl + 1.0% NP-40 + 0.5% sodium deoxycholate + 0.1% SDS. Tris was purchased from HiMedia (Cat. no. MB029), Glycine from Fisher Scientific (Cat. no. 56406), Sodium bicarbonate from Sigma (Cat. no. S6297), Methanol from Fisher Scientific (Cat. no. 67561), PVDF membranes from Millipore (Cat. no. IPVH00010) and BSA from Sigma (Cat. no. A2153). Chemiluminescent reagents for Western blotting Immobilon Western Chemiluminescent HRP Substrate was purchased from Millipore (Cat. no. WBKLS0500), SuperSignal West Femto Maximum Sensitivity Substrate from ThermoFisher (Cat. no. 34096).

Pre-cast gels for SDS-PAGE silver staining: Any kD™ Mini-PROTEAN® TGX™ Precast Gel (Cat. no. 456-9034). Iso-electric focussing (IEF) IPG strips for 2D-GE: Biorad IPG, 7cm long, pH 3-10 (Cat. no. 163-2000); pre-cast gels for IEF strip: 12% Mini-PROTEAN® TGX™ Precast Gel (Cat. no. 456-1041). Silver Staining Plus kit Biorad (Cat. no. 161-0449).

*Reagents and instruments for caveolae isolation:* Sucrose (Sigma Cat. no. S8501), Tricine (Sigma Cat. no. T5816), EDTA (Sigma Cat. no. E6758), Percoll (17-0891-01), OptiPrep (D1556), Beckman ultracentrifuge tubes (Cat. nos. 355618, 344059, 349622), Wheaton Dounce homogenizer (Cat no. 432-1270), Peristaltic pump (GE Healthcare Cat. no. 18-1110-91), Gradient maker (GE Healthcare Cat. no. 80-6197-80) with appropriate silicone tubing, Sonicator probe (3mm).

*Reagents for focal adhesion isolation:* Triethanolamine (Sigma Cat. no. 90279), dental water jet (Oracura OC001), BSA (Sigma Cat. no. A2153).

### **Suspension and re-adhesion of cells**

WTMEFS, IP6K<sup>+/+</sup>MEFs or NIH3T3 cells were cultured in complete DMEM in four 6 cm dishes (one for each time point) to ~70% confluence. Cells were serum starved for 14h with low serum DMEM. Cells from 3 dishes were detached using trypsin-EDTA (Invitrogen) at 37°C and trypsin neutralized with low-serum DMEM. This processing took ~5 min and these detached cells represent the 5'SUSP time point. Detached cells were mixed with 15ml low serum DMEM and 15ml of 2% methylcellulose (final 1% methylcellulose) and incubated at 37°C for 20 min (20'SUSP) or 120 min (120'SUSP) respectively. For re-plating on fibronectin (FN), cells held in suspension for 120 min (120'SUSP) were used. Following incubation for required time in methylcellulose media, cells were carefully washed by addition of low-serum DMEM followed by centrifugation at 1250 rpm in a cooled table-top Eppendorf centrifuge for 7 min at 4°C. After this centrifugation cells appeared as loose pellet distributed over the conical edge of the 50ml tube, which was carefully dislodged using a 1ml micropipette (cut tip). Cells were washed once again with low-serum media followed by centrifugation 1000 rpm in a cooled table-top Eppendorf centrifuge for 7 min at 4°C, after which pellet was resuspended in low-serum media. These cells now represent the 20'SUSP and 120'SUSP time points. For re-adhesion time points, 120'SUSP cells were re-plated in low-serum DMEM for 15min (15'FN) or 4h (4hFN) on tissue culture dishes pre-coated with 10µg/ml FN. Adherent fibroblasts serum starved for 14h were lysed to represent stably adherent (ADH) cells. Cells were lysed in RIPA buffer for protein estimation using BCA assay and 20µg total protein used for Western blotting.

### ***FAK inhibitor treatment in suspension and re-adhesion assay***

Adherent WTMEFs were pre-treated with DMSO or FAK inhibitor PF-228 (10 $\mu$ M) in DMEM with 0.2% FBS for 14h before being detached and held in suspension for 120 min with 1% methyl cellulose in the presence of PF-228 (10 $\mu$ M) or DMSO (CNT). Cells were washed and collected as the 120'SUSP time point or re-plated on 10 $\mu$ g/ml FN for 15min (15'FN) and 4h (4hFN) in the presence of PF-228 (10 $\mu$ M) or DMSO (CNT). All cells were lysed in RIPA, protein estimated and used for Western blotting as described above.

### **Surface labelling and endocytosis of GM1**

#### ***Surface labelling***

WTMEFs and Cav1-/-MEFs serum-starved for 14h were trypsinised (0'SUSP) and held in suspension for 2h (120'SUSP). Cells at respective time points were labelled with 10 $\mu$ g/ml of CTxB-Alexa 594 in PBS for 15 min on ice. Cells were then washed thrice using cold PBS followed by fixation with 3.5% paraformaldehyde. Cell suspension in leftover ~20ul PBS was mounted on slides with Fluoromount. Imaging was done using Zeiss LSM710 laser confocal microscope, 40X oil objective and identical microscopy settings were used for all samples in that experiment. Image analyses were done using ImageJ (NIH). For quantitation of surface GM1 levels using ImageJ, intensity threshold was set to map the entire cell and a mask was created to measure intensity in that cell. Total integrated density in cells was measured, average integrated density calculated and was represented in arbitrary units in the graphs.

#### ***Endocytosis***

Cells were processed as described above with one major difference: all cells were detached and labelled using 10 $\mu$ g/ml of CTxB-Alexa 594 in PBS for 15 min on ice. Cells were then washed thrice using cold PBS. At this point, one third of cells were aliquoted and fixed with PFA, designated as 0'SUSP time point. Remaining cells were mixed with low serum DMEM, mixed with methyl cellulose containing media and held in suspension as described for 20 min and 120 min. After suspension at required time points, cells were washed, fixed with PFA and mounted on slides as described.

### **Detergent-free caveolae isolation**

Caveolae isolation was done using detergent-free isolation method developed in the lab of Dr. Richard Anderson (Smart *et al*, 1995). Briefly, cells from 10 confluent T75 flasks were washed twice with 5ml of 1X PBS and the cells were collected by scraping (for ADH) or after

suspension (20'SUSP and 120'SUSP) in 5ml of 1X PBS + 1mM PMSF. Cells were pelleted by centrifugation for 5 min, at 2000 rpm, 4°C in a cooled table-top Eppendorf centrifuge. The pellet was resuspended in 1ml of Buffer A (0.25M Sucrose, 1mM EDTA, 20mM Tricine pH 7.8) + protease and phosphatase inhibitors (1X PIC+1mM PMSF+10mM NaF+1mM Na-orthovanadate) designated as WCL. The sample was then placed in a 2ml Wheaton Dounce homogeniser (Cat. no. 0841416A) on ice, and homogenized with 30 strokes of the tight-fitting plunger. The homogenate was transferred to a 1.5ml centrifuge tube and centrifuged at 3000 rpm for 7 min at 4°C in an Eppendorf centrifuge. The post-nuclear supernatant (PNS) fraction was removed and stored on ice. The pellet was resuspended in fresh 1ml of Buffer A, homogenized, and centrifuged once more at 3000 rpm for 7 min at 4°C and PNS re-collected. Both PNS fractions were combined and carefully layered on the top of a 22.5ml of 30% Percoll (7.5ml 100% Percoll + 12.5ml 2X Buffer A + 5ml MilliQ water) + protease and phosphatase inhibitors, and centrifuged at 86,330g for 30 min at 4°C in a Beckman Ti70 rotor. The plasma membrane fraction visible as a band ~4.5 cm from the bottom of the centrifuge tube was collected (PM1). This fraction was adjusted to 2ml with Buffer A, and placed in a Beckman tube (Cat. no. 349622) tube on ice and sonicated with 3mm probe and following settings: 90% output – 40 sec ON – 10 sec OFF – 40 sec ON. The tube was then incubated on ice for 2 min to maintain the sample at 4°C before a second round of sonication under the same conditions. This sonicated sample now labelled as PM2 (2ml) was then mixed with 1.84ml 50% Optiprep + 0.16ml Buffer A, and placed at the bottom of a Beckman centrifuge tube (Cat. no. 344059). This mixture has a final Optiprep concentration of ~23%. A continuous 20% to 10% OptiPrep gradient was prepared on top of the sample using a gradient maker, and centrifuged at 52,000g for 90 min in a Beckman SW40 swinging bucket rotor. At the end of the spin the top 5ml of the gradient was collected as Opti1 and mixed with 5ml of 50% Optiprep in a 13ml centrifuge tube. This 10ml sample (now in 25% Optiprep) was overlaid with 2ml of 5% OptiPrep and centrifuged at 52,000g for 90 min at 4°C. After the spin, 1ml fractions were collected using a micropipette tip from the interface between 5% and 25% Optiprep (Fr.1) and then from the top of meniscus (Fr.2). These fractions (1ml each of Fr.1 and Fr.2) were then concentrated by mixing with 2ml of PBS + protease and phosphatase inhibitors, and spun at 100,000g for 1h, at 4°C (43,000 rpm fixed-angle TLA100.3 rotor). Supernatant was discarded after the spin and 50µl 1X Laemmli sample buffer added directly to the tubes. These samples concentrated from Fr.1 and Fr.2 were designated as caveolar membranes CM1 and CM2 respectively. All samples were subject to Western blotting with loading as described in Table 1. Calculations to

determine purity of the preparation from Western blotting data were done as follows: band intensity for each protein (Cav1, Cavin, Paxillin, GM130, RhoGDI) in respective fraction was multiplied by loading factor for that fraction (Table 1). This value was normalized to WCL and represented as percentage of protein in CM2 relative to WCL.

**Table 1:**

Sample	Total lysate (µl)	Volume run on gel (µl)	Loading factor
WCL	2000	1	2000
PNS	1900	2	950
PM1	2000	3	666.6666667
PM2	2000	3	666.6666667
Opti1	5000	24	208.3333333
Fr.1	1000	24	41.66666667
Fr.2	1000	24	41.66666667
CM1	50	25	2
CM2	50	25	2

### **Cav1 immunoprecipitation**

WTMEFs at ~80% confluency adherent for at least 24h on 60mm dish (per sample) were scraped in 2ml DPBS, and spun at 2000 rpm to obtain cell pellet. Pellet was reconstituted in 1ml of Buffer A containing protease and phosphatase inhibitors. Cells were homogenised using a Dounce homogeniser (used in Caveolae isolation protocol). Post-nuclear supernatant (PNS) was collected by spinning the homogenate at 3000 rpm, 7 min, 4°C. The homogenisation and spin was repeated and PNS pooled. Cav1 N20 (Santa Cruz) antibody, crosslinked to Dynabeads using Dynabeads Antibody Coupling Kit (Invitrogen, Cat. no. 14311D) according to manufacturer's instructions, was used for immunoprecipitation to minimise IgG elution in IP complexes. Beads crosslinked to Cav1 antibody were washed with IP buffer (20mM Tricine, pH 7.8 + 1mM EDTA pH 8.0 + protease and phosphatase inhibitors), added to PNS and incubated with constant rotation for 2h at 4°C. Immuno-precipitates bound to beads were washed thrice with IP buffer to remove unbound fractions. Washed beads were transferred to a fresh tube after the third wash. Elution of IP reaction was done using 100µl each of the following mild elution buffers: (1) 0.1M glycine, pH 2.5, (2) 0.2M KCl-HCl, pH 1.5, or (3) 0.1M Citrate, pH 3.1; by incubation with gentle mixing for 30 min, at 4°C. Eluates (supernatants) were mixed with Laemmli's buffer and subjected to Western blotting.

### **Focal adhesion (FA) isolation**

Focal adhesion isolation was done using the method described by Kuo *et al*, 2011. Briefly, six T25 flasks were coated with 10µg/ml FN overnight at 4°C, and blocked using sterile 5% BSA in complete DMEM for 1 h at 37°C. Flasks were washed with media before plating WTMEFs for 24h at ~50% confluence (typically 2x10<sup>5</sup> cells per flask). For FA isolation, cells were given a hypotonic shock for 3 min with 2ml triethanolamine-containing low-ionic-strength buffer (2.5mM triethanolamine (TEA) in water at pH 7.0). Cells were moved to ice and buffer used for hypotonic shock (2ml) removed from each flask. Cell bodies left back were removed using hydrodynamic force with 20ml PBS with 1X PIC+1mM PMSF+10mM NaF+1mM Na-orthovanadate from a dental water jet (setting used - gentle). Two rapid washes of the flask surface were done as above. The buffer (~20ml) collected from flask 1 was used to similarly wash cells off in the remaining 5 flasks, the pooled cellular wash collected at the end and designated as cell body fraction (CB). All 6 flasks were then rinsed with 50ml of PBS containing protease and phosphatase inhibitors using the water jet, followed by one last rinse with 2ml each of distilled water with protease and phosphatase inhibitors. Any remaining liquid in the flask was drained by placing the flask tilted on ice, and FAs left adherent to the dish were collected in 200µl RIPA buffer containing 1X PIC+1mM PMSF+10mM NaF+1mM Na-orthovanadate using a cell scraper. 200µl RIPA with focal adhesions from flask 1 was then transferred to each of the other 5 flasks in succession and focal adhesions collected and pooled together. FA and CB fractions so collected were TCA-precipitated (Link & Labaer, 2011). In brief, 22µl of ice-cold 100% TCA was added to 200 µl of the sample, mixed and incubated on ice for 10 min. 500µl of ice-cold 10% TCA was then added to the tube, mixed and incubated on ice for 20 min. Following this incubation, samples were centrifuged at 20,000g for 30 min at 4°C, supernatant removed and pellets washed with 500µl of acetone and centrifuged at 20,000g for 10 min at 4°C. Protein pellets were dried for 5 min and resuspended in 50µl RIPA buffer containing protease and phosphatase inhibitors. This is now the FA or CB fraction used for Western blotting. WTMEFs (2x10<sup>5</sup>) plated on one FN+BSA coated dish and lysed in 200µl RIPA served as the whole cell lysate (WCL). WCL, FA and CB samples were protein estimated using BCA assay and 15µg protein used for Western blotting.

## **Western Blotting**

Samples for Western blotting were mixed with Laemmli buffer before resolving by SDS-PAGE. 12.5% polyacrylamide gels were prepared and run using Tris-glycine running buffer containing 0.1% SDS in Bio-Rad mini apparatus. Resolved proteins were transferred onto PVDF membrane with sodium bicarbonate or Tris-glycine-methanol running buffer. All blotted membranes were blocked with 5% non-fat milk in TBS + 0.1% Tween-20 (TBST) at RT for 60 minutes with gentle rocking. Blocked blots were incubated overnight at 4°C with primary antibodies at indicated dilutions made in 5% BSA in TBST. After primary antibody incubation, blots were washed thrice with TBST on a rotary shaker for 10 min each. Blots were incubated at RT for 60 min with secondary antibodies at indicated dilutions made in 2.5% BSA in TBST. Blots were washed again thrice with TBST on a rotary shaker for 10 min each. Blots were developed on ImageQuant LAS-4000 (Fujifilm Life Sciences) with chemiluminescent substrate. Densitometry analyses of Western blotting data were done using ImageJ software.

## **Two-dimensional gel electrophoresis (2D-GE)**

BioRad setup was used for 2D gel electrophoresis. Sample preparation and electrophoresis runs were done according to manufacturer's instructions (BioRad "2D-electrophoresis workflow: How to guide"). In brief, caveolae isolated using the detergent-free fractionation method were eluted in 2D sample buffer (8 M urea, 4% CHAPS, 100 mM DTT, 0.05% SDS, 0.5% ampholyte 3–10 and a trace of bromophenol blue). 125µl of sample was passively rehydrated onto a 7cm IPG strip (BioRad) initially for 1h, followed by overnight incubation after mineral oil overlay. Iso-electric focusing (IEF) was performed in BioRad Protean IEF cell (Dr. Anjan Banerjee lab, Biology department, IISER, Pune), with the following program: S01 linear voltage ramp 250V over 30 min, S02 linear ramp 3000V over 1.5h, S03 3000V for 10,000 Volt-hours. Following IEF, IPG strips were subjected to 15 min of reduction with 2% DTT and 15 min of alkylation with 2.5% IAA, both made in equilibration buffer (6M urea, 375mM Tris-HCl (pH 8.8), 2% SDS, 20% glycerol). Strips were then mounted on top of a 12% polyacrylamide gel with low-melting agarose (made in PAGE running buffer with trace of BPB) and electrophoresed. Silver staining was done using BioRad kit.

## **Sample preparation and immunogold labelling for FESEM imaging**

### ***Adherent WTMEFs***

$2 \times 10^5$  WTMEFs were seeded on silicon wafers placed in wells of a 48-well plate and allowed to spread for at least 24h. Media was removed and cells were washed twice with PBS. Cells



were fixed with 3.5% paraformaldehyde in PBS for 15 mins at room temperature, and washed thrice with PBS. The wafers were blocked with 2% BSA in PBS for 1h at RT. Labelling was done using anti-Cav1 antibody (Santa Cruz) diluted in 2% BSA at 1:50 dilution in PBS for 1h at RT. The wafers were incubated overnight at 4°C in a humidified chamber (petri dish with moist Whatman paper). Wafers were washed thrice with PBS. Secondary labelling was done using gold-conjugated Protein A diluted in 2% BSA in PBS at 1:50 dilution, followed by incubation for 1h, RT. Following gold labelling, cells were washed thrice with PBS (5 min each). Wafers were then air-dried for 15-20 mins under laminar flow, followed by vacuum-drying in a desiccator with calcium carbonate overnight.

### ***Caveolae membranes***

CM2 pellet after caveolae isolation was dissolved in 30µl of DPBS, and further diluted 1:10 with DPBS. 30µl of this was drop-casted on a silicon wafer and allowed to air-dry. (Blocking was not done for caveolae membranes since background due to BSA may be too high.) 30µl of the 1:50 primary antibody solution made in DPBS was added to this air-dried CM2, and incubated for 1h, RT. The surface was washed thrice with gentle aspiration. Protein A-gold at 1:50 dilution made in DPBS was added to the wafer and incubated for 1h, RT. The surface was washed thrice with gentle aspiration. Wafers were then air-dried for 15-20 mins under laminar flow, followed by vacuum-drying in a desiccator with calcium carbonate overnight. Secondary control samples were treated similarly without primary antibody treatment.

### ***Gold sputter-coating for FESEM***

Caveolae membranes drop-casted and processed as above – without immunolabelling – on silicon wafers (Sigma). Post vacuum-drying the samples, 10nm gold sputter-coating was done at the FESEM facility, Physics department, IISER, Pune before imaging.

### ***Sample preparation for TEM***

CM2 pellet was reconstituted in 50µl of Ca<sup>2+</sup> and Mg<sup>2+</sup> free PBS. This was applied on TEM grids prepared in the lab of Dr. Atanu Basu, NIV, Pune. Negative staining of the samples was done using 2% phosphotungstic acid as a negative stain. Stained samples were allowed to dry before imaging.

## **Electron microscopy**

### ***Field emission scanning electron microscopy (FESEM)***

Imaging was done at the FESEM facility, Physics department, IISER, Pune with help from Anil Prathamshetti. Microscopy settings differ in terms of keV and magnification for every image captured, and are mentioned in detail in every image.

### ***Transmission electron microscopy (TEM)***

The imaging was done at 120keV on HR-TEM facility at NIV, Pune with help from Nitali Tadmalkar and Dr. Atanu Basu.

## **Fluorescence and confocal microscopy imaging**

GM1 surface labelling or endocytosis images were acquired using a 63X oil immersion objective on Zeiss LSM 780 multiphoton confocal microscope, NA 1.4. Phase contrast images were acquired using a 20X objective of EVOS FL Auto Imaging system (ThermoFisher AMAFD1000). Fluorescence intensity analysis was performed using ImageJ software.

## **Statistical analysis**

Statistical analyses of data were done using unpaired two-tailed t-test. All analyses were done using Prism Graphpad analysis software. Statistical significance was considered at  $p < 0.05$ .

## RESULTS

---

### *pY14Cav1 regulates GM1 endocytosis upon loss of adhesion*

One of the most recognized but least studied functions of pY14Cav1 is its requirement for caveolar endocytosis. Caveolar endocytosis of raft microdomains occurs in response to loss of cell-ECM adhesion, to downregulate growth signaling (del Pozo *et al*, 2005). Moreover, although rafts microdomains are endocytosed through different routes (Torgersen *et al*, 2001), their endocytosis upon loss of adhesion is primarily *via* caveolae (del Pozo *et al*, 2005). Hence in order to establish that pY14Cav1 drives caveolar endocytosis of rafts, we surface-labelled the glycosphingolipid, ganglioside GM1 (a raft microdomain marker), in Cav1<sup>-/-</sup>-MEFs reconstituted with Cav1. Fluorescently-conjugated cholera toxin subunit B (CTxB), known to specifically bind clustered GM1 (Kabbani *et al*, 2020), was used to study these dynamics. Cells were detached (0'SUSP) using trypsin (trypsinization does not affect GM1) and held in methyl cellulose suspension for (120'SUSP). Detached or suspended cells were labelled on ice with Alexa-conjugated CTxB, fixed, imaged and fluorescence intensity quantified using ImageJ as described in Materials and Methods. Surface GM1 fluorescence intensity was comparable in 0'SUSP and 120'SUSP Cav1<sup>-/-</sup>-MEFs, indicating lack of GM1 endocytosis (Fig. 1.1) under these conditions. Surface GM1 levels in Cav1<sup>-/-</sup>-MEFs expressing Flag WT-Cav1 show a marked decrease upon loss of adhesion, whereas those in phosphodeficient Y14F-Cav1 expressing cells stayed similar to Cav1<sup>-/-</sup>-MEFs expressing no Cav1. Expression of Flag-WT-Cav1 and Y14FCav1 were comparable as confirmed by Western blot detection with anti-Flag antibody. These results confirm pY14Cav1 to be required for loss of adhesion-mediated caveolar endocytosis of raft microdomains marked by GM1.

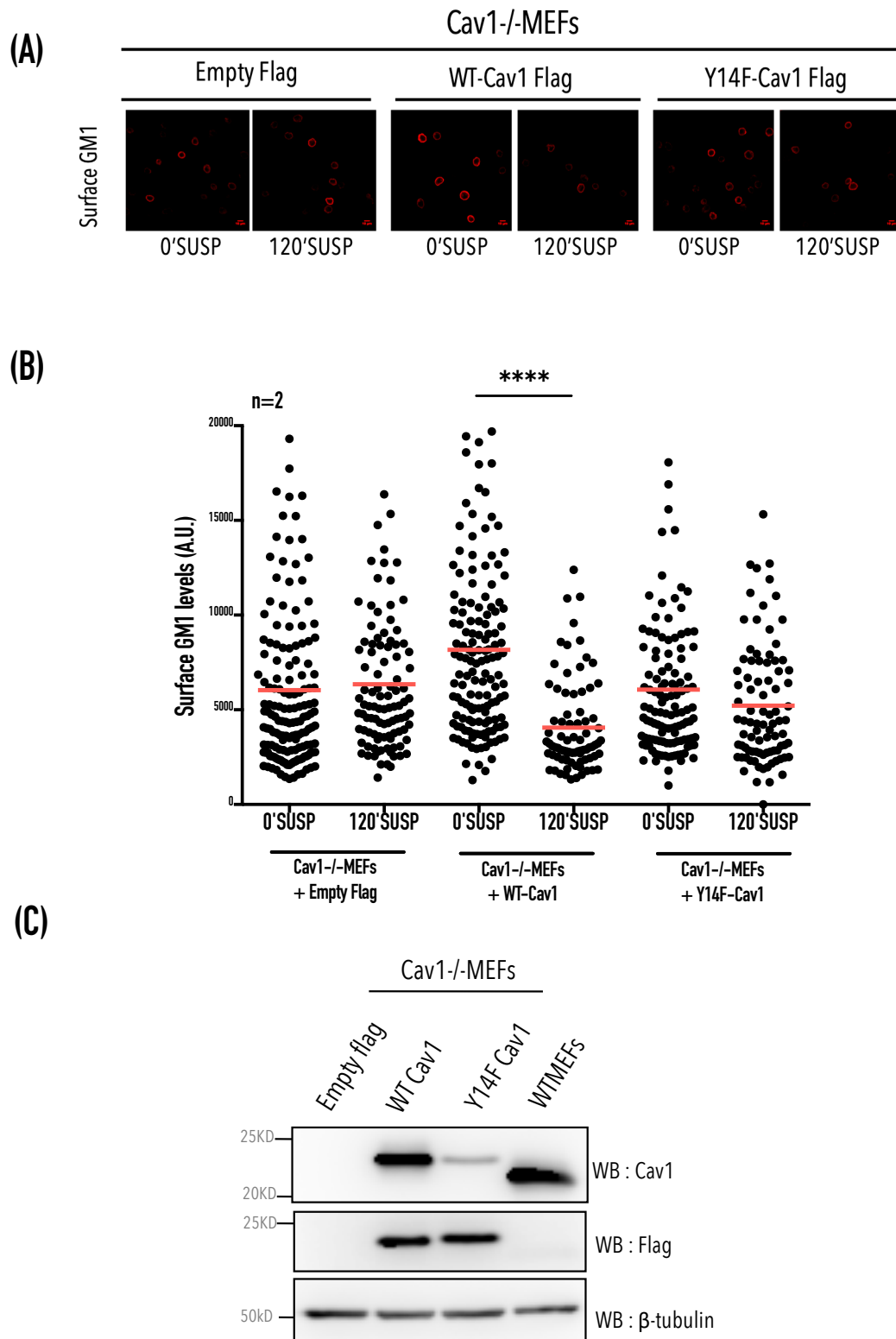


**Figure 1.1. pY14Cav1 regulates GM1 endocytosis upon loss of adhesion.** (A) Cell surface GM1 levels in Cav1<sup>-/-</sup>-MEFs expressing Empty Flag, WT-Cav1 or Y14F-Cav1. (B) Fluorescence intensity of surface GM1 quantitated using integrated density from ImageJ software. (C) Expression levels of Cav1 determined by Western blotting.

### ***Cav1 phosphorylation is regulated upon loss of adhesion in mouse fibroblasts***

Loss of cell-matrix adhesion while downregulating integrin-dependent signaling can also cause a distinct change in membrane tension allowing cells to adopt an energetically favourable spherical form. In suspended cells, membrane endocytosis triggered through caveolae is dependent on pY14Cav1 (del Pozo *et al*, 2005), which is also known to have a mechanotransducory role (Joshi *et al*, 2012). We hence asked if loss of adhesion regulates Cav1 phosphorylation in mouse fibroblasts. Serum-deprived WTMEFs and NIH3T3 cells held in suspension using methylcellulose for 5, 20 and 120 min (5'SUSP, 20'SUSP and 120'SUSP), show a rapid decrease in total pY14Cav1 levels in the first 5 min in suspension. Normalized to their total Cav1 levels, this drop in pY14Cav1 is maintained in suspended cells at 20 min and 120 min (Fig. 1.2). The observed drop in pY14Cav1 levels between stably adherent (ADH) vs 5 min, 20 min and 120 min suspended WTMEFs and NIH3T3 fibroblasts is largely comparable (62%, 64% and 67% respectively in WTMEFs and 58%, 69% and 72% in NIH3T3). WTMEFs from a different source (IP6K<sup>+/+</sup>MEFs, Dr. Rashna Bhandari, CDFD) also gave comparable results (Fig. 1.2). Loss of cell-matrix adhesion hence leads to a rapid and sustained decrease in Cav1 phosphorylation (Buwa *et al*, 2020a).

### ***Cav1 phosphorylation is restored on re-adhesion to fibronectin in mouse fibroblasts***

Loss of adhesion-mediated decrease in pY14Cav1 levels could be a result of decreased integrin-mediated adhesion and hence signaling. We hence tested if re-adhesion of suspended cells affects pY14Cav1 levels. Re-adhesion of 120'SUSP cells to fibronectin for 15 min (15'FN) in low-serum conditions recovered pY14Cav1 levels in both WTMEFs and NIH3T3 cells. pY14Cav1 levels continue to be maintained 4h after re-plating (4hFN) (Fig. 1.3). In the absence of serum growth factors the drop and recovery of pY14Cav1 seen in these cells is comparable to integrin-dependent regulation of FAK activation (pY397FAK) and Paxillin phosphorylation (pY118Paxillin) (Fig. 1.3). This suggests Cav1 phosphorylation to be regulated by cell-matrix adhesion (Buwa *et al*, 2020a).

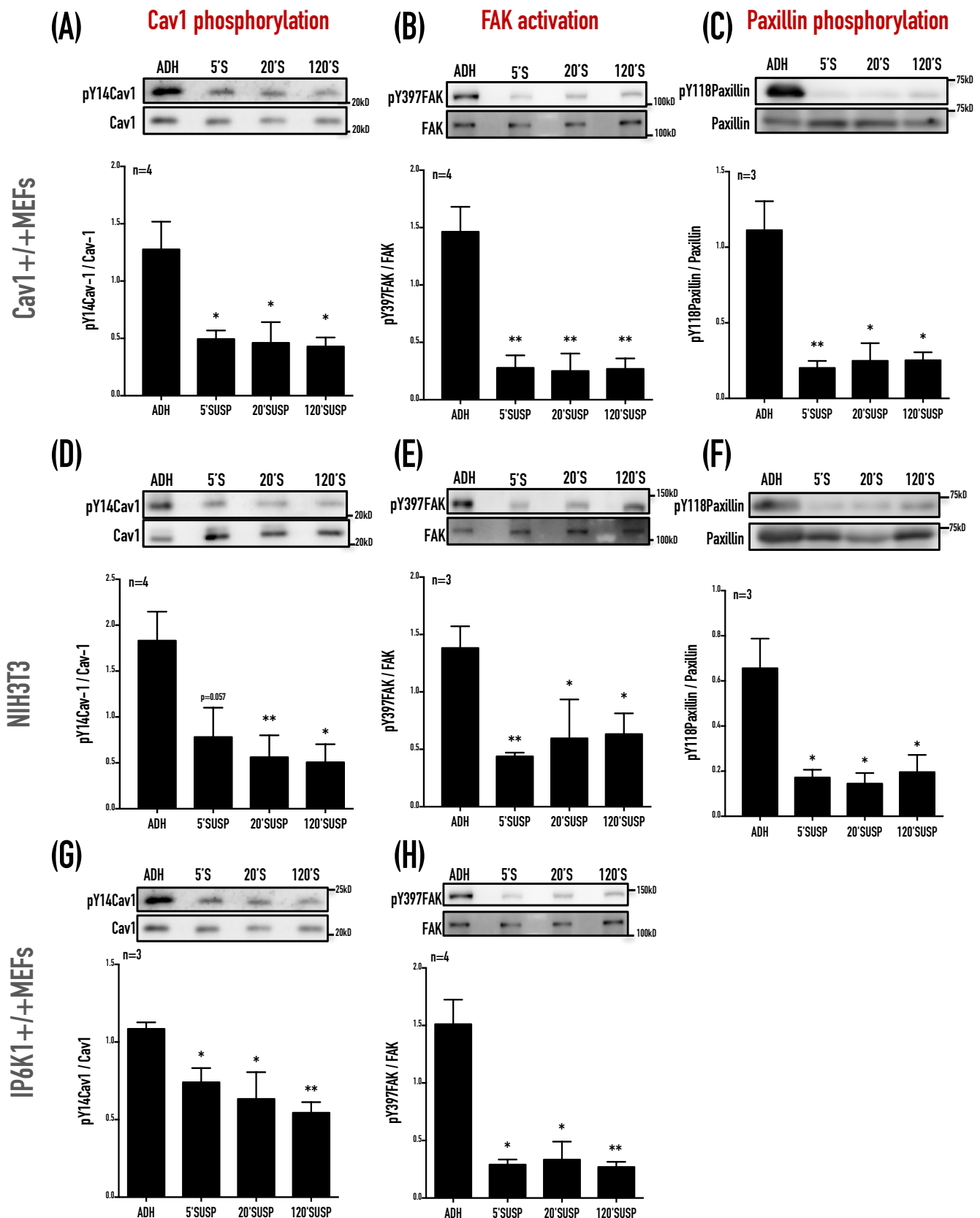


**Figure 1.2. Cav1 phosphorylation is regulated upon loss of adhesion in mouse fibroblasts.** (A-H) Western blot analysis of phosphorylated and total FAK, Cav1 and Paxillin in adherent (ADH), detached (5'SUSP), suspended for 20min (20'SUSP) and suspended for 120min (120'SUSP) Cav1+/+MEFs, NIH3T3 cells and IP6K1+/+MEFs, as mentioned. Graphs represent densitometry analysis of Western blotting data from 4 independent experiments, with ratios of band intensities of phosphorylated protein to respective total protein plotted as mean  $\pm$  SE. Statistical analysis was done using unpaired two-tailed t-test.

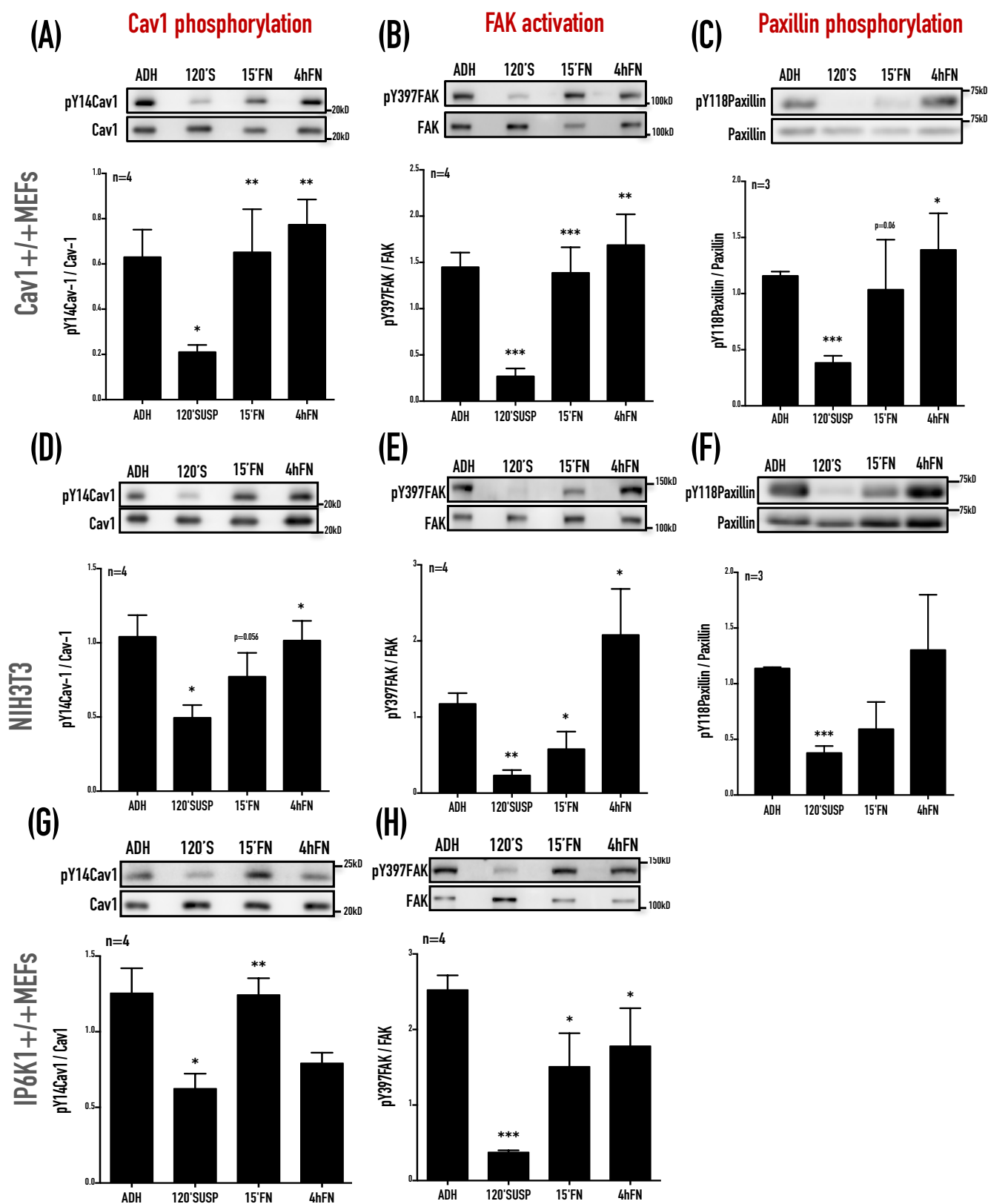


**Figure 1.3. Cav1 phosphorylation is upregulated upon re-adhesion to fibronectin in mouse fibroblasts.** (A-H) Western blot analysis of phosphorylated and total FAK, Cav1 and Paxillin in adherent (ADH), suspended for 120min (120'SUSP), re-adherent for 15min (15'FN) and re-adherent for 4h (4hFN) WTMEFs, NIH3T3 cells and IP6K1+/+MEFs, as mentioned. Graphs represent densitometry analysis of Western blotting data from four independent experiments, with ratios of band intensities of phosphorylated protein to respective total protein plotted as mean  $\pm$  SE. Statistical analysis was done using unpaired two-tailed t-test.

### ***pY14Cav1 is detected in isolated caveolae in MEFs***

Cav1 can get phosphorylated in response to extracellular stimuli and localize to caveolae or non-caveolar sites such as focal adhesions. The relative localization of pY14Cav1 at these sites could change in response to external stimuli. But the localization of endogenous pY14Cav1 under stimulated or basal, non-stimulated conditions is not known. Most studies have evaluated the role of pY14Cav1 using overexpressed, fluorescently-tagged, phosphorylatable (WT), phosphodeficient (Y14F) or phosphomimetic (Y14D or Y14E) mutants. Knowing loss of adhesion to significantly affect total pY14Cav1 levels (Fig. 1.2), we first asked if this affects caveolar pY14Cav1 levels. We sought to answer this query by isolating caveolae using the detergent-free protocol developed in Richard Anderson's lab (Smart *et al*, 1995) from stably adherent (ADH) and WTMEFs suspended for 20 min or 120 min (20'SUSP and 120'SUSP) (Fig. 1.4A). The suspended cells represent the early and late endocytosis events (Fig. 1.4B). Cav1 levels in WCL from ADH vs 20'SUSP vs 120'SUSP WTMEFs when run together are comparable, though pY14Cav1 levels showed an expected decrease in suspended (20 min and 120 min) cells (Fig. 1.4C). Detergent-free lysis of WTMEFs (WCL) was used to obtain a post-nuclear supernatant (PNS) by Dounce homogenisation. PNS was separated on a Percoll gradient and to obtain plasma membrane (PM1), which appears as a clear visible band (Fig. 1.4D). This was sonicated (PM2) and separated on a continuous Optiprep gradient (10%-20%) (Opti1), and then a discontinuous Optiprep gradient (5% and 25%) and the caveolar fractions collected (Fr.1, Fr.2) and concentrated (CM1 and CM2). All of these fractions from ADH, 20'SUSP and 120'SUSP cells were processed and amounts of lysates to be loaded was calculated as described in Fig. 1.4E. Samples were resolved by SDS-PAGE and probed for caveolar markers Cav1 and Cavin1 and non-caveolar markers Paxillin, GM130 and RhoGDI (Fig. 1.5). The percentage of each marker protein in the caveolar CM2 fraction relative to WCL was calculated accounting for the loading factor as detailed in the methods section (Fig. 1.4E). This was plotted and relative enrichment of caveolar proteins confirmed over non-caveolar proteins (Fig. 1.5). We see a significant enrichment of Cav1 in caveolae (CM2) compared to the non-caveolar proteins (Fig. 1.5). This confirms the purity of caveolae isolated to be comparable in ADH, 20'SUSP and 120'SUSP cells.



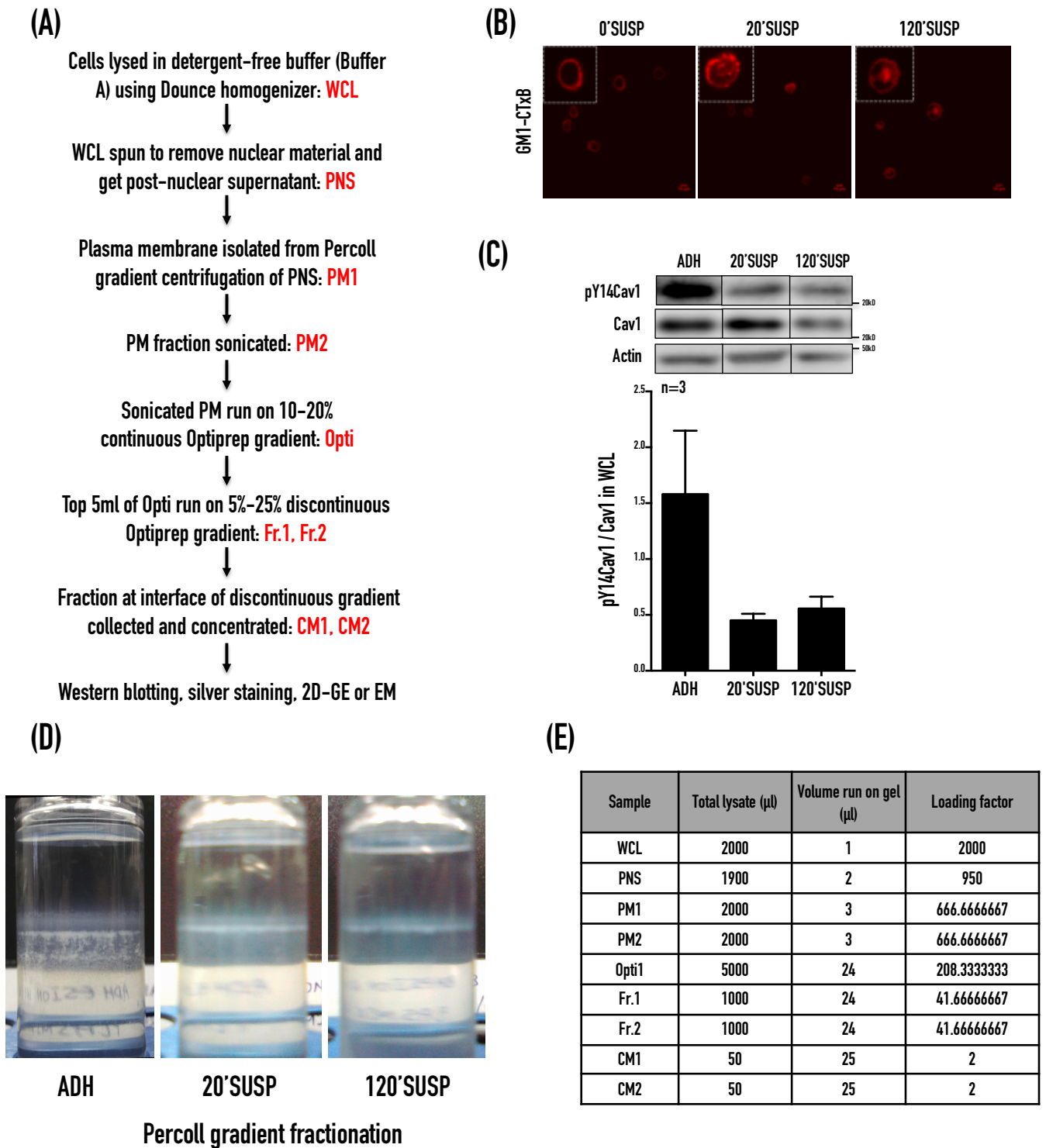


**Figure 1.4. Detergent-free caveolae isolation from WTMEFs** (A) Schematic for detergent-free caveolae isolation from adherent (ADH) and suspended (20'SUSP, 120'SUSP) WTMEFs. (B) Representative images for GM1 endocytosis in trypsinised (0'SUSP) and cells suspended for 20 min or 120 min. (C) Western blot analysis of pY14Cav1, total Cav1 and Actin in adherent (ADH), 20min suspended (20'SUSP) and 120min suspended (120'SUSP) WTMEFs, with WCL from same experiments as used for caveolae isolation run on same gel for comparison. Blots are cropped for representation in the right order. Graph represents ratio of band intensities of phosphorylated Cav1 to total Cav1 plotted as mean  $\pm$  SE from 3 independent experiments. (D) Representative images for Percoll gradient fractionation of lysates from adherent or suspended cells. Plasma membrane (PM) band appears as a white, thick band ~4 cm from the bottom of tube. (E) Calculations for enrichment of caveolar proteins and exclusion of non-caveolar ones in caveolae. Band intensity of each protein from densitometry of Western data multiplied by respective loading factor for every sample to calculate amount of protein in that sample.

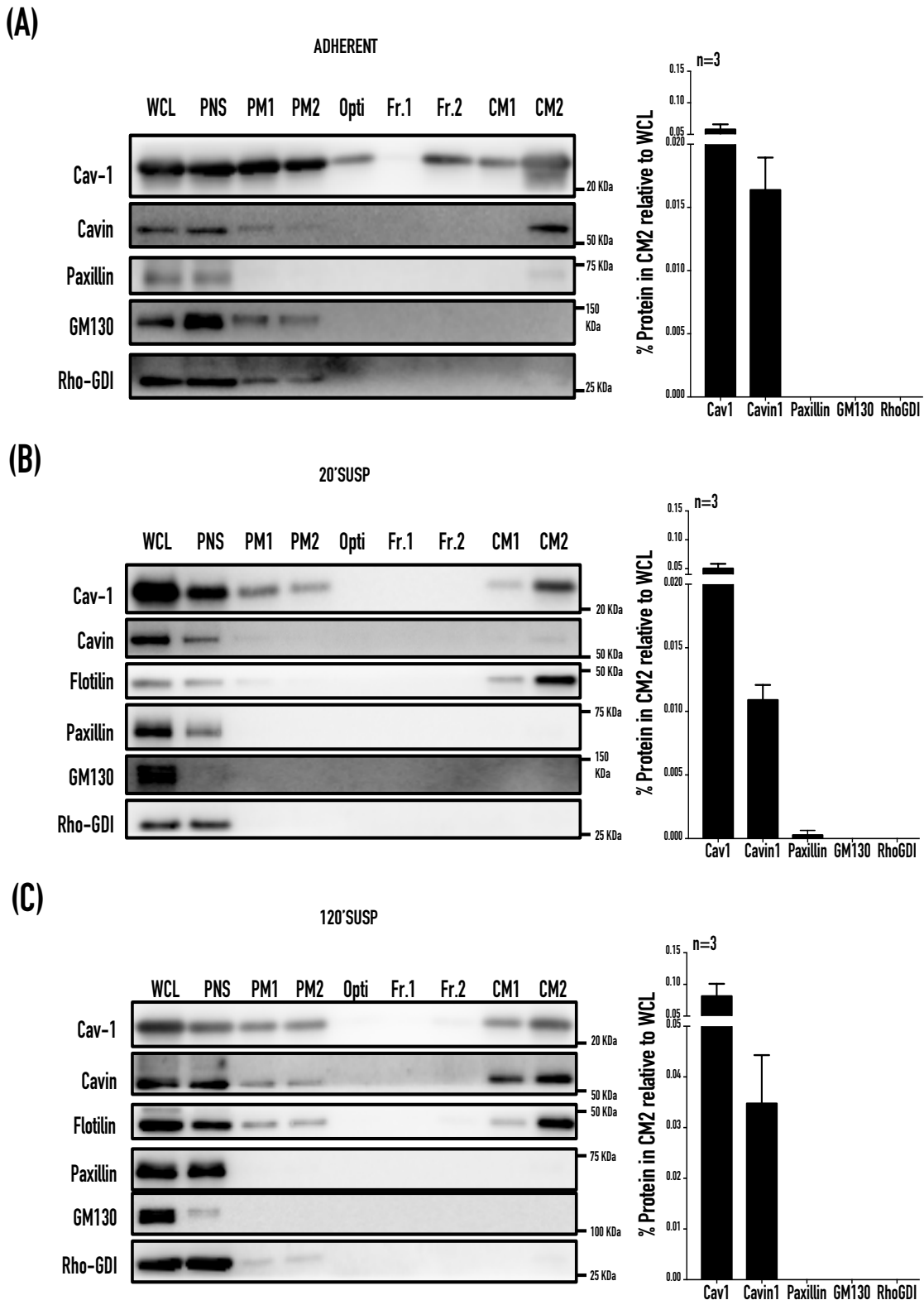


**Figure 1.5. Caveolae isolation from adherent and suspended WTMEFs - purity and enrichment.** Purity of caveolar membranes isolated from adherent (A), 20'SUSP (B) or 120'SUSP (C) WTMEFs using detergent-free method, confirmed by Western blotting. Lanes in Western blotting data represent samples collected at different stages of the purification procedure. Graphs represent densitometry analysis of Western blotting data. Band intensities for WCL and CM2 for each protein were normalized to respective loading factor (Fig. 1.4E), CM2 values normalized to WCL and this ratio represented as percentage  $\pm$  SE of respective protein in CM2.

We further evaluated the proteomic profiles of these caveolae membranes using silver staining of CM2 run on SDS-PAGE and 2D-gel electrophoresis (Fig. 1.6). In SDS-PAGE gels, we find caveolae isolated from adherent and suspended cells show remarkably different profiles, with only a some bands conserved (marked in green arrowheads) across the samples (Fig. 1.6A). 2D-GE profiles similarly show a different spot profile for caveolae isolated from adherent and suspended cells (Fig. 1.6B).

The detergent-free method for caveolae isolation uses the buoyant properties of caveolae membranes. Furthermore, the lack of detergent at any point in the protocol ensures that lipids in these membranes are not disrupted. Hence caveolar proteins are expected to be membrane-bound and retain their native properties. Preliminary studies using electron microscopy reveal caveolae membranes (CM2) to be vesicular structures with an average diameter of ~100-200 nm by FESEM (Appendix Figure 1A-B) and TEM (negatively stained CM2) (Appendix Figure 1C). Immuno-gold labeling of CM2 with the Cav1 antibody followed by IEM revealed the membranes to be lined with Cav1 (data not shown).

Thus satisfied with the purity of these detergent-free caveolae preparations, we evaluated the presence of pY14Cav1 in caveolae isolated from ADH vs 20'SUSP vs 120'SUSP WTMEFs (Fig. 1.7). Similar number of adherent or suspended WTMEFs were subjected to detergent-free fractionation to isolate caveolae. Isolated caveolae were resolved by SDS-PAGE and subjected to Western blotting to detect for the presence of endogenous pY14Cav1 (Fig. 1.7). The phosphorylated Cav1 detected in caveolae fraction (CM2) was normalized to total Cav1 present in CM2, and this ratio further normalized to the pY14Cav1/Cav1 ratio similarly calculated in respective WCL. pY14Cav1 levels so calculated in caveolae isolated from adherent (ADH) and suspended cells (20'SUSP and 120'SUSP) are comparable (Fig. 1.7). This suggests loss of adhesion to not affect the caveolar pY14Cav1 pool, and leads us to speculate that this pool could indeed be adhesion-independent (Buwa *et al*, 2020a), an interesting prospect that needs to be explored further in detail. This also leads us to speculate that the significant adhesion-mediated changes in total cellular pY14Cav1 levels (Fig. 1.2, 1.3) could hence be prominently from their non-caveolar localization at sites such as focal adhesions.

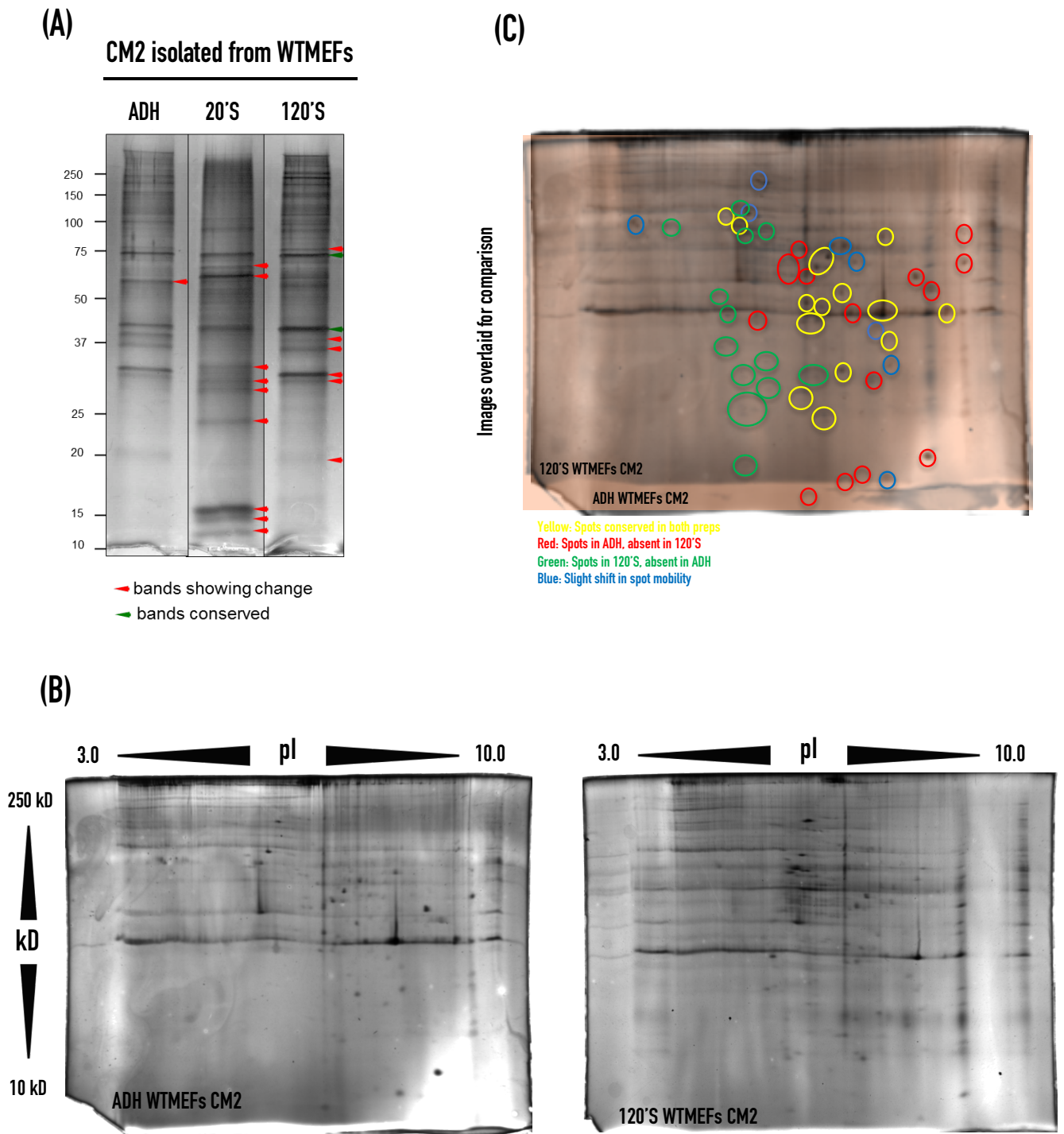


**Figure 1.6. Protein profiles of caveolae isolated from adherent and suspended WTMEFs.** (A) Caveolae isolated using detergent-free method (CM2) from adherent (ADH) and cells suspended for 20 min (20'SUSP) and 120 min (120'SUSP) were resolved by PAGE and subjected to silver staining. (B) Caveolae similarly isolated from adherent (ADH, left) and cells suspended for 120 min (120'S, right) were subjected to iso-electric focussing followed by a second dimension run on PA gels. (C) 2D-GE gel images were overlaid to detect similarities, differences and shift in spot patterns.

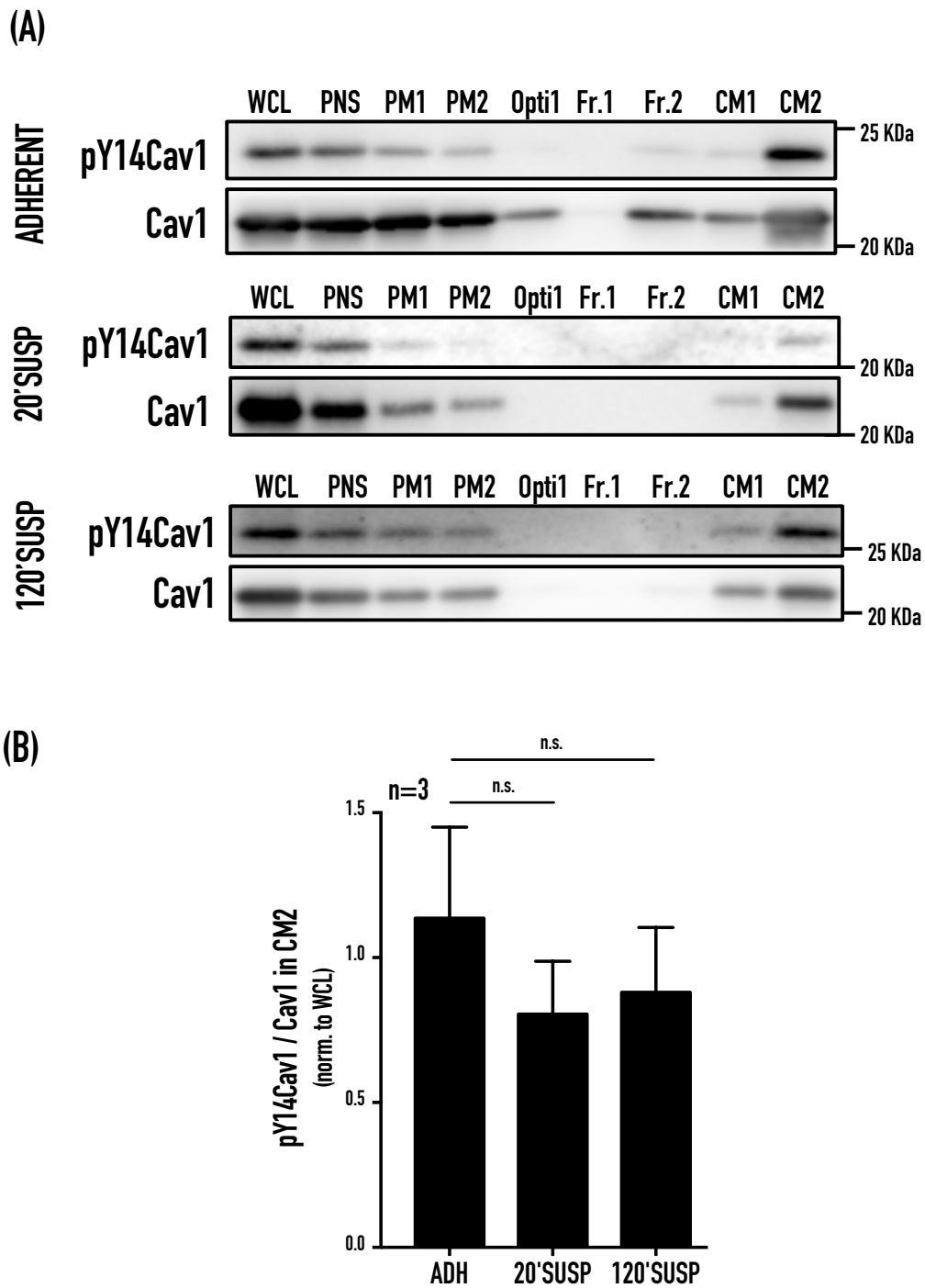


**Figure 1.7. Endogenous pY14Cav1 in caveolae isolated from adherent and suspended WTMEFs.** (A) Cav1 phosphorylation in caveolar membranes (CM2) isolated from WTMEFs by the detergent-free method, confirmed by Western blotting. (B) Graph represents densitometry analysis of Western blotting data. Ratio of pY14Cav1 to total Cav1 in CM2 was normalized to ratio of pY14Cav1 to total Cav1 in WCL, plotted as mean  $\pm$  SE from three independent experiments. Statistical analysis was done using unpaired two-tailed t-test.

### ***pY14Cav1 is detected in isolated focal adhesions (FA) in MEFs***

The localization of endogenous pY14Cav1 is not well-established at any sub-cellular locations, including focal adhesions. We hence employed the method devised by Kuo *et. al.* using a short, pH-balanced hypotonic treatment of cells, to isolate FAs. Triethanolamine (TEA) was used to hypotonically shock the cells. Since mechanical stresses are known to affect Cav1 phosphorylation (Radel & Rizzo, 2005), it was crucial to determine if this treatment and resulting swelling of cells affected the same. We hence did a time course experiment to determine if TEA treatment affects total cellular pY14Cav1 levels. Adherent WTMEFs were treated with 2.5mM TEA for varying time points, starting from 1 min to 40 min of treatment. Cells started to slightly swell at 4-5 min post-treatment (5' TEA), and had started to come off the tissue culture dish at ~10 min (Fig. 1.8A). Although cells had started to swell, pY14Cav1 levels remained comparable to untreated (CNT, 0' TEA) at least until 5 min post TEA treatment (Fig. 1.8B, C), after which these levels start to decrease by >20% at 10 min, and by ~33% at later time points. We hence chose to treat the cells with TEA for 3 min to isolate FAs.

Focal adhesions were isolated from WTMEFs adherent on fibronectin, precipitated using TCA, reconstituted and protein estimated as described (Fig. 1.9A). Equal amounts of WCL, FA and CB protein were resolved by SDS-PAGE. FA fractions thus isolated are found to be enriched in the FA proteins FAK and Paxillin when compared to WCL and CB. Cytosolic RhoGDI on the other hand was clearly absent from FAs and detectable in only WCL and cell bodies (CB), signifying purity of FA preparations (Fig. 1.9B). We are also able to detect Cav1 in these FA fractions, although it is not as enriched as *bona fide* FA proteins. FA fractions however show detectable enrichment of endogenous pY14Cav1 (Fig. 1.9C). Quantitation also suggests a significantly higher percentage of Cav1 in FA to be phosphorylated, relative to that seen in WCL. We thus find endogenous pY14Cav1 to be abundantly present in FAs isolated from adherent mouse fibroblasts (Buwa *et al*, 2020a). Since loss of adhesion leads to loss of FAs, they could not be isolated and evaluated in suspended cells. Importantly, loss of FAs could be leading to the rapid reduction in pY14Cav1 levels upon loss of adhesion.

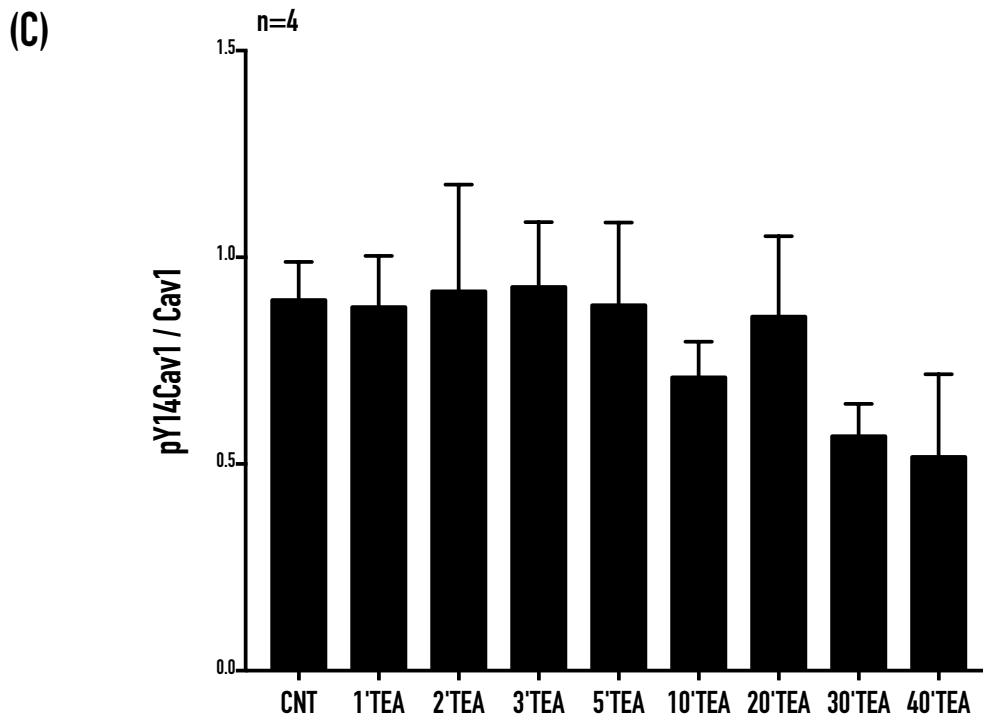
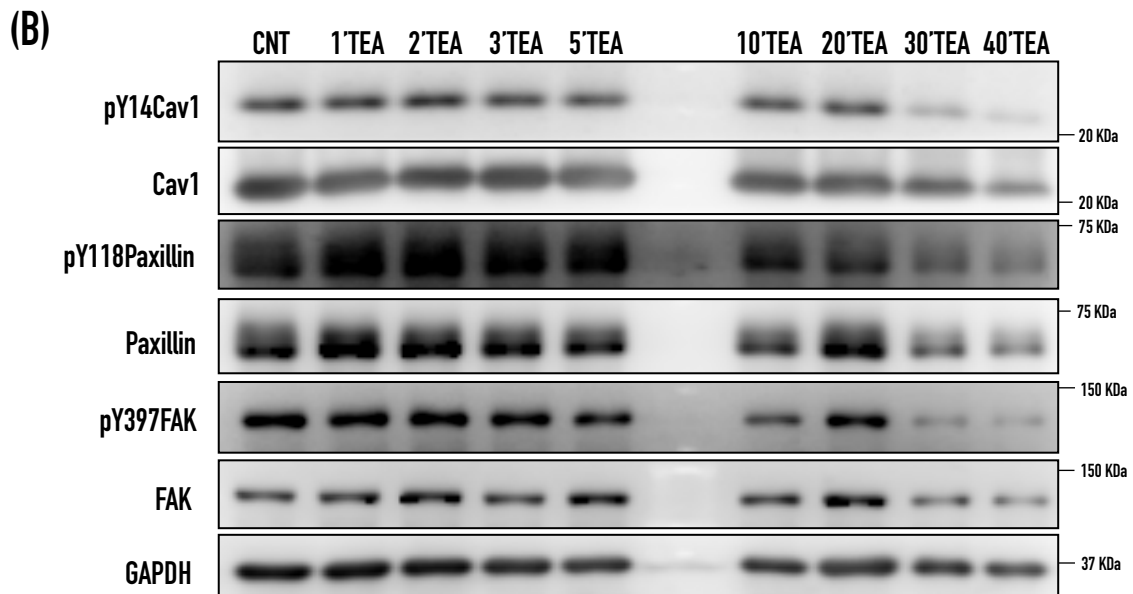
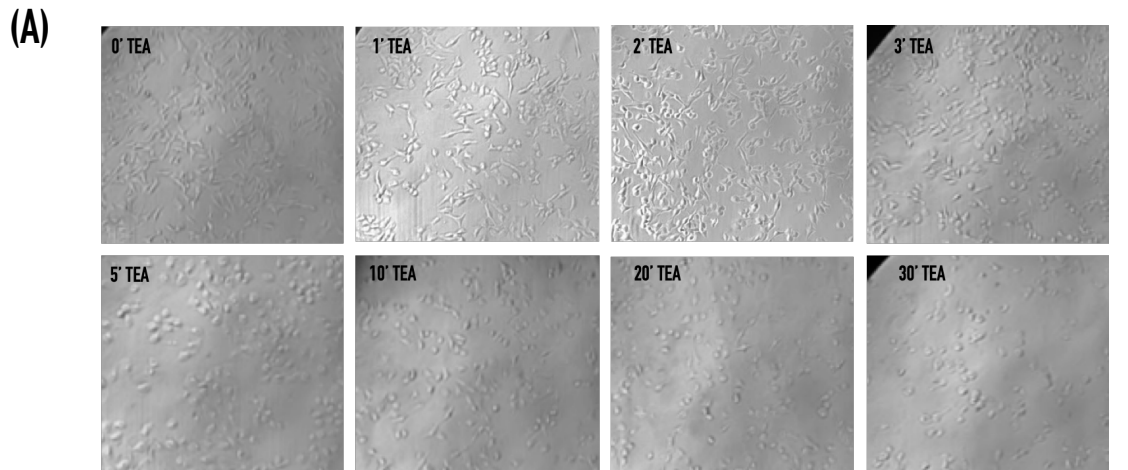


**Figure 1.8. Effect of hypotonic shock on total pY14Cav1 levels - time kinetics.** (A) Cell morphology in WTMEFs treated with Triethanolamine buffer to hypotonically shock cells. (B) Phosphorylated and total cellular Cav1, Paxillin and FAK in WTMEFs treated with Triethanolamine buffer, confirmed by Western blotting. (C) Densitometry analyses of Western data, with ratio of pY14Cav1 to total Cav1 represented as mean  $\pm$  SE from 4 independent experiments.

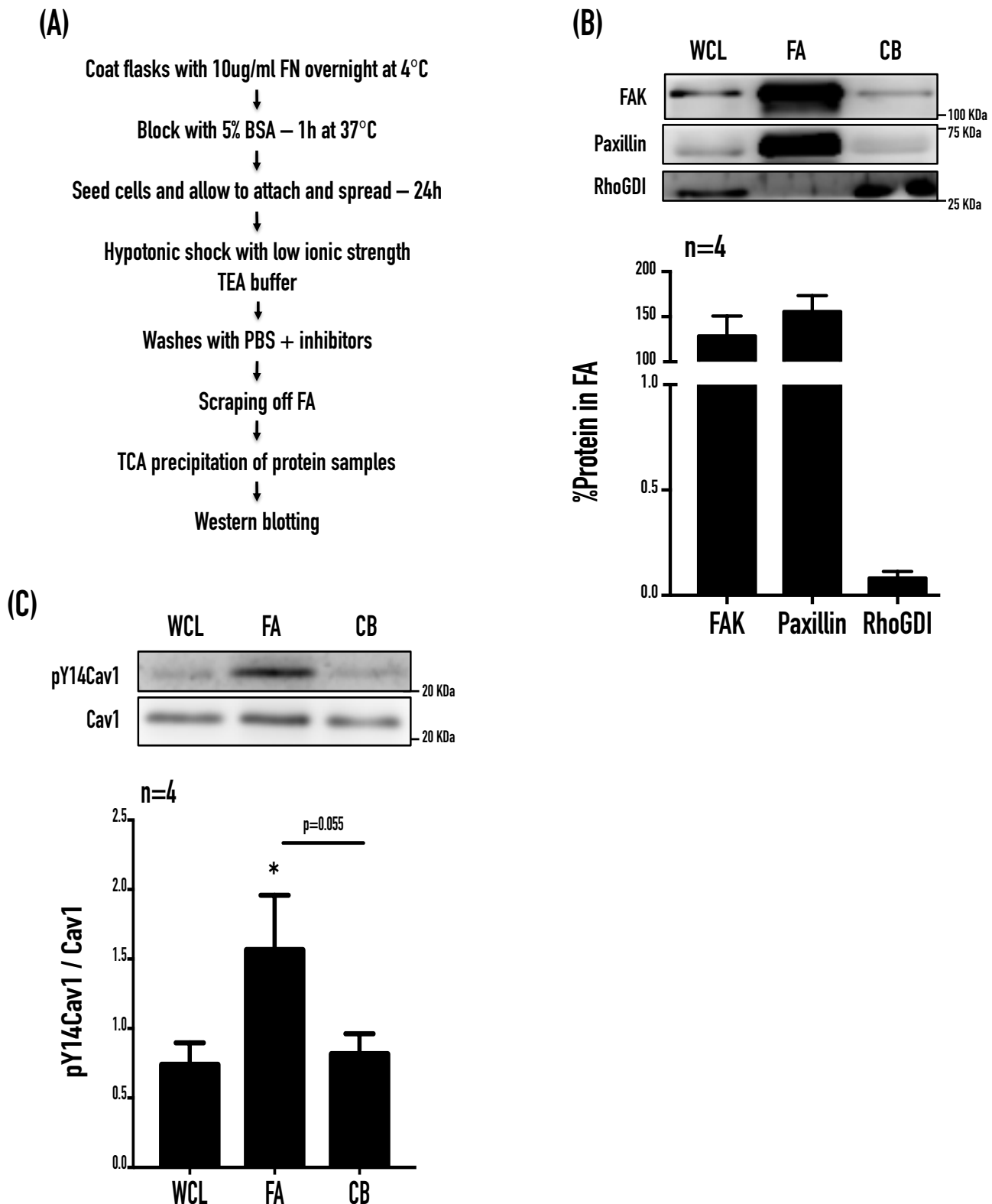


**Figure 1.9. Endogenous pY14Cav1 in focal adhesions isolated from adherent WTMEFs.** (A) Schematic for FA isolation from WTMEFs plated on FN using hypotonic shock method. (B) Purity and enrichment of FA proteins FAK and Paxillin in FAs isolated from WTMEFs, confirmed by Western blotting. Lanes in Western blotting data represent equal protein loaded for whole cell lysates (WCL), focal adhesions (FA) and cell bodies (CB). Graph represents densitometry analysis of Western blotting data. Band intensities for FA were normalized to WCL for respective protein and ratio represented as percentage  $\pm$  SE of that protein in focal adhesions. (D) Western blot analysis of pY14Cav1 and total Cav1 in FAs from adherent WTMEFs, with equal protein loaded for whole cell lysates (WCL), focal adhesions (FA) and cell bodies (CB). Graph represents densitometry analysis of Western data, with ratio of pY14Cav1 to total Cav1 plotted as mean  $\pm$  SE from 4 independent experiments. Statistical analysis was done using unpaired two-tailed t-test.



### ***Re-adhesion mediated recovery of pY14Cav1 is dependent on FAK activation in MEFs***

FAK is a prominent FA protein and also an important regulator of FA mediated signaling in adherent cells (Schaller, 2010). FAK forms a complex with Src upon integrin engagement and activation. We hence tested the effect of inhibition of FAK, using a FAK-specific small molecule inhibitor – PF-228 (Slack-Davis *et al*, 2007), on Cav1 phosphorylation in fibroblasts re-adherent on fibronectin. PF-228 treatment expectedly blocks FAK activation (pY397FAK) in re-adherent cells at early (15'FN) and late (4hFN) time points (Fig. 1.10A). pY397FAK levels decrease by ~65% in cells re-adherent for 15 min and by ~45% in 4h re-adherent cells upon PF-228 treatment. Interestingly, FAK inhibition significantly also inhibits Cav1 phosphorylation in 15'FN and 4hFN re-adherent cells respectively (Fig. 1.10B). pY14Cav1 levels similarly decrease by ~65% in cells re-adherent for 15 min and by ~45% in 4h re-adherent cells upon PF-228 treatment. PF-228 treatment seems to affect phosphorylation of Paxillin at early (15'FN) with a ~42% decrease, but not later adhesion time points (4hFN) (Fig. 1.10C). This further emphasizes the prominent presence of pY14Cav1 in focal adhesions and its distinct regulation by FAK. The caveolar pool of pY14Cav1 being unaffected on loss of adhesion (Fig. 1.7), suggests the observed change in net pY14Cav1 levels in suspended cells (Fig. 1.2, 1.3) could majorly result from the loss of FAs in these cells (Buwa *et al*, 2020a).

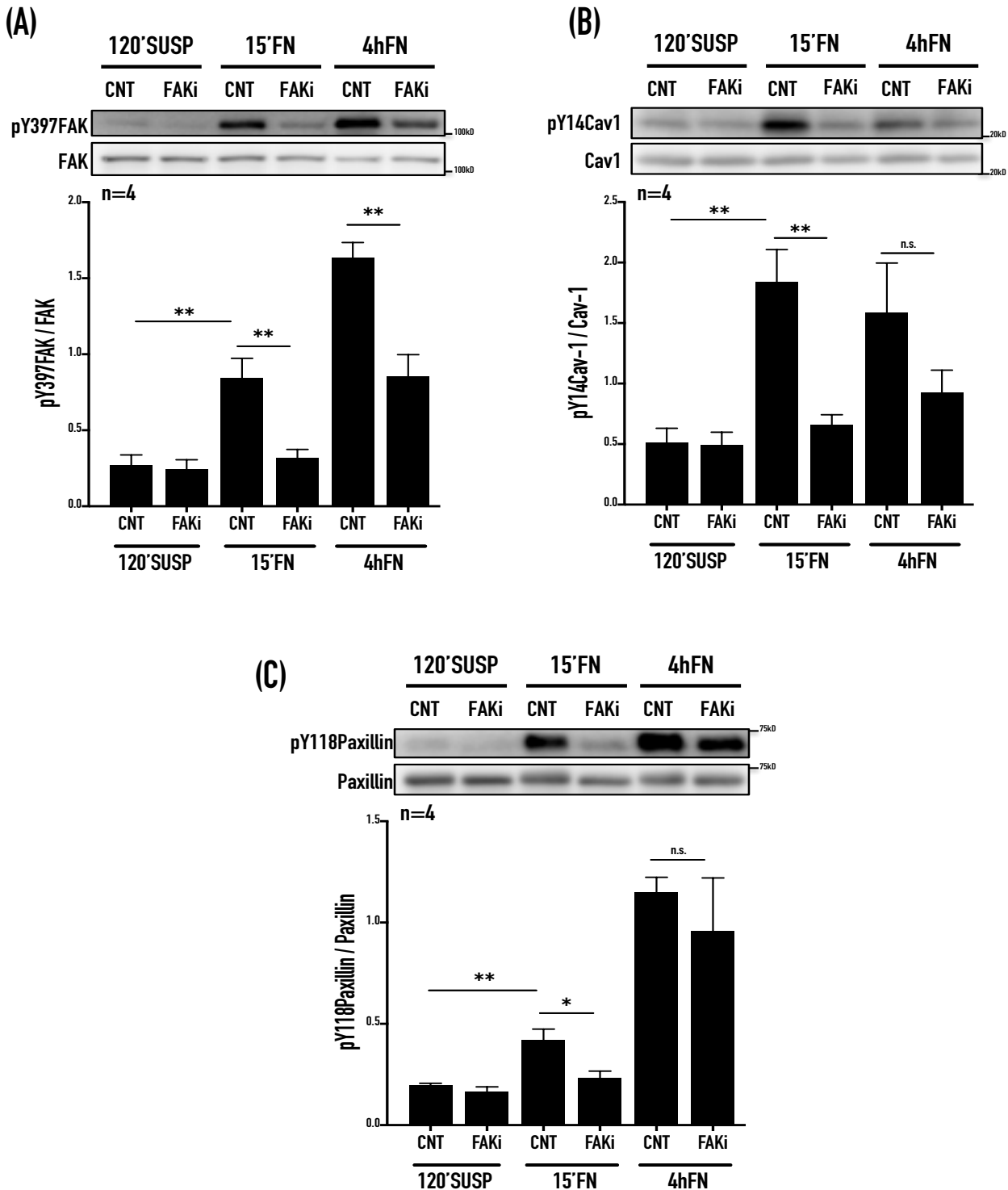


**Figure 1.10. Loss of adhesion-mediated regulation of Cav1 phosphorylation by FAK.** Western blot analysis of phosphorylated and total FAK (A), Cav1 (B) and Paxillin (C) in WTMEFs suspended for 120min (120'SUSP), re-adherent for 15min (15'FN) and re-adherent for 4h (4hFN). pY14Cav1, pY1397FAK and pY118Paxillin are probed for in the same blot and hence share a GAPDH loading control represented with the pY14Cav1 blot. WTMEFs were pretreated for 12h with 10uM PF-228 (FAKi) or DMSO (CNT) and then subjected to methyl cellulose suspension followed by re-plating on FN, with FAK inhibitor in media at all steps of processing. Graphs represent densitometry analysis of Western blotting data, with ratios of band intensities of phosphorylated protein to respective total protein plotted as mean  $\pm$  SE from four independent experiments. Statistical analysis was done using unpaired two-tailed t-test.

## DISCUSSION

---

Loss of cell-ECM adhesion triggers a drastic change in the mechanical properties of cells, going from being a stretched adherent cell to a round non-adherent one. Also accompanying this process is the disruption of focal adhesions (Parsons *et al*, 2010; Sen & Kumar, 2009) and triggering of caveolar endocytosis of raft microdomains (del Pozo *et al*, 2005), both of which are dependent on Cav1 phosphorylation (del Pozo *et al*, 2005; Goetz *et al*, 2008a; Joshi *et al*, 2008). Studies evaluating the role of pY14Cav1 in cellular functions at caveolae and non-caveolar sites have relied on the use of phosphodeficient (Y14F) and phosphomimetic (Y14D) Cav1 mutants, which have then been extrapolated to the behavior of endogenous pY14Cav1 in cells. But overexpression of Cav1 is associated with saturation of caveolae and associated increase in non-caveolar caveolins, thus overthrowing their finely tuned regulation (Pol *et al*, 2020). We evaluate endogenous pY14Cav1 in this study, and confirm its presence in both caveolae and focal adhesions. We also show that re-adhesion of suspended fibroblasts regulates Cav1 phosphorylation, which is differentially regulated by FAK likely at FAs (Buwa *et al*, 2020a).

Caveolar endocytosis upon cell detachment is initiated as early as ~30 s (del Pozo *et al*, 2005), and stays active after 120 min in suspension (Fig. 1.1, 1.4). pY14Cav1 levels in isolated caveolae from actively endocytosing early suspended (20'SUSP) and late suspended cells (120'SUSP) are comparable to stable adherent cells (ADH) (Fig. 1.7). This ensures pY14Cav1 stays available in caveolae to support endocytosis in suspended cells. Internalized pY14Cav1 could additionally support intracellular signaling on caveolae. Tyr14 phosphorylated motif of Cav1 forms an SH2-binding domain capable of binding Src kinase, tumor necrosis factor- $\alpha$  receptor-associated factor 2 (TRAF2), Csk and SH2 domain-containing protein tyrosine phosphatase 2 (SHP-2) (Radel *et al*, 2007; Caselli *et al*, 2002; Jo *et al*, 2014). Interaction of some proteins with pY14Cav1, especially TRAF2 and Csk is primarily Cav1 phosphorylation-dependent (Cao *et al*, 2002). It is thus likely that upon caveolar endocytosis, caveolae-associated pY14Cav1 could act as a signaling platform on early endosomes to sequester or recruit downstream signaling players. A proteomic screen of Cav1-binding proteins in caveolae isolated from adherent *vs* suspended cells identifying differentially recruited players, could help reveal such a regulatory mechanism. It would also help uncover the basic components and regulators of the machinery necessary to regulate internalization of caveolae.

The observed adhesion-dependent change in total cellular pY14Cav1 levels (Fig. 1.2, 1.3) in fibroblasts could hence come from a non-caveolar, likely focal adhesion pool. Studying

pY14Cav1 localization by immunostaining is limited by the known cross-reactivity of the pY14Cav1 antibody with phosphorylated Paxillin (Hill *et al*, 2007). Furthermore, Cav1 overexpression and fluorescent tagging has been reported to affect its localization and function in cells (Han *et al*, 2015; Hanson *et al*, 2013; Parton & Howes, 2010; Pol *et al*, 2020; Payne-Tobin Jost & Waters, 2019). Thus biochemical studies for isolation of focal adhesions followed by Western blotting detection allow us to confirm the presence of endogenous pY14Cav1 in FAs (Fig. 1.9) (Buwa *et al*, 2020a). The role of pY14Cav1 at FAs could include their stabilization during migration, (Meng *et al*, 2017) promoting signaling and turnover of focal adhesions (Joshi *et al*, 2008; Goetz *et al*, 2008a; Grande-García *et al*, 2007).

FAK could regulate Cav1 phosphorylation (Park *et al*, 2011; Yeh *et al*, 2017; Konkel *et al*, 2013), and PF-228 mediated inhibition of FAK in FN re-adherent cells confirms the same (Fig. 1.10). Indeed when re-adhesion mediated recovery of pY397FAK (essential for FA formation) is blocked using PF-228, pY14Cav1 levels also fail to recover (Fig. 1.10). On loss of adhesion, the drop in FAK activation is not affected further by PF228 treatment (Fig. 1.10A, 120'SUSP) and hence does not affect pY14Cav1 levels (Fig. 1.10B). On the other hand, pY397FAK inhibition completely abrogates early (15'FN) adhesion-mediated recovery of pY14Cav1 levels. PF228 treatment in re-adherent cells (15'FN) blocks the recovery of ~65% of pY14Cav1 by inhibiting ~65% of active FAK. This lack of a complete inhibition of FAK by PF228 could in part be responsible for the partial inhibition of pY14Cav1 on re-adhesion.

In cells adherent for 4h, PF-228 treatment inhibits ~48% of FAK activation, causing an equivalent ~44% inhibition of pY14Cav1 in these cells. This suggests a strong correlation between extent of FAK inhibition and inhibition of pY14Cav1 levels at early and late adhesion time points. Interestingly, FAK-mediated regulation of pY118Paxillin occurs at early adhesion, but not at late adhesion time points (Fig. 1.10C). This suggests FAK-mediated regulation of Paxillin and Cav1 in focal adhesions to likely be different (Buwa *et al*, 2020a). Indeed, Paxillin is known to be phosphorylated by other kinases like Src and JNK, in addition to FAK (López-Colomé *et al*, 2017). It also has multiple known phosphorylation sites (Tyr31, Ser273), which could regulate its tyrosine phosphorylation and activation (López-Colomé *et al*, 2017). FAK and Paxillin are both additionally thought to be part of different functional modules that separately regulate integrin-mediated cellular responsiveness (Stutchbury *et al*, 2017).

Integrin-mediated adhesion induces FAK Tyr397 autophosphorylation and activation of (Mitra & Schlaepfer, 2006; Huvneers & Danen, 2009), allowing for the binding of SH2 domain containing proteins like Src and Csk (Mitra & Schlaepfer, 2006; Li *et al*, 2002). This FAK-

mediated recruitment of Src could drive early re-adhesion mediated Cav1 phosphorylation. pY14Cav1 further binds and could recruit more Src to FA (Gottlieb-Abraham *et al*, 2013) which can phosphorylate FAK to regulate FA signaling (Westhoff *et al*, 2004). pY14Cav1 mediated recruitment of Csk at FAs in response to mechanical stress (Radel & Rizzo, 2005; Radel *et al*, 2007; Yang *et al*, 2011) could further regulate Src activity. Such a FAK-Src-pY14Cav1 crosstalk could in turn regulate pY14Cav1-dependent FA dynamics and turnover (Joshi *et al*, 2008). FA-associated pY14Cav1 could thus be the major pool affected by FAK, but it remains to be determined if *caveolar* pY14Cav1 could also be regulated by FAK activation. pY14Cav1 remains dependent on the status of FAK activation at late adhesion time points (4h) (Fig. 1.10) reflecting a sustained FAK-pY14Cav1 crosstalk, which in turn could regulate FA-dependent processes in these cells. Tyr14 phosphorylation of Cav1 is also an important regulator of actomyosin contractility. Indeed, pY14Cav1-mediated regulation of focal adhesion dynamics is known to affect the polarization and migration of cells through Rho GTPase activation (Grande-García *et al*, 2007). The Src-p190RhoGAP (Grande-García *et al*, 2007) and Rho/ROCK dependent (Joshi *et al*, 2008) control of FA dynamics is regulated by Cav1 Tyr14 phosphorylation and drives cancer cell migration and invasion.

Our studies identify the presence of endogenous pY14Cav1 in caveolae as well as focal adhesions and suggest cell-matrix adhesion to differentially regulate pY14Cav1 at these distinct sites (Buwa *et al*, 2020a). These studies done in mouse fibroblasts also suggest pY14Cav1 present at these distinct locations could regulate caveolae and FA function simultaneously in these cells. Caveolae disassembly leads to release of caveolins into the bulk PM, and caveolar endocytosis leads to removal of caveolins to intracellular sites like endosomes. Caveolar endocytosis is regulated by cell-matrix adhesion, and adhesion also activates FA dependent signaling in cells. It is hence possible that there exists a dynamics between the caveolar and non-caveolar (FA) pools of pY14Cav1, which is likely dependent on the stimuli that cells are experiencing. Understanding the nature of this crosstalk and the impact these pools of pY14Cav1 have on each other remains an important question to be addressed. Taken together, the regulatory crosstalk between FAK and pY14Cav1 downstream of adhesion could also contribute to how cells respond to mechanical cues and impact diverse cellular outcomes. The differential regulation of this crosstalk on changing mechanical stimuli could further help fine tune mechano-signaling pathways downstream of focal adhesions to regulate cellular function.

## **CHAPTER 2:**

### **Cav1 phosphorylation: Matrix stiffness-dependent regulation in 3D and 2D microenvironments**

## ABSTRACT

---

Cell matrix-adhesion regulates cellular responses to changing mechanical properties of the extracellular matrix, which are primarily sensed and communicated in cells by integrins. Tyr14 phosphorylation of Cav1 (pY14Cav1) is detected in both caveolae and focal adhesions. Our studies in mouse fibroblasts have shown cell-matrix adhesion to regulate endogenous pY14Cav1 levels at focal adhesions. Increasing matrix stiffness (on collagen-coated 2D polyacrylamide gels) promotes total pY14Cav1 levels in mouse fibroblasts, comparable to the known activation of FAK. PF-228 mediated inhibition of FAK, while comparable across increasing stiffness, affects Cav1 phosphorylation (pY14Cav1) more at higher than at lower stiffness. This differential regulation is not seen for Paxillin (pY118Paxillin). This suggests the FAK-Cav1 crosstalk to have a unique sensitivity to changing integrin-mediated mechano-signaling. Together, these findings highlight the presence of FAK-mediated regulation of pY14Cav1 downstream of integrins, that could be vital to the mechano-responsiveness of cells.

## INTRODUCTION

---

### *Mechanical forces in cells*

Cells in physiology experience a variety of mechanical forces including tensile stress caused by stretch and hypo-osmotic conditions, compressive and shear stresses, and cues exerted by the ECM like topography and stiffness (Le Roux *et al*, 2019; Janmey *et al*, 2020; Hoon *et al*, 2016; Northcott *et al*, 2018). Extracellular stresses bring about changes in PM tension, curvature or domain rearrangement (Le Roux *et al*, 2019; Thottacherry *et al*, 2018), *via* contractility of underlying actomyosin network (Heer & Martin, 2017) to regulate downstream signaling. The rapid responsiveness of the PM to mechanical stress is for the most part localised and energy-independent (Kosmalska *et al*, 2015). Mechanical stress-induced changes in PM also trigger cascades involving transmembrane proteins that can sense these changes and transduce them into biochemical responses (Le Roux *et al*, 2019). Mechanically-gated channels like Piezo (Ranade *et al*, 2015; Cox *et al*, 2016; Zhao *et al*, 2016), G-proteins (White & Frangos, 2007), phospholipase D2, mTORC2, actin assembly (Diz-Muñoz *et al*, 2016) and membrane curvature sensing proteins like BAR domain proteins (Vidal-Quadras *et al*, 2017; Sathe *et al*, 2018) are all involved in this responsiveness (Le Roux *et al*, 2019).

In physiology, a major mechanical force that cells experience comes from the ECM stiffness and is mediated by integrins, downstream FA signaling and YAP/TAZ mediated mechanotransduction (Humphrey *et al*, 2014; Keely, 2011; Panciera *et al*, 2020). Stiffness of the ECM is influenced by its composition, crosslinking and remodelling by cells, and regulates survival, proliferation and differentiation (Bonnans *et al*, 2014; Handorf *et al*, 2015; Humphrey *et al*, 2014). Integrin signaling and cell proliferation are promoted by increasing ECM stiffness, and deregulation of stiffness leads to several pathological conditions ranging from cardiovascular disease and fibrosis to cancer (Wells, 2008; Dufort *et al*, 2011; Northcott *et al*, 2018; Lampi & Reinhart-King, 2018). ECM stiffness not only accompanies but also precedes disease and drives its progression, and hence ECM stiffness as well as its cellular responses are emerging as potential therapeutic targets in various disease conditions (Lampi & Reinhart-King, 2018; Pickup *et al*, 2014; Panciera *et al*, 2020). Some of the major players in sensing and transducing matrix microenvironment stiffness are integrins and their regulation of FA dependent signaling, Rho GTPase activation and YAP/TAZ mediated mechanotransduction (Humphrey *et al*, 2014; Keely, 2011; Panciera *et al*, 2020).



### ***Mechanosensing through Caveolae, Cav1 and pY14Cav1***

Buffering of PM tension in response to mechanical stress could be mediated by the combined effect of endocytosis (Apodaca, 2002; Thottacherry *et al*, 2018), exocytosis (Gauthier *et al*, 2011), flattening and reforming of PM folds (Kosmalska *et al*, 2015) and caveolae (Sinha *et al*, 2011). The PM responds to mechanical forces from the extracellular microenvironment and intracellular actin cortex (Martino *et al*, 2018; Dufort *et al*, 2011) which regulate caveolar architecture, endocytosis and/or signaling (Golani *et al*, 2019; Torrino *et al*, 2018; Joshi *et al*, 2012). Caveolae are abundant in muscle, endothelial, fibroblast, and adipocytes cells, all of which are found in tissues exposed to significant mechanical stress. In muscle cells, EM studies show caveolae respond to mechanical stress and change their morphology (Gabella & Blundell, 1978; Dulhunty & Franzini-Armstrong, 1975; Prescott & Brightman, 1976). Caveolae flatten in response to mechanical stresses like shear stress, uniaxial stretch and osmotic swelling in a multitude of systems including endothelial cells, fibroblasts, skeletal muscle cells and the notochord of fish (Cheng *et al*, 2015; Lim *et al*, 2017; Lo *et al*, 2016; Sinha *et al*, 2011; Yeow *et al*, 2017; Gervásio *et al*, 2011). This addition of caveolar membrane into the bulk PM may be a first step to prevent lysis of cells, acting as a reservoir to buffer membrane tension.

Mechanical cues are seen to regulate pY14Cav1 levels to control caveolar density at the PM (Joshi *et al*, 2012; del Pozo *et al*, 2005) and cellular area (Yeh *et al*, 2017). While it is not known what fraction of Cav1 in caveolae is phosphorylated, studies using phosphodeficient (Y14F-Cav1) and WT-Cav1 show they both make comparable number of caveolae, suggesting pY14Cav1 to not be required for caveolae formation (del Pozo *et al*, 2005). Expression of phosphomimetic Y14D-Cav1 does increase the number of caveolae in certain cell types (Joshi *et al*, 2012; Zimnicka *et al*, 2016). Cav1 phosphorylation regulates transcription factor Egr1 to promote the expression of Cav1 and Cavin1 (Joshi *et al*, 2012). This positive feedback loop is thought to promote caveola biogenesis in response to cyclic stretch (Joshi *et al*, 2012). In bovine aortic endothelial cells chronic exposure to unidirectional laminar shear stress is seen to cause a ~45% increase in the total number of caveolae (Boyd *et al*, 2003). Along with the changes in pY14Cav1 levels its localization in and outside caveolae could also be vital to its role in the cellular response to mechanical cues (del Pozo *et al*, 2005; Zimnicka *et al*, 2016; Meng *et al*, 2017; Nah *et al*, 2017).

Loss of adhesion causes a rapid drop in PM tension (Thottacherry *et al*, 2018) and dissolution of FAs (Parsons *et al*, 2010; Sen & Kumar, 2009), which triggers pY14Cav1-dependent caveolar endocytosis of raft microdomains (del Pozo *et al*, 2005). This adhesion-dependent

regulation significantly decreases membrane order (Gaus *et al*, 2006) and downregulates anchorage-dependent signaling (del Pozo *et al*, 2005). On loss of adhesion a drop in net pY14Cav1 levels (Chapter 1 of this dissertation) which recovers on re-adhesion (Ortiz *et al*, 2016) could support this regulation. Cav1 phosphorylation is indispensable for loss of adhesion mediated endocytosis of raft microdomains and signaling (del Pozo *et al*, 2005). Mechanisms for pY14Cav1-mediated regulation of caveolar endocytosis have not been studied thoroughly. One proposed mechanism is the spatial distancing or separation of Cav1 molecules within the oligomeric caveolar coat due to charge repulsion (Zimmnicka *et al*, 2016). pY14Cav1 could also regulate caveolar endocytosis by its recruitment of membrane scission molecules like Dynamin2. pY14Cav1 also regulates Cdc42-dependent fluid phase endocytosis through the CLIC/GEEC pathway (Cheng *et al*, 2010; Chaudhary *et al*, 2014), which is upregulated in response to reduction in PM tension in a Vinculin- and GBF1-dependent manner (Thottacherry *et al*, 2018).

Relative contribution loss of adhesion mediated change in membrane tension and dissolution of FAs have in regulating pY14Cav1 function in and out of caveolae to regulate the response of cells remains to be fully understood. pY14Cav1 is known to increase the activation of Src kinase by creating an SH2 docking site and preventing Src inactivation by Csk (Cao *et al*, 2002). Activated Src activates Rac and Cdc42 (Yang *et al*, 2011) and inhibits Rho through activation of p190RhoGAP, in turn increasing RhoA activation (Grande-García *et al*, 2007). pY14Cav1 thus follows the Src-ROCK-p190RhoGAP-RhoA pathway in regulating Rho GTPase activation. Another study showed that phosphorylation of Cav1 happens in response to shear stress via Src family kinases (Radel & Rizzo, 2005). This leads to association of Csk at integrin sites, which in turn brings about phosphorylation of myosin light chain, and hence mechanotransduction by involvement of Rho GTPases (Radel *et al*, 2007; Yang *et al*, 2011). Cav1 scaffolding domain (CSD) contains a motif conserved in small GTPase guanine nucleotide dissociation inhibitors (GDIs) (Nevins & Thurmond, 2006). Indeed, Cav1 has been reported to act as a Cdc42 GDI, with Cav1 preferentially binding to GDP-Cdc42 over GTP-Cdc42 (Cheng *et al*, 2010). Another downstream effector of pY14Cav1 that could regulate a mechanotransduction response is VAV2, a GEF for Rho and Rac GTPases (Boettcher *et al*, 2010). Cav1 is recruited to the membrane and phosphorylated upon bacterial infection. This leads to increased interaction with VAV2, hence regulating actin cytoskeletal rearrangements mediated by change in activation of RhoA. These studies outline the crucial role of Tyr14 phosphorylation of Cav1 in regulation of Rho GTPase activation and actomyosin contractility.

Cav1 is known to have a differential role and localization in 3D trans-migration (during angiogenesis) compared to 2D planar migration (during wound healing) at non-caveolar vs caveolar sites (Parat *et al*, 2003). Cav1 is released from caveolae at the rear end of cells migrating in 3D to relocate at pseudopodia at the cell front, whereas caveolae polarize at the rear end of endothelial cells, fibroblasts and neurons during planar migration but not in cancer cells (Parat *et al*, 2003; Beardsley *et al*, 2005; Lentini *et al*, 2008; Urra *et al*, 2012). Moreover, pY14Cav1 is required for dissociation of Cav1 from caveolae and its re-localization in trans-migrating cells (Parat *et al*, 2003). It is hence very likely that pY14Cav1 plays distinct roles at distinct sub-cellular localizations depending on the microenvironment, which our studies aim to explore.

## MATERIALS AND METHODS

---

### Cell culture

Wild-type (WT) and Cav1-knockout (Cav1<sup>-/-</sup>) mouse embryonic fibroblasts (MEFs) (from Dr. Richard Anderson's lab, University of Texas Health Sciences Center, Dallas TX) were cultured in high glucose DMEM medium with 5% foetal bovine serum (FBS), penicillin and streptomycin (Invitrogen) (hereby referred to as complete DMEM). Cells were regularly checked for and found to be devoid of bacterial or mycoplasma contamination. Serum starvation of cells, where mentioned, was done for 14h using DMEM medium with 0.2% FBS, penicillin and streptomycin (low-serum DMEM). For transfections,  $1 \times 10^5$  cells were seeded in 1.5ml of DMEM in a 6-well plate. 3h post-seeding cells started to spread and were transfected with PEI (Sigma Cat. no. 408727) or Lipofectamine-LTX (Invitrogen Cat. no. 15228100). Transfection mixes containing 2 $\mu$ g plasmid (per well) were made in 450 $\mu$ l of Opti-MEM (Gibco Cat. no. 22600050) with 6 $\mu$ l of 1mg/ml PEI (for PEI transfections) or 2 $\mu$ l Plus reagent and 5 $\mu$ l LTX reagent (for LTX transfections). Transfection mixes were incubated for 30 min at room temperature before addition to cells. Cells were incubated with transfection mixes for ~14h before changing media to complete DMEM. 48h post transfections, cells were used for subsequent experiments.

### Antibodies and Reagents

Primary antibodies used for Western blotting were diluted in 5% BSA made in TBST at following dilutions: Cav1 (Santa Cruz Biotech SC-894) at a dilution of 1:2000, pY14Cav1 (BD 611338) at 1:500, FAK (Cell Signaling Technology (CST) 3285) at 1:1000, pY397FAK (CST 3283) at 1:1000, Cavin1 (BD 611258) at 1:500, Flotillin (BD 610820) at 1:1000, pY118Paxillin (BD 611725) and Paxillin (BD 610052) at 1:2000, GM130 (BD 610822) at 1:500, RhoGDI (Millipore 06-730) at 1:2000, Actin (DSHB JLA20) at 1:2000 and  $\beta$ -tubulin (DSHB Clone E7) at 1:2000. HRP-conjugated secondary antibodies (anti-rabbit and anti-mouse) were purchased from Jackson Immuno Research Laboratories and used at a dilution of 1:10000. Methylcellulose for suspension assay was purchased from Sigma (Cat. no. M0262). Fibronectin (FN) was purchased from Sigma (Cat. no. F2006). FAK inhibitor PF-228 (Slack-Davis *et al*, 2007) was purchased from Sigma (Cat. no. PZ0117). Protease inhibitor cocktail PIC was purchased from Roche (04693132001), and phenylmethanesulfonyl fluoride (PMSF), sodium orthovanadate and sodium fluoride from Sigma. BCA assay kit used for protein estimation was purchased from Thermo Fisher (Cat. no. 23225). RIPA buffer composition:

50mM Tris-HCl at pH 8.0 + 150mM NaCl + 1.0% NP-40 + 0.5% sodium deoxycholate + 0.1% SDS. Tris was purchased from HiMedia (Cat. no. MB029), Glycine from Fisher Scientific (Cat. no. 56406), Sodium bicarbonate from Sigma (Cat. no. S6297), Methanol from Fisher Scientific (Cat. no. 67561), PVDF membranes from Millipore (Cat. no. IPVH00010) and BSA from Sigma (Cat. no. A2153). Chemiluminescent reagents for Western blotting Immobilon Western Chemiluminescent HRP Substrate was purchased from Millipore (Cat. no. WBKLS0500), SuperSignal West Femto Maximum Sensitivity Substrate from ThermoFisher (Cat. no. 34096).

*Reagents for making 2D polyacrylamide gels of varying stiffness:* Acrylamide (HiMedia Cat. no. MB068), bis-acrylamide (HiMedia Cat. no. MB005), APS, TEMED (Sigma Cat. no. T9281), MES buffer (Sigma Cat. no. M8250), NHS (Sigma Cat. no. 130672), EDC (Sigma Cat. no. E1769), Toluene (Qualigen Cat. no. 32507), Silane (Sigma Cat. no. 440159), Phalloidin conjugated to Alexa Fluor 488 (Invitrogen, Cat. no. A12379) at a dilution of 1:400, Phalloidin conjugated to Alexa Fluor 594 (Invitrogen, Cat. no. A12381) at a dilution of 1:100, DAPI (Invitrogen Cat. no. D1306) and Fluoromount-G (Southern Biotech Cat. no. 0100-01). Collagen was purchased from Gibco (Collagen I, Rat Tail Cat. no. A1048301) and used at a concentration of 25µg/ml in 1X PBS for coating PA gels.

*Reagents for 3D collagen gels:* Collagen Type-1, Rat tail (Corning - Cat no. 354236) 10X PBS (Gibco - 70011044), Collagenase P (Roche - 11213865001), HBSS (Gibco – 14025076), LabTek chambers (Thermo Scientific - 155409), Fluorescently conjugated CTxB-488 (Cat. No. C34775), CTxB-594 (Cat. No. C22842) were procured from Molecular Probes, Invitrogen.

## **2D polyacrylamide gels of varying stiffness**

40% acrylamide and 2% bis-acrylamide and MES buffer solutions were made in autoclaved milli-Q water and filter-sterilized. Acrylamide solutions for respective stiffness gels were made by varying the proportion of acrylamide and bis-acrylamide, as described below in Table 2.

**Table 2:**

<b>Gel stiffness</b>	<b>40% Acrylamide (ml)</b>	<b>2% Bis-acrylamide (ml)</b>	<b>Water (ml)</b>	<b>% Acrylamide in final gel</b>	<b>% Bis-acrylamide in final gel</b>
0.5kPa	0.75	0.3	8.95	3%	0.06%
2.5kPa	1.0	0.75	8.25	4%	0.15%
23kPa	2.5	1.125	6.375	10%	0.225%

### ***Preparation of glass slides and coverslips***

Glass slides were cut into 2.5x2.5 cm squares and coated with a drop of nail paint (that forms a hydrophobic layer) using a spin coater for homogenous distribution. The slides were allowed to air-dry and then treated to a UV cycle for 25 min in the tissue culture hood before use. 12mM round glass coverslips were activated using a Toluene-Silane activating solution in a 9:1 ratio. Activation was done at room temperature for 30 min on a rotary shaker. Coverslips were air-dried before use.

### ***Preparation of polyacrylamide gels***

To the polyacrylamide (PA) gel solution made as described above (Table 1), APS and TEMED were added in a 1:1000 ratio. For each gel, 45 $\mu$ l of each solution was placed as a drop on the nail paint-coated glass slide and an activated, dried coverslip was placed on top. Gels were allowed to polymerize for 20 min, after which they stay attached to coverslip, which was then transferred to a well of a 24-well plate. Gels were washed with 1X PBS before being treated each with 50 $\mu$ l of 0.1M NHS and 0.2M EDC in 0.1M MES buffer for 20 min in the dark. Gels were washed again with 500 $\mu$ l of 1X PBS and coated with 25 $\mu$ g/ml of collagen solution, diluted in 1X PBS, overnight at 4°C. After collagen coating, gels were washed with 500 $\mu$ l of 1X PBS, given 3 UV cycles and 30 min of antibiotic treatment (Pen-Strep diluted 1X in PBS). Gels were washed with 500 $\mu$ l of 1X PBS and equilibrated in 500 $\mu$ l of media for at least 30 min before seeding of cells.

### ***Plating cells on PA gels***

3x10<sup>4</sup> and 7.5x10<sup>4</sup> WTMEFs were seeded on gels for cell spreading and Western blotting experiments respectively. Cells were allowed to attach and grow for 24h and processed thereafter. For cell spreading experiments, cells were fixed with 3.5% paraformaldehyde and then stained with phalloidin diluted in 1X PBS, in a humid chamber at 4°C overnight. Samples were also stained with DAPI for 2 min at room temperature, and then washed twice with 1X PBS before mounting on glass slides using fluoromount. For Western blotting, cells on each coverslip were lysed in 80 $\mu$ l of RIPA buffer containing protease and phosphatase inhibitors on ice. Samples were collected, protein estimated using BCA assay and 30 $\mu$ g total protein used for Western blotting.

### ***FAK inhibitor treatment in cells plated on PA gels***

WTMEFs were seeded on gels as described and allowed to spread for 8h with complete DMEM. 8h post-seeding on gels, cells in each well were treated with 10 $\mu$ M FAK inhibitor (PF-228) or DMSO-containing media for 24h. Cells were lysed in RIPA at the end of 24h to be processed for Western blotting as described above.

### ***Embedding cells in 3D collagen gels***

Cells were embedded 48h post-transfection in 1.0 or 1.5mg/ml collagen type-1 as follows. A mixture of 10X PBS, sterile milli-Q water and collagen (to make final concentration to 1.0 or 1.5mg/ml) was made in a total volume of 400 $\mu$ l. This amount will vary according to stock bottle concentration. This mixture was kept on ice for 5 min. Cells were detached with trypsin, spun at 1000 rpm for 5 min at 4°C and the pellet was resuspended in 1X PBS.

4X10<sup>4</sup> cells for imaging or 12X10<sup>4</sup> cells for gel extraction were added to the collagen gel solution in a volume of 100 $\mu$ l, mixed, and 1N NaOH was added at a final concentration of 0.006N in the gel. The final volume of this solution is 400 $\mu$ l. After thorough mixing by gentle pipetting, the solution was added to a well of a LabTek chamber (imaging) or 24-well plate (gel extraction). The gels were incubated at 37°C and 5% CO<sub>2</sub> in the incubator for 30 min until gels visibly polymerised. After ensuring complete polymerisation, 400 $\mu$ l of complete DMEM was gently added on top and the cells were re-incubated for 12h (imaging) or 3h (gel extraction).

### ***Coating coverslips with collagen***

Coverslips (VWR) were cleaned with glass cleaning solution (25g KOH in 500ml methanol), thoroughly washed with MilliQ water and stored in 100% ethanol. Before use, coverslips were flame-dried and subjected to UV sterilization for 30 min. Each well of a 24-well plate was coated with 400 $\mu$ l of 100 $\mu$ g/ml collagen solution, diluted in 1X PBS, overnight at 4°C. After aspirating collagen solution, the coverslips were washed with 1X PBS before plating cells.

### ***Extraction of cells from 3D collagen gels using collagenase***

After 3h of embedding, cells were extracted using collagenase as follows. Media was removed from the wells and gels were washed twice with 400 $\mu$ l of 1X PBS for 2 min each. 4mg/ml collagenase solution was diluted in HBSS in the dark and stored on ice. 400 $\mu$ l of this collagenase solution was added to each gel and 24-well plate was kept in a 37°C incubator at 75 rpm for ~10-12 min till the gels dissolved. Once dissolved, 800 $\mu$ l of cold media was added

to each solution, collected in a tube and spun at 2000 rpm, 4°C for 10 min. The cell pellets were lysed in 30µl of 1X Laemmli's buffer for further processing by Western blotting.

### ***Labelling cells in 3D collagen***

WTMEFs were embedded in collagen gels of appropriate concentrations as described. After complete gel polymerization, labelling with CTxB was carried out on ice. CTxB at a dilution of 1:2000 in DMEM was added to gels, with incubation on ice for 20 min. After 20 min fresh DMEM was added and cells were further incubated for 3h at 37°C. Fixation of gels was done using 4% PFA at RT for 20 min, followed by three washes with 1X PBS (incubate gel with PBS for 5 min), before imaging.

### **Western Blotting**

Samples for Western blotting were mixed with Laemmli's buffer before resolving by SDS-PAGE. 12.5% polyacrylamide gels were prepared and run using Tris-glycine running buffer containing 0.1% SDS in Bio-Rad mini apparatus. Resolved proteins were transferred onto PVDF membrane with sodium bicarbonate or Tris-glycine-methanol running buffer. All blotted membranes were blocked with 5% non-fat milk in TBS + 0.1% Tween-20 (TBST) at RT for 60 minutes with gentle rocking. Blocked blots were incubated overnight at 4°C with primary antibodies at indicated dilutions made in 5% BSA in TBST. After primary antibody incubation, blots were washed thrice with TBST on a rotary shaker for 10 min each. Blots were incubated at RT for 60 min with secondary antibodies at indicated dilutions made in 2.5% BSA in TBST. Blots were washed again thrice with TBST on a rotary shaker for 10 min each. Blots were developed on ImageQuant LAS-4000 (Fujifilm Life Sciences) with chemiluminescent substrate. Densitometry analyses of Western blotting data were done using ImageJ software.

### **Microscopy imaging**

#### ***EVOS imaging (2D gels)***

Following settings were used for all images captured. Images were acquired using a 40X oil immersion objective on EVOS FL Auto Imaging system (ThermoFisher AMAFD1000). For each gel stiffness at least 80-100 cells were imaged per biological replicate. Cell spread area analysis was performed using ImageJ software (NIH).

#### ***Confocal imaging (3D gels)***

Images were acquired using a 63X oil immersion objective on Zeiss LSM 780 multiphoton confocal microscope, NA 1.4. For Z-stacks, the step size was kept at 0.8µm. Z-stacks were



reconstructed using Huygens software and object analyzer module was used to calculate volume and surface area.

### **Statistical analysis**

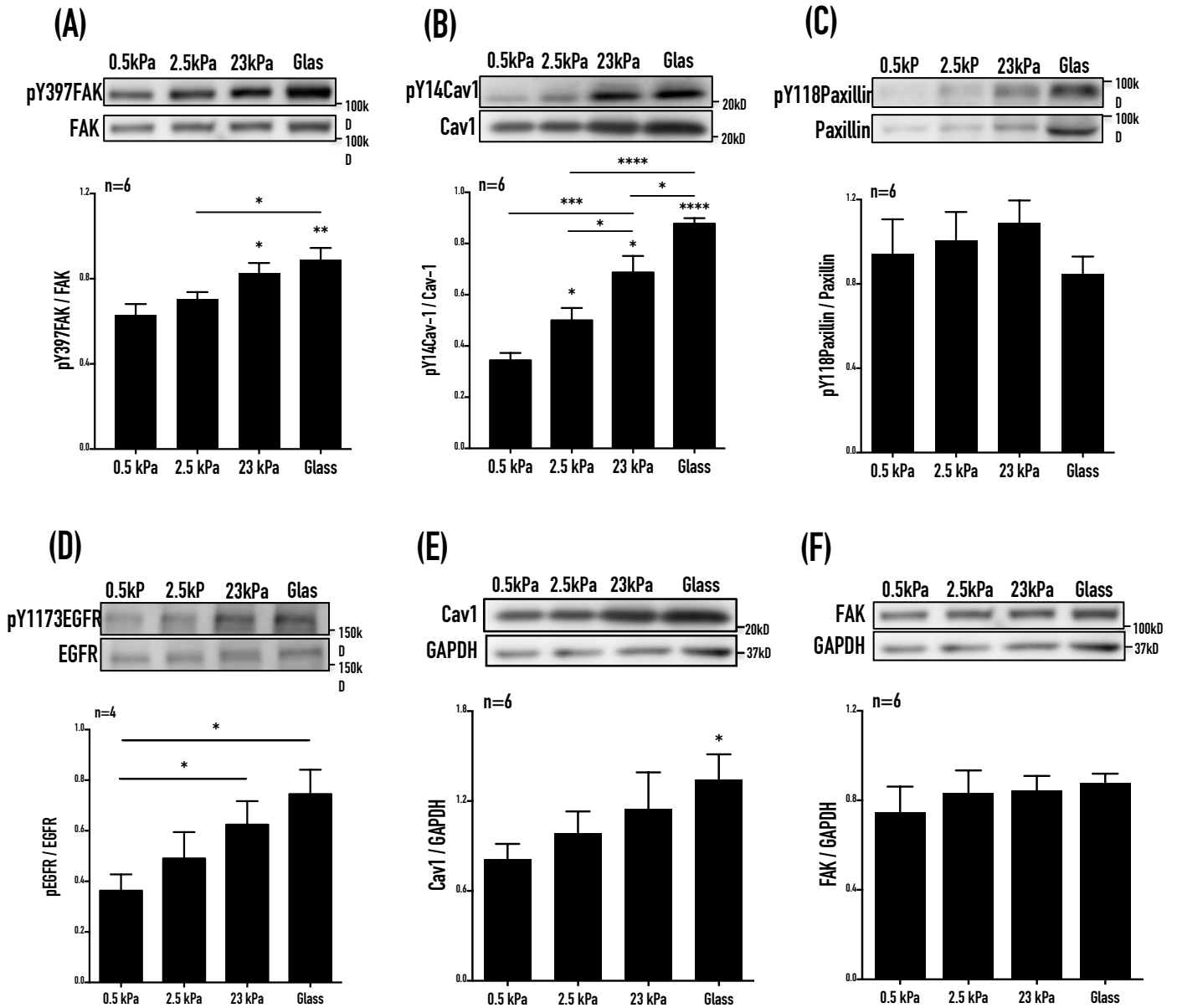
Statistical analysis of data was done using unpaired two-tailed t-test. All analyses were done using Prism Graphpad analysis software. Statistical significance was considered at  $p < 0.05$ .

## RESULTS

---

### *Cav1 phosphorylation is regulated by matrix stiffness*

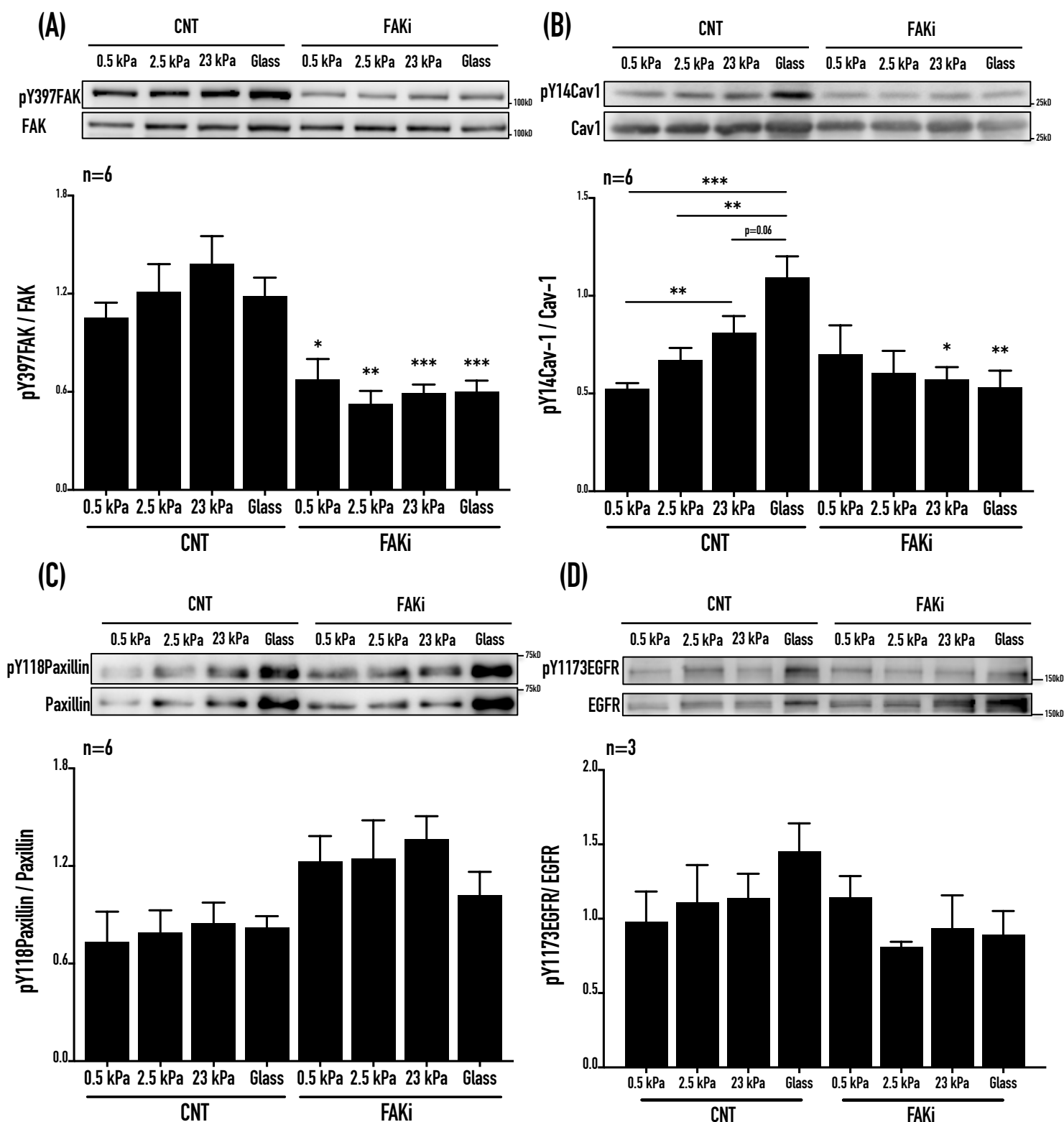
Focal adhesions formed in response to integrin-ECM engagement are among the early responders to changing ECM stiffness (Schwartz, 2010; Levental *et al*, 2009; Friedland *et al*, 2009; Gehler *et al*, 2009). Matrix stiffness regulates both FA number and FA size, with cells on soft matrices having less and smaller FAs compared to stiff matrices (Riveline *et al*, 2001; Schiller & Fässler, 2013; Yeh *et al*, 2017). In comparison to suspended *vs* re-adherent cells (Fig. 1.2), cells adherent on collagen-coated 2D polyacrylamide (PA) gels of varying stiffness allow for more subtle changes in cell-matrix adhesion and signaling. Fibroblasts adherent on increasing matrix stiffness for 24h show a steady increase in FAK activation (pY397FAK normalized to total FAK) (Fig. 2.1A). pY397FAK levels increase by 10% from 0.5kPa to 2.5kPa; ~14% increase from 2.5kPa to 23kPa; and an eventually ~7% increase on Glass. The overall increase in FAK activation (pY397FAK) between the lowest (0.5kPa) and highest stiffness (Glass) is ~28%. pY14Cav1 normalized to total Cav1 levels shows a more pronounced increase in cells across increasing stiffness (Fig. 2.1B). pY14Cav1 levels increase by ~30% from 0.5kPa to 2.5kPa; ~25% increase from 2.5kPa to 23kPa; and ~22% increase at Glass. The overall increase between lowest (0.5kPa) and highest stiffness (Glass) is ~61%, and more pronounced than seen for pY397FAK. Phosphorylation of Paxillin (pY118Paxillin normalized to total Paxillin) is however not seen to be regulated by changing matrix stiffness (Fig. 2.1C), as has been reported earlier (Stutchbury *et al*, 2017). EGFR activation known to be regulated by increasing matrix stiffness is confirmed by its increasing phosphorylation at Tyr1173 (pY1173EGFR) (Fig. 2.1D). Total Cav1 levels normalized to GAPDH show an increase with increasing matrix stiffness (Fig. 2.1E), as reported earlier (Yeh *et al*, 2017). Total FAK levels normalized to GAPDH show no such differences across matrices of varying stiffness (Fig. 2.1F) as is also reported (Wang *et al*, 2019b; Wei *et al*, 2008; Schlunck *et al*, 2008). Cav1 phosphorylation is thus regulated by increasing matrix stiffness on collagen-coated 2D polyacrylamide gels (Buwa *et al*, 2020a).



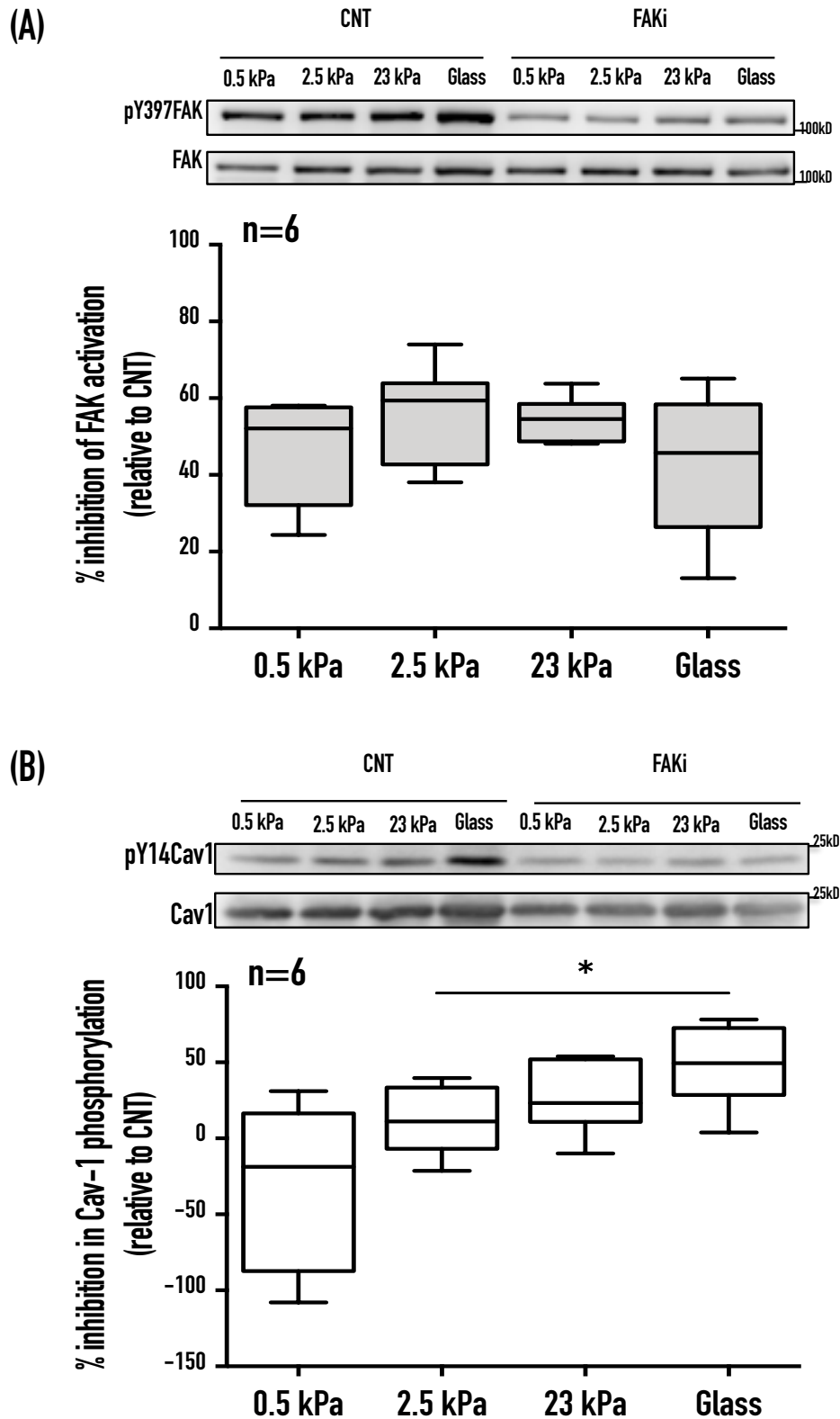
**Figure 2.1. Cav1 phosphorylation is regulated by matrix stiffness on collagen-coated 2D gels.** (A) Western blot analysis of phosphorylated and total FAK (A), Cav1 (B), Paxillin (C) and EGFR (D) in WTMEFs adherent on polyacrylamide gels of varying stiffness for 24h. Graphs represent ratios of band intensities of phosphorylated protein to respective total protein plotted as mean  $\pm$  SE from at least four independent experiments. Western blot analysis of total FAK (E), Cav1 (F) in WTMEFs adherent on polyacrylamide gels of varying stiffness for 24h. Graph represents mean  $\pm$  SE ratio of band intensity of total FAK or total Cav1 to respective GAPDH from 6 independent experiments.

### ***Matrix-stiffness dependent regulation of Cav1 phosphorylation is FAK-dependent***

Knowing that cell-matrix adhesion regulates Cav1 phosphorylation downstream of FAK (Buwa *et al*, 2020a), we tested the FAK-Cav1 crosstalk across changing matrix stiffness by inhibiting FAK activation with PF-228. Since cells are treated after they have spread on these gels, PF-228 treatment does not affect cell morphology (data not shown). PF-228 inhibits more than 50% of FAK activation across all stiffness (Fig. 2.3A). Cav1 phosphorylation on the other hand is inhibited differentially across matrix stiffness. pY14Cav1 levels remain largely unaffected by FAK inhibition at 0.5kPa (relative to DMSO CNT), drop by ~10% at 2.5kPa and drop significantly by ~28% at 23kPa and ~40% on Glass, relative to their respective DMSO CNT (Fig. 2.2B). Plotting the percentage inhibition (Fig. 2.3) of FAK and Cav1 phosphorylation gives us an idea of the relative impact of changing matrix stiffness in regulating the same. FAK inhibition is comparable across increasing stiffness (Fig. 2.3A). PF-228-mediated inhibition of pY14Cav1 gradually increases across increasing stiffness, being most prominent on glass, significantly better than 2.5kPa (Fig. 2.3B). Paxillin phosphorylation is not affected by FAK inhibition, indeed increasing slightly (Fig. 2.2C), while EGFR activation is inhibited comparably across all stiffnesses (Fig. 2.2D). These results suggest FAK-mediated regulation of pY14Cav1 to be distinctly different from that of Paxillin (as seen in early *vs.* late adherent cells, Fig. 1.10) (Buwa *et al*, 2020a). FAK-mediated regulation of pY14Cav1 being matrix stiffness dependent could affect FA assembly and turnover. This could further impact their roles in FA-dependent sensing and transducing of mechanical cues.



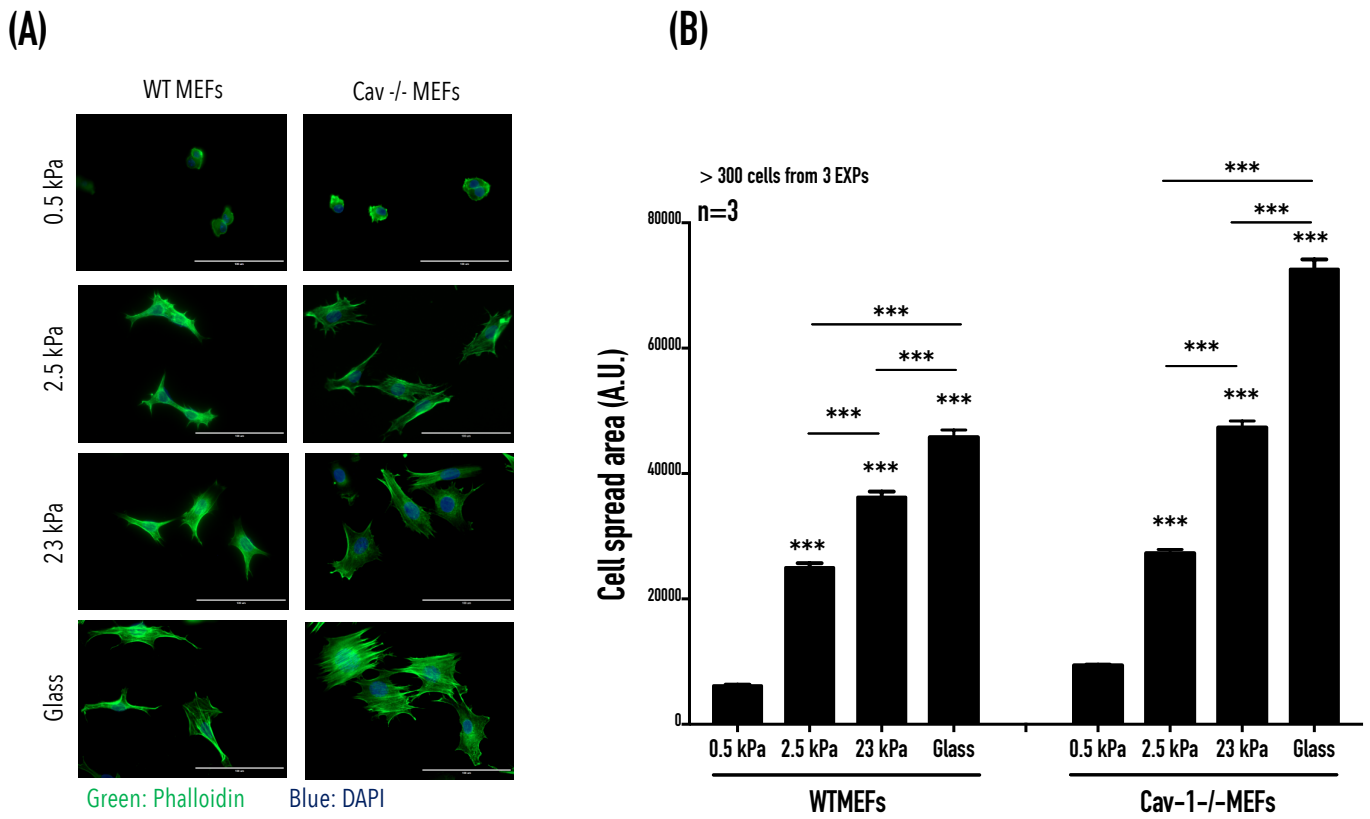
**Figure 2.2. Cav1 phosphorylation is regulated by FAK activation in a matrix stiffness-dependent manner.** (A) Western blot analysis of phosphorylated and total FAK (A), Cav1 (B), Paxillin (C) and EGFR (D) in WTMEFs adherent on polyacrylamide gels of varying stiffness for 24h. WTMEFs were allowed to spread on polyacrylamide gels of varying stiffness for 8h, after which cells were treated with 10mM PF-228 (FAKi) or DMSO (CNT) for 24h and processed for Western blotting as described. Statistical analysis was done using unpaired two-tailed t-test. Graphs represent ratios of band intensities of phosphorylated protein to respective total protein plotted as mean  $\pm$  SE from at least four independent experiments.



**Figure 2.3. Matrix stiffness-dependent regulation of Cav1 phosphorylation by FAK on 2D gels - percent inhibition.** Ratios of phosphorylated to total FAK and Cav1 in FAKi cells from Western blotting data in Fig. 2.2 were normalized to those in CNT cells for each stiffness, and data from six independent experiments represented in graphs as percentage inhibition upon FAK inhibition.

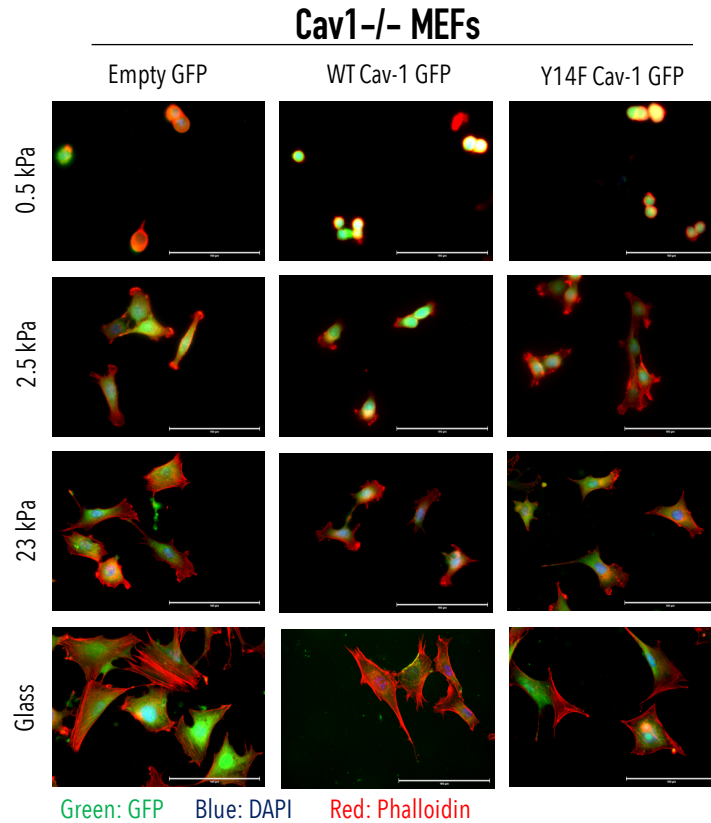
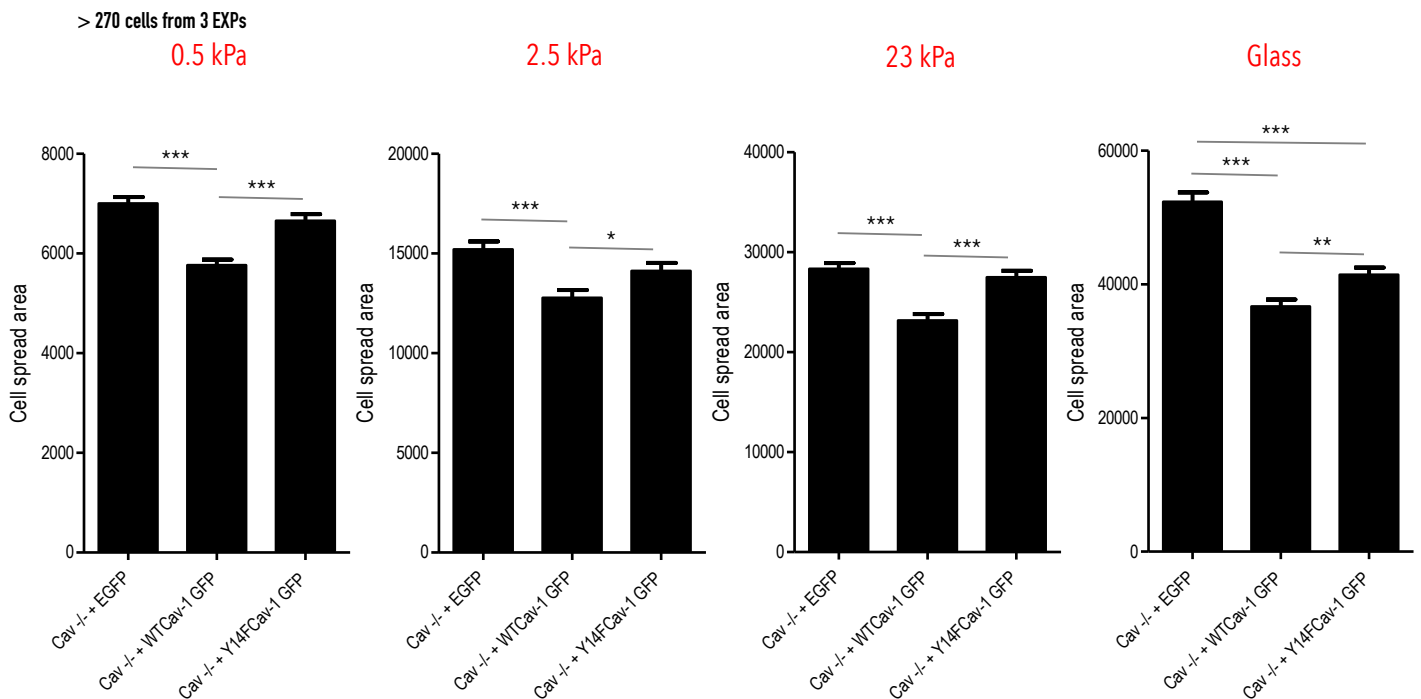
### ***Cav1 phosphorylation regulates differential spreading of WTMEFs on 2D gels of varying stiffness***

Fibroblasts plated on collagen-coated polyacrylamide gels of increasing matrix stiffness expectedly show a steady increase in cell spread area (Fig. 2.4). Cell spread area of WTMEFs shows ~300% increase from 0.5kPa to 2.5kPa gels, ~45% increase from 2.5kPa gels to 23kPa gels and ~25% increase from 23kPa gels to Glass (gPa). Cav1 phosphorylation has a potential role in mediating cell polarisation (Grande-García *et al*, 2007), and could mediate spreading dependent on matrix stiffness. To test whether this is regulated by pY14Cav1, we transiently transfected Cav1<sup>-/-</sup>-MEFs with phosphorylatable WT-Cav1 GFP and phospho-deficient Y14F-Cav1 GFP, and seeded these cells on 2D polyacrylamide gels of varying stiffnesses. Cav1<sup>-/-</sup>-MEFs also show an increase in cell spread area with increasing substrate stiffness, similar to WTMEFs. However the overall area of Cav1<sup>-/-</sup>-MEFs is significantly higher than that of WTMEFs at all stiffnesses (Fig. 2.4B). Cav1<sup>-/-</sup>-MEFs reconstituted with WT-Cav1 GFP show overall decreased cell spread area than Cav1<sup>-/-</sup>-MEFs (Fig. 2.5). Difference in cell spread area between Cav1<sup>-/-</sup>-MEFs vs WT-Cav1 expressing cells is ~18% on 0.5kPa, ~15% on 2.5kPa, ~18% on 23kPa, and ~29% on Glass. This difference, though seen across all stiffness, is most prominent at the highest stiffness (Glass). Expression of Y14F-Cav1 GFP does not affect cell spread area of Cav1<sup>-/-</sup>-MEFs across stiffnesses (Fig. 2.5). This suggests Cav1 phosphorylation does play a role in regulation of cell spreading in fibroblasts adherent on matrices of increasing stiffness.



**Figure 2.4. Differential spreading of WTMEFs and Cav1<sup>-/-</sup>MEFs on 2D PA gels of varying stiffness.** (A) Fluorescent microscopy images of WTMEFs and Cav1<sup>-/-</sup>MEFs on 2D gels of varying stiffness, as indicated. Cells were stained with DAPI (blue) and phalloidin (green). (B) Bar graph represents mean  $\pm$  SE of cell spread area calculated using ImageJ (NIH), from at least 15 different frames each from three independent experiments. Statistical analysis of the data was done using unpaired two-tailed t-test.



**(A)****(B)**

**Figure 2.5. Role of Cav1 phosphorylation in regulating cell spreading on 2D PA gels of varying stiffness.** (A) Fluorescent microscopy images of Cav1<sup>-/-</sup> MEFs expressing EGFP, WT-Cav1-GFP and Y14F-Cav1-GFP on 2D gels of varying stiffness, as indicated. Cells were stained with DAPI (blue) and phalloidin (red). (B) Bar graphs represent mean  $\pm$  SE of cell spread area calculated using ImageJ (NIH), from at least 15 different frames each from three independent experiments. Statistical analysis of the data was done using unpaired two-tailed t-test.

### ***Regulation and Role of Cav1 phosphorylation in 3D collagen gels***

pY14Cav1 has been implicated in regulation of cellular morphology in 3D collagen gels as well (Goetz *et al*, 2011). 3D collagen gels represent a scenario closer to the *in vivo* microenvironment of cells. Moreover, fibroblasts and collagen are abundantly found in connective tissue and stroma, and collagen has been widely used to study fibroblast functions (Tang, 2020). We find morphology of fibroblasts embedded in collagen gels to also be dependent on pY14Cav1 (Fig. 2.6). WTMEFs and Cav1<sup>-/-</sup>-MEFs reconstituted with WT-Cav1 GFP and Y14F-Cav1 GFP were embedded in 1.5mg/ml collagen gels for 12h before imaging. Surface area and volume measurements in these cells do not show any significant differences (Fig. 2.6). Aspect ratio (ratio of longest axis to the shortest axis) was seen to be significantly pronounced in WTMEFs relative to Cav1<sup>-/-</sup>-MEFs. WTMEFs appear elongated and display more protrusions, compared to Cav1<sup>-/-</sup>-MEFs that appear round with almost no protrusions. Interestingly, both protrusivity and aspect ratio seem to recover in Cav1<sup>-/-</sup>-MEFs expressing phosphorylatable WT-Cav1, but not the phospho-deficient Y14F variant (Fig. 2.6). This suggests Cav1 phosphorylation to be required to rescue the phenotype of Cav1<sup>-/-</sup>-MEFs in 3D collagen gels.

Given that cellular morphology in 3D is dependent on Cav1 phosphorylation, it was interesting to ask if other pY14Cav1-dependent processes are similarly regulated, and more importantly whether they are differentially regulated in gels of varying stiffness. Earlier studies in the lab show that GM1 endocytosis is differentially regulated in WTMEFs embedded in 3D collagen gels of two different stiffnesses, *viz.*, 1.0mg/ml and 1.5mg/ml (Unpublished data: Trupti Thite and Nagaraj Balasubramanian), which was corroborated (Fig. 2.7A). GM1 endocytosis (marked by fluorescent CTxB) is seen to happen at 1.0mg/ml, but at 1.5mg/ml there is no endocytosis (Fig. 2.7A). Interestingly, Cav1<sup>-/-</sup>-MEFs in 3D show GM1 endocytosis at both 1.0mg/ml and 1.5mg/ml, signifying that GM1 is *not* endocytosed through caveolae in cells in 3D microenvironments (Unpublished data: Trupti Thite and Nagaraj Balasubramanian). Indeed, GM1 is known to be endocytosed *via* caveolae-independent, Cdc42-mediated fluid phase endocytosis (Thottacherry *et al*, 2018), which could be the pathway used for endocytosis of GM1 in 3D, and remains to be tested.

3D collagen gels of 1.0 and 1.5mg/ml do however offer an interesting window where Cav1-containing cells are able to sense the change in mechanical properties of the collagen matrix (stiffness, pore size, extent of polymerisation) and accordingly differentially regulate endocytosis. Stiffness and crosslinking of 3D collagen gels of 1.5mg/ml is significantly higher

than a 1.0mg/ml gel (Miron-Mendoza *et al*, 2010; Carey *et al*, 2017). Given that pY14Cav1 is a mechanotransducer (Joshi *et al*, 2012), we asked whether pY14Cav1 levels are regulated differently in 1.0 and 1.5mg/ml 3D collagen gels (similar to 2D gels). WTMEFs embedded in 3D gels were extracted using collagenase and subjected to Western blotting. Cav1 phosphorylation in WTMEFs embedded in 3D collagen gels is significantly lower compared to collagen-coated 2D plastic (Fig. 2.7B). There is a modest ~18% increase in Cav1 phosphorylation in 1.5mg/ml gels as compared to 1.0 mg/ml gels, though the difference is not statistically significant. Cells embedded in 3D collagen gels are reported to not form as many focal adhesions as cells cultured on 2D. Additionally, cells in 3D have significantly lower FAK activation compared to 2D (King & Parsons, 2011), which we also observe in our studies (Fig. 2.7C). Furthermore, FAK activation in 1.5mg/ml gels is also marginally (~12%) higher than that in 1.0mg/ml gels, although this difference is not statistically significant. It is likely that these differences would be more prominent in a wider range of 3D collagen stiffness gels, although this as well as the dependence of pY14Cav1 on FAK in 3D gels remains to be established.

*Experiments in this chapter were done with help from project student Nivedhika Kannan and project assistant Shaunak Kanade who worked under my supervision.*

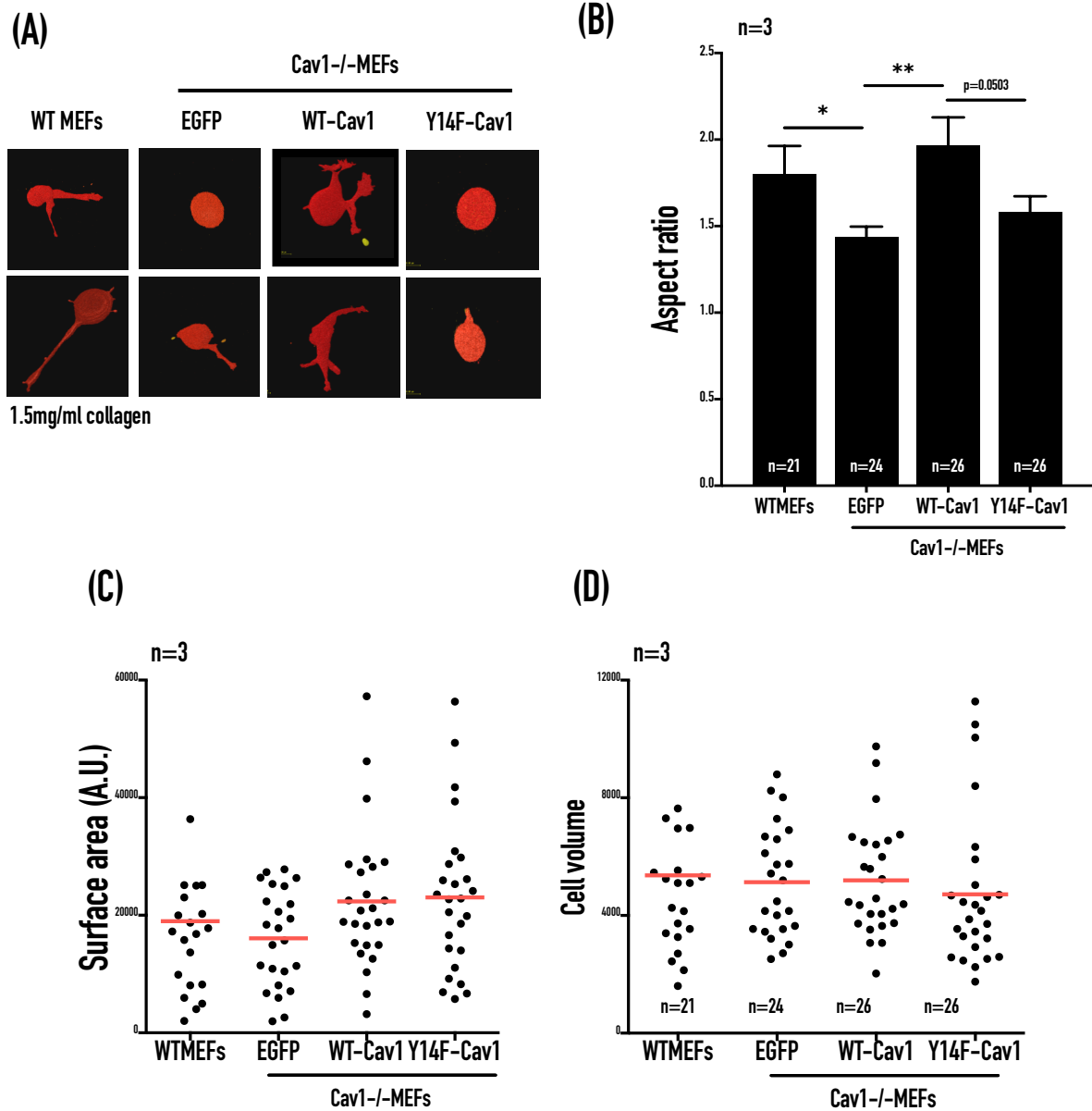


**Figure 2.6. Role of pY14Cav1 in regulating cell morphology in 3D collagen.** (A) Fluorescent microscopy images of WTMEFs and Cav1<sup>-/-</sup> MEFs expressing EGFP, WT-Cav1-GFP and Y14F-Cav1-GFP embedded in collagen gels of 1.5mg/ml, as indicated. Aspect ratio (B), surface area (C) and volume (D) of these cells represented as mean  $\pm$  SE calculated using ImageJ (NIH), from three independent experiments. Statistical analysis of the data was done using unpaired two-tailed t-test.

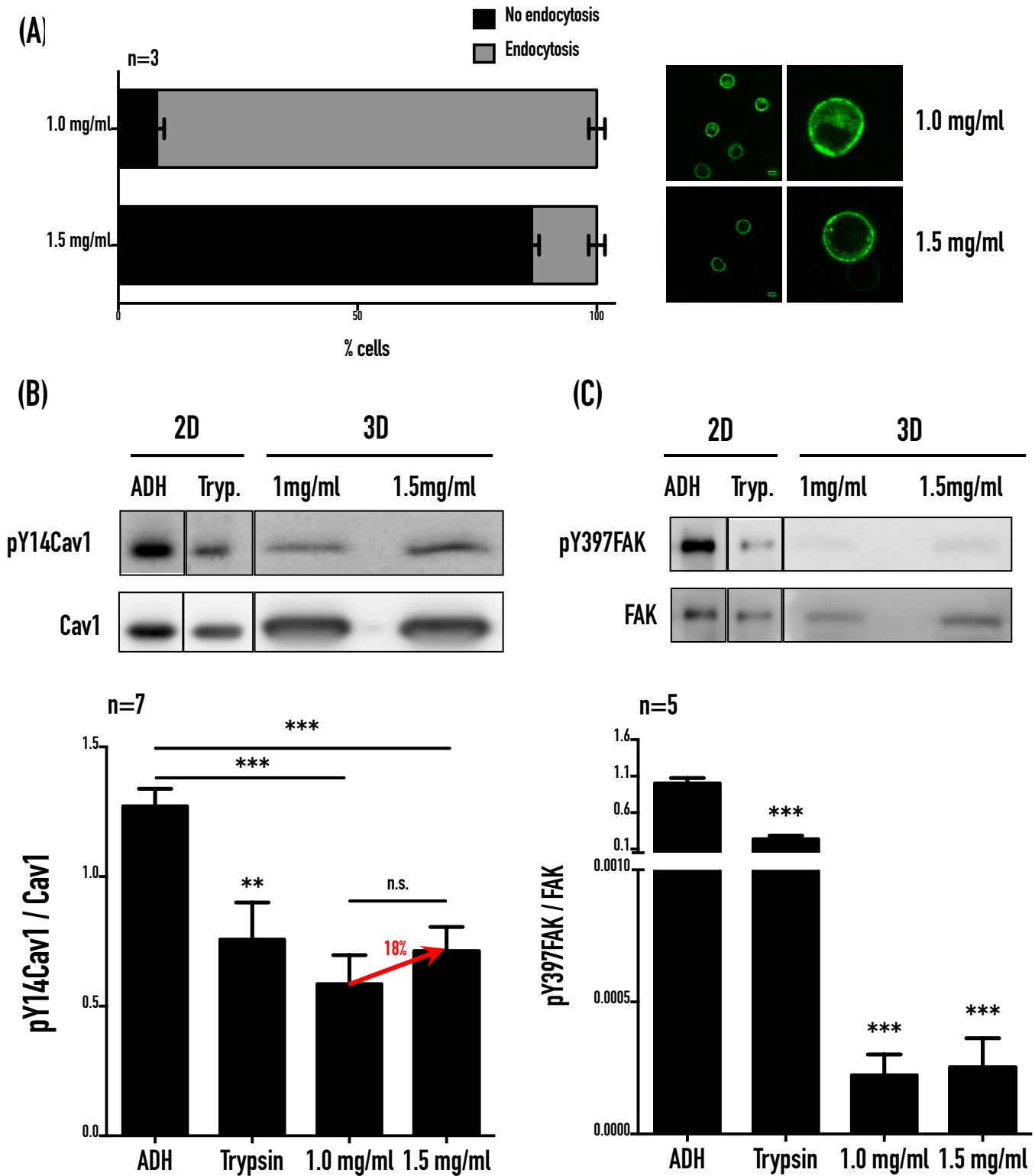


**Figure 2.7. Regulation of pY14Cav1 levels in 3D collagen gels of varying stiffness.** (A) Confocal microscopy images of WTMEFs embedded in collagen gels of 1.0mg/ml and 1.5mg/ml stained for GM1, as indicated. Bar graph represents mean  $\pm$  SE of cells scored for GM1 endocytosis, calculated using ImageJ (NIH), from at least 15 different frames each from three independent experiments. Western blot analysis of phosphorylated and total Cav1 (B) and FAK (C) in adherent (ADH), detached (Trypsin) or WTMEFs embedded in 1.0mg/ml and 1.5mg/ml collagen gels. Bar graphs represent mean  $\pm$  SE of densitometry of Western data using ImageJ (NIH), from at least five independent experiments. Statistical analysis of the data was done using unpaired two-tailed t-test.

## DISCUSSION

---

Focal adhesions are some of the most direct responders to changing ECM stiffness (Schwartz, 2010; Levental *et al*, 2009; Friedland *et al*, 2009; Gehler *et al*, 2009). ECM stiffness regulates both FA number and size – cells on soft matrices have less number of, and smaller FAs compared to stiff matrices (Yeh *et al*, 2017). Adhesion of fibroblasts on increasing matrix stiffness expectedly promotes cells spreading (Fig. 2.4), known to be regulated by integrin mediated signaling (Wolfenson *et al*, 2014). This reflects in the stiffness-dependent activation of FAK and increased Cav1 phosphorylation (Fig. 2.1). A significant fraction of pY14Cav1 resides in FAs (Fig. 1.9) and pY14Cav1 is sensitive to re-adhesion-mediated recovery of FAK (Fig. 1.10). FAK activation on changing ECM stiffness could hence drive Cav1 phosphorylation downstream of integrins. PF-228 mediated inhibition of FAK does indeed affect matrix stiffness-dependent Cav1 phosphorylation (Fig. 2.2, 2.3), further confirming the presence of an integrin-FAK-pY14Cav1 axis. The gradual increase in total Cav1 levels across increasing stiffness could be a result of increased pY14Cav1 (Joshi *et al*, 2012), and could affect Cav1 levels in caveolae and/or FAs. The relative impact this, along with the observed activation of FAK across increasing stiffness, could have on Cav1 phosphorylation does remain to be determined. Also it remains to be determined if *caveolar* pY14Cav1 could be sensitive to FAK activation.

On loss of adhesion no significant change in pY14Cav1 levels are observed in caveolae (Buwa *et al*, 2020a). This could also be the case in cells adherent on matrix of increasing stiffness. Interestingly, the degree/extent of dependence of Cav1 phosphorylation on FAK activation is variable on matrices of varying stiffness. On the least stiff matrix (0.5 kPa) inhibition of pY397FAK does not lead to any change in pY14Cav1 levels between CNT *vs.* FAKi (Fig. 2.2, 2.3). This is reminiscent of FAK inhibition in non-adherent cells (Fig. 1.10) where pY14Cav1 seems to be independent of the status of FAK phosphorylation. As matrix stiffness increases, the effect of FAK inhibition on Cav1 phosphorylation also increases, with the highest inhibition seen on glass (Fig. 2.2, 2.3). Taken together, these results suggest that increase in pY14Cav1 levels upon increasing matrix stiffness could primarily be an increase in FA-associated pY14Cav1. Additionally, a considerable fraction of the net pY14Cav1 levels in cells on softer gels (e.g. 0.5 kPa) is likely to be caveolar pY14Cav1, with the FA-associated pY14Cav1 increasing with increasing matrix stiffness.

Cell spreading on 2D gels of increasing stiffness is regulated by Cav1 and its phosphorylation (Fig. 2.5). pY14Cav1 is known to affect activation of the Rho GTPases, with Cav1<sup>-/-</sup> cells

showing decreased RhoA and increased Cdc42 and Rac1 activation (Grande-García *et al*, 2007; Joshi *et al*, 2008). Furthermore, RhoA inhibition is known to enhance cell spreading and migration by altering cell polarity and protrusion (Arthur & Burridge, 2001). The difference in cell spreading seen in our studies (Fig. 2.5) could hence be a result of differential regulation of Rho GTPases by pY14Cav1.

Cav1 phosphorylation is dispensable for caveolae formation (del Pozo *et al*, 2005), but *density* of caveolae on the PM is known to be influenced by pY14Cav1, especially in response to external stimuli known to affect it (Joshi *et al*, 2012; Orlichenko *et al*, 2006b). Our results do not rule out the possibility that the role of pY14Cav1 in regulating matrix-dependent cell spreading could be influenced by its ability to regulate caveolae formation and/or caveolar trafficking (by regulating the total available cell surface area for spreading).

Despite both FAK and pY14Cav1 being regulated by changing matrix stiffness, their crosstalk is seen to be variable across 2D gels of varying stiffnesses. Integrin-dependent signaling is distinctly altered on increasing stiffness and could reflect the greater impact FAK has on Cav1 phosphorylation at higher stiffness. Both Src activation (Wang *et al*, 2019a; Görtzen *et al*, 2015) and Src binding to FAK (Provenzano *et al*, 2009) increase on stiffer matrices and could impact FAK-dependent regulation of pY14Cav1 across changing matrix stiffness. c-Abl also possesses intrinsic mechanosensitivity, its activity significantly increased in cells exposed to hypo-osmotic swelling, on stiff substrates and on mechanical stretching (Echarri *et al*, 2019). The relative contribution of these kinases in regulating pY14Cav1 downstream of FAK remains to be evaluated. This adhesion- and FAK-dependent regulation of Cav1 phosphorylation is summarized as a model in Fig. 2.8.

Cells in 3D microenvironments have distinct differences in their morphology and functions compared to those growing on 2D (Baker & Chen, 2012; Stock *et al*, 2016). The role and regulation of Cav1 and pY14Cav1 in cells in 3D could indeed be distinctly different than in 2D. Mouse fibroblasts with (WTMEFs) and without (Cav1<sup>-/-</sup>-MEFs) Cav1, embedded in 3D collagen gels have distinctly different morphology (Fig. 2.6) (Goetz *et al*, 2011) and across changing stiffness (1.0 vs 1.5mg/ml), show strikingly different endocytosis behaviour. Morphology of cells in 3D is thus dependent on phosphorylation of Cav1 (pY14Cav1) while differential endocytosis is not. Indeed, GM1 internalization can occur through caveolae-independent routes. Cav1 is known to regulate fluid phase endocytosis, with its Tyr14 phosphorylation reducing Cdc42-mediated endocytosis (Chaudhary *et al*, 2014; Cheng *et al*, 2010). Cav1 and pY14Cav1 regulate Rho GTPase activation that in turn reduces Cdc42

activation (Grande-García *et al*, 2007). It is hence likely that pY14Cav1, by regulating Cdc42 activation, could affect Cdc42-dependent fluid phase endocytosis of GM1 in 3D as well. The role and regulation of non-caveolar, Cdc42-mediated GM1 endocytosis in 3D collagen gels remains to be further tested. pY14Cav1 is known to regulate Rho GTPase activation (Grande-García *et al*, 2007); and protrusion formation, cell polarization and contractility are all regulated by Rho GTPases (Zegers & Friedl, 2014; Ridley, 2015). pY14Cav1-regulation of protrusivity in 3D could hence be dependent on Rho GTPase activation.

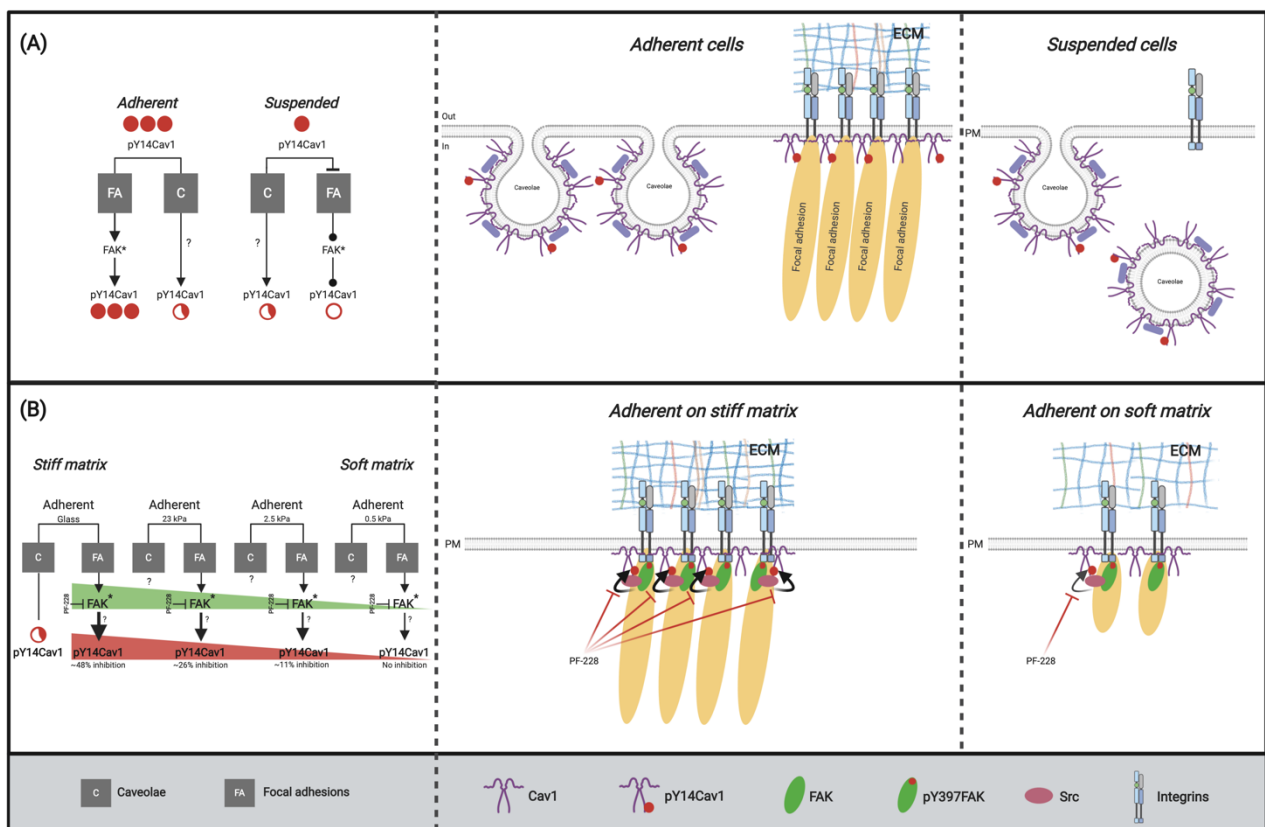


**Figure 2.8. Model for adhesion-dependent regulation of pY14Cav1.** (A) Endogenous pY14Cav1 (closed red dot) is regulated by cell-matrix adhesion in mouse fibroblasts, with adherent cells having significantly higher pY14Cav1 compared to suspended cells. Endogenous pY14Cav1 is localised to both caveolae and focal adhesions in adherent cells. On loss of adhesion (suspended cells) caveolar pY14Cav1 levels are not affected (partly closed red dot), suggesting the loss of FA-associated pY14Cav1 (open red dot) to affect total pY14Cav1 levels. (B) Cells adherent on stiff matrices, with more active FAK, have greater Cav1 phosphorylation compared to soft matrices. Changing matrix stiffness (0.5 kPa, 2.5 kPa, 23 kPa and Glass) shows a steady increase in FAK activation (FAK\*) (green sloping bar) and Cav1 phosphorylation (red sloping bar). PF-228-mediated inhibition of FAK activation inhibits Cav1 phosphorylation differentially on changing matrix stiffness (% inhibition). FAK-dependent regulation of pY14Cav1 could be mediated by FA-associated Src kinase. The effect of changing matrix on caveolar pY14Cav1 remains to be tested.



Additionally, cells embedded in 3D gels do not form as many focal adhesions, with FAK activation being significantly lower (King & Parsons, 2011) as also seen in our studies (Fig. 2.7B, C). This could reflect the FAK-pY14Cav1 crosstalk being much subdued in these cells. In agreement with this, only a modest increase in pY397FAK and pY14Cav1 levels is seen across increasing stiffness in 3D collagen gels (1.0 vs 1.5mg/ml): FAK activation increases at 1.5mg/ml by a small margin of ~12%, with ~18% increase in pY14Cav1. It is likely that higher stiffnesses of 3D collagen gels could promote their levels, although this as well as the FAK-pY14Cav1 regulation in 3D gels remains to be established.

Taken together, our studies indicate that FAK regulates pY14Cav1 differentially on changing matrix stiffness. Matrix stiffness-dependent regulation of pY14Cav1 through FAK could further regulate pY14Cav1-dependent functions. In conjunction, pY14Cav1 could regulate Rho GTPase and FA-dependent cellular responses like cell migration and invasion in response to changing matrix stiffness. Cell migration involves turnover of FAs which is dependent on the FAK-Src crosstalk at the leading edge (Webb *et al*, 2004) and RhoA-dependent disassembly at the trailing edge (Ridley, 2015). This is influenced by matrix stiffness during migration in 3D gels (Hetmanski *et al*, 2019). pY14Cav1 levels, sensitive to ECM stiffness (Buwa *et al*, 2020a), could regulate FA dynamics (Joshi *et al*, 2008; Goetz *et al*, 2008a) as well as RhoA activation (Boscher & Nabi, 2013; Grande-García *et al*, 2007). pY14Cav1 also dampens fluctuations in Vinculin tension, thereby maintaining FAs at high tension to drive membrane protrusion and cell migration (Meng *et al*, 2017). High traction at FAs (through both FAK and Vinculin) enables cells to sample ECM rigidity and guide ECM-stiffness dependent migration (Plotnikov *et al*, 2012). pY14Cav1 is also known to be a mechanotransducer, and its levels are regulated by mechanical stimuli like stretch and laminar shear stress (Joshi *et al*, 2012; Zhang *et al*, 2007). This regulates its interaction with MT1-MMP affecting its localization in invadopodia (Yang *et al*, 2016; Pu *et al*, 2020; Labrecque *et al*, 2004), which could regulate remodeling of the microenvironment to influence matrix-dependent signaling and migration in cancer cells.

***Part of Chapters 1 and 2 have been recently published:***

*Buwa N, Kannan N, Kanade S & Balasubramanian N (2020a) Adhesion-dependent Caveolin 1 Tyrosine-14 phosphorylation is regulated by FAK in response to changing matrix stiffness. FEBS Lett. 595: 532–547.*

## **CHAPTER 3:**

### **Cav1 phosphorylation in cancers: PTP-mediated regulation and role in anchorage-independence**

## ABSTRACT

---

The role of Cav1 as a tumor suppressor or promoter has been contentious, and could at least in part be dependent on its Tyr14 phosphorylation. Apart from its role in caveolar endocytosis and focal adhesion function in non-transformed cells, pY14Cav1 is thought to have a regulatory role in cancers. Cav1 is known to have a role in tumor cell migration and invasion, of which Cav1 phosphorylation is a critical determinant. We find that adhesion regulates pY14Cav1 levels in some, but not all, Cav1-expressing cancer cell lines. Regulation of pY14Cav1 levels could hence contribute to the role Cav1 has in cancers. Protein tyrosine phosphatase (PTP) levels and activation are known to be deregulated in many cancers and could help mediate the same. We screened pY14Cav1 levels across cancers and used siRNA-mediated targeting of PTPs to evaluate the effect they have on pY14Cav1 levels. Their impact across cancer cell lines is variable, and supports anchorage-independent signaling in T24 bladder cancer cells. Taken together, these studies reveal the possible role pY14Cav1 and its regulation could have in cancers.

## INTRODUCTION

---

Anchorage-dependent membrane raft microdomain recycling through caveolar endocytosis is known to regulate growth signaling in cells (del Pozo *et al*, 2005; Del Pozo *et al*, 2004). Deregulation of this recycling pathway is one of the many ways in which cancer cells could acquire anchorage-independence. Cav1 was initially thought to be a tumour suppressor since deletion of the *CAV1* gene locus was found to be associated with loss of tumorigenicity in many cancers (Williams, 2004). But up-regulation of Cav1 and its requirement for tumorigenesis and metastasis have also been reported in many cancer types (Goetz *et al*, 2008b; Simón *et al*, 2020). Role of Cav1 as a tumor suppressor or promoter in cancers is hence likely to be tissue- and/or stage-specific. These roles could at least in part be dependent on its Tyr14 phosphorylation. Cav1 Tyr14 phosphorylation is a critical determinant of cell migration and invasion in some cancer types (Joshi *et al*, 2019; Díaz-Valdivia *et al*, 2020). Migration in cells expressing phosphorylatable Cav1, but not non-phosphorylatable Y14F-Cav1, is seen to be elevated and become Src-dependent (Joshi *et al*, 2019; Goetz *et al*, 2008a).

### ***pY14Cav1: Role in migration and invasion in cancers***

Cells devoid of Cav1 lack cell polarity, show reduced wound healing and altered Rho GTPase activities (Grande-García *et al*, 2007). This change in the activation status of Rho GTPases is mediated by pY14Cav1, since phospho-deficient mutants of Cav1 decreased RhoA activation which in turn translated into aberrant directional migration (Grande-García *et al*, 2007). Elevated pY14Cav1 levels correspond with increased RhoA activation, and expression of dominant negative RhoA or active Rac1 leads to a reduction of pY14Cav1 levels. pY14Cav1 levels are Rho/ROCK and Src-dependent, since inhibition of either leads to decreased pY14Cav1 (Joshi *et al*, 2008). Interestingly pY14Cav1 also imparts Src- and ROCK inhibitor-sensitive stabilization of FAK in FAs and *de novo* focal adhesion formation. This points to a regulatory feedback loop between pY14Cav1, Src and Rho/ROCK, where Rho/ROCK and Src regulate pY14Cav1 which acts as an effector for Rho signaling, and pY14Cav1 in turn regulates Rho GTPase activation. The Src-p190RhoGAP (Grande-García *et al*, 2007) and Rho/ROCK dependent (Joshi *et al*, 2008) control of focal adhesion dynamics is regulated by Cav1 Tyr14 phosphorylation to mediate cancer cell migration and invasion. In cancer cells migrating in 3D matrices caveolae appear at the rear end in response to significantly lower membrane tension which drives RhoA activation and local actin contractility promoting cell rear retraction (Hetmanski *et al*, 2019). This could be mediated by pY14Cav1-mediated regulation of RhoA activation (Boscher & Nabi, 2013).

Cav1 and pY14Cav1 also play a central role in force-dependent stromal remodeling of the tumor microenvironment (Goetz *et al*, 2011). Cav1-expressing cancer-associated fibroblasts (CAFs) regulate matrix alignment and modulate ECM stiffening through Rho-dependent regulation of cell contractility (Goetz *et al*, 2011), both of which are regulated by pY14Cav1 (Nethe & Hordijk, 2011; Yang *et al*, 2011; Grande-García *et al*, 2007). This pY14Cav1-dependent stromal remodeling promotes tumor invasion and metastasis *in vivo*. Osmotic and hydrostatic pressure in the tumor microenvironment could regulate Cav1-dependent matrix metalloproteinases (MMP) expression in glioblastoma cell lines (Pu *et al*, 2020). These forces are also known to regulate Cav1 phosphorylation. MMPs and Cav1 (supported by its Tyr14 phosphorylation) colocalize to pseudopodia and invadopodia (Murphy & Courtneidge, 2011; Caldieri *et al*, 2009; Yamaguchi *et al*, 2009; Joshi *et al*, 2019) to drive invasion. Fluid shear stress in breast cancer cells also promotes Cav1 phosphorylation and MT1-MMP localization in invadopodia, to drive metastasis (Yang *et al*, 2016). Src-dependent Cav1 phosphorylation regulates its interaction with MT1-MMP (Labrecque *et al*, 2004) and could thus regulate force-induced, MMP-dependent stromal remodeling. This could further influence matrix-dependent signaling and function in cancer cells.

#### ***pY14Cav1: Role in caveolar endocytosis in cancers***

Interestingly, caveolar endocytosis has recently been shown to regulate surface availability of the EGFR family member HER2. HER2 surface expression in cancer cells is critical for targeting and binding of Trastuzumab (a therapeutic anti-HER2 antibody) or Ab-drug conjugates like Trastuzumab-emtansine (T-DM1) (Pereira *et al*, 2018; Li *et al*, 2018). HER2 co-fractionates with Cav1 in the same lipid-rich fractions, and Cav1 expression levels regulate HER2 localization at PM without affecting total HER2 protein levels. This observation is consistent with HER2-positive tumor samples from gastric cancer patients (Pereira *et al*, 2018). Lovastatin, a cholesterol-lowering drug, downregulates Cav1 expression, thus increasing HER2 availability for Trastuzumab binding at the PM (Pereira *et al*, 2018). A recent study finds Cav1 phosphorylation to be required for HER2/Trastuzumab internalisation, as both phospho-deficient Cav1 or hypoxic conditions that reduce pY14Cav1 levels, inhibit T-DM1 internalization and cytotoxicity (Chandran *et al*, 2020). This suggests a specific role for Cav1 phosphorylation in HER2 trafficking.

Invasive cancer cells migrating in complex 3D matrices have been shown to induce caveolae formation in response to significantly lower tension at the rear end of the cells along the axis of migration (Hetmanski *et al*, 2019). This accumulation leads to activation of RhoA signaling

to control local actin contractility thus promoting cell rear retraction (Hetmanski *et al*, 2019). Cav1-mediated endocytosis of inactive Rac1 at the rear end of migrating cells has also been shown to regulate Rac1 trafficking and degradation (Williamson *et al*, 2015; Nethe *et al*, 2010). Moreover, this pathway was preferred by cells upon engagement of fibronectin receptor syndecan-4 (Bass *et al*, 2011; Williamson *et al*, 2015), suggesting a preference of Cav1-mediated endocytosis in exclusive scenarios. To add another level of complexity in Cav1/caveolae-dependent cell migration, it has been observed that Cavin1 expression in cell lines lacking it (prostate cancer cells PC3) induces caveolae formation at the cell rear, decreasing migration potential and inhibiting EMT (Aung *et al*, 2011). This is brought about by neutralizing non-caveolar Cav1 (Moon *et al*, 2014) to drive caveolae formation, inhibiting accumulation and trafficking of non-caveolar Cav1 at the leading edge. Other caveolar proteins EHD2 and Pacsin2 have also been shown to have an inhibitory effect on migration in cancer cells (Meng *et al*, 2011; Li *et al*, 2013), but it is unclear whether this happens in response to caveolae formation at cell rear. Indeed, Cav1 appears to be associated with the leading edge in migrating cancer cells (Urrea *et al*, 2012; Joshi *et al*, 2008), very likely in non-caveolar domains. The central theme of these studies seems to be caveolae formation in response to reduced membrane tension at the trailing end in migrating cells, and it remains to be determined if and how Cav1 phosphorylation plays a role in these processes.

### ***pY14Cav1 regulation by protein tyrosine phosphatases (PTPs) in cancers***

Protein phosphorylation/dephosphorylation events are crucial regulators of signal transduction cascades. Phosphorylation can drive the activation of signal transduction pathways, regulating survival, growth and proliferation. Dephosphorylation events mediated by protein tyrosine phosphatases (PTPs) can turn down signaling pathways, resulting in inhibition of growth and proliferation (Bollu *et al*, 2017). Kinases and phosphatases thus regulate a fine balance between activation and termination of signaling events in non-transformed cells. Tumorigenesis entails dysregulation of this balance, either by hyperactivation of kinases or loss of PTPs. Indeed, expression profile of PTPs has been reported to be altered across multiple cancers including human breast cancer samples (Hollander *et al*, 2016).

PTEN was one of the first identified PTPs found to be frequently lost or mutated in many human cancers (Bollu *et al*, 2017). Genetic ablation of another PTP, *viz.*, PTP1B accelerates lymphomagenesis in p53-null mice, suggesting it can function as a tumour suppressor (Dubé *et al*, 2005). PTP1B expression regulates apoptosis and inhibits growth, migration and invasion of cancer cells (Hoekstra *et al*, 2016), and is associated with poor prognosis in gastric, ovarian,

breast and prostate cancers (Bollu *et al*, 2017). PTP1B expression is elevated in HER2-positive breast and non-small cell lung cancers (Liu *et al*, 2015), its inhibition delaying onset of tumour formation and reducing lung metastasis (Julien *et al*, 2007). Another PTP, PTPN14, regulates cell-matrix adhesion, migration, anchorage-independent growth and metastasis of colorectal and breast cancer cells (Zhang *et al*, 2013).

Interestingly, PTP1B and PTPN14 are both known to dephosphorylate pY14Cav1 to regulate cancer cell migration, invasion and metastasis (Martínez-Meza *et al*, 2019; Díaz-Valdivia *et al*, 2020). PTP1B was shown to be activated by angiotensin type 2 receptor (AT2R), which in turn led to Cav1 dephosphorylation and inhibition of Cav1-enhanced melanoma metastasis (Martínez-Meza *et al*, 2019). PTPN14 was found to be associated with Cav1-immunoprecipitates, where it dephosphorylates pY14Cav1. Further, PTPN14 expression and activity blocked Cav1-enhanced migration, invasion and metastasis of cancer cells (Díaz-Valdivia *et al*, 2020). The relative impact of PTP-mediated dephosphorylation on caveolar vs. non-caveolar pY14Cav1 is an open question. The role of PTPs in regulating pY14Cav1-mediated anchorage-independent signaling and growth also remains to be fully studied, which we further explore in our studies.

## MATERIALS AND METHODS

---

### Cell culture

Calu1, MiaPaCa2, HCT116, PC3, UMUC3, T24, DU145, MDA-MB-231, HT1080, CFPAC1, U87MG, SKOV3 were from ECACC, and cultured in high glucose DMEM or RPMI1640 medium (according to ECACC guidelines) with 5% foetal bovine serum (FBS), penicillin and streptomycin (Invitrogen) (hereby referred to as complete DMEM). Cells were regularly checked for and found to be devoid of bacterial or mycoplasma contamination. Serum starvation of cells, where mentioned, was done for 14h using DMEM medium with 0.2% FBS, penicillin and streptomycin (low-serum DMEM). For siRNA-mediated knockdowns,  $0.5 \times 10^5$  cells were seeded in 60 mm dishes. 3h post-seeding cells started to spread and were transfected with 5pmol of SMARTPool siRNA mix using RNAiMax transfection reagent. This was similarly repeated after 24h (Day 2) and cells were processed or used for experiments after 48h of the second shot of knockdown. Transfection mixes containing siRNA were made in 450 $\mu$ l of Opti-MEM (Gibco Cat. no. 22600050), and incubated for 30 min at room temperature before addition to cells.

### Antibodies and Reagents

Primary antibodies used for Western blotting were diluted in 5% BSA made in TBST at following dilutions: Cav1 (Santa Cruz Biotech SC-894) at a dilution of 1:2000, pY14Cav1 (BD 611338) at 1:500, FAK (Cell Signaling Technology (CST) 3285) at 1:1000, pY397FAK (CST 3283) at 1:1000, Cavin1 (BD 611258) at 1:500; Actin (DSHB JLA20) at 1:2000 and  $\beta$ -tubulin (DSHB Clone E7) at 1:2000. HRP-conjugated secondary antibodies (anti-rabbit and anti-mouse) were purchased from Jackson Immuno Research Laboratories and used at a dilution of 1:10000. Methylcellulose for suspension assay was purchased from Sigma (Cat. no. M0262). Fibronectin (FN) was purchased from Sigma (Cat. no. F2006). FAK inhibitor PF-228 (Slack-Davis *et al*, 2007) was purchased from Sigma (Cat. no. PZ0117). Protease inhibitor cocktail PIC was purchased from Roche (04693132001), and phenylmethanesulfonyl fluoride (PMSF), sodium orthovanadate and sodium fluoride from Sigma. BCA assay kit used for protein estimation was purchased from Thermo Fisher (Cat. no. 23225). RIPA buffer composition: 50mM Tris-HCl at pH 8.0 + 150mM NaCl + 1.0% NP-40 + 0.5% sodium deoxycholate + 0.1% SDS. Tris was purchased from HiMedia (Cat. no. MB029), Glycine from Fisher Scientific (Cat. no. 56406), Sodium bicarbonate from Sigma (Cat. no. S6297), Methanol from Fisher Scientific (Cat. no. 67561), PVDF membranes from Millipore (Cat. no. IPVH00010) and BSA from



Sigma (Cat. no. A2153). Chemiluminescent reagents for Western blotting Immobilon Western Chemiluminescent HRP Substrate was purchased from Millipore (Cat. no. WBKLS0500), SuperSignal West Femto Maximum Sensitivity Substrate from ThermoFisher (Cat. no. 34096). TRIzol was purchased from Invitrogen (Ambion, Cat. no. 15596018); iScript cDNA synthesis kit from Biorad (Cat. no. 1708891); SYBR RT-PCR mix (SYBR® FAST Master Mix (2X) Universal) from Kapa Biosystems (Cat. no. KK4601); RT-PCR plates from Biorad Multiplate™ 96-Well PCR Plates, low profile, unskirted, white (Cat. no. MLL9651). RT-PCR machine: Bio-Rad CFX96 Real Time System.

**SMARTPool oligos:** siRNA oligos targeting specific PTPs were purchased from Dharmacon. Catalog numbers for each of these sequences are listed in the tables at the end of this section.

### **Suspension and re-adhesion of cells**

Cells were cultured in complete DMEM or RPMI to ~70% confluence. Cells were detached using trypsin-EDTA (Invitrogen) at 37°C, neutralised and spun down to get a cell pellet. The pellet was reconstituted, mixed with 15ml media and 15ml of 2% methylcellulose and incubated at 37°C for 120 min (120'SUSP). For re-plating on fibronectin (FN), cells held in methylcellulose suspension were carefully washed, followed by centrifugation at 1250 rpm in a cooled table-top Eppendorf centrifuge for 7 min at 4°C. After this centrifugation cells appeared as loose pellet distributed over the conical edge of the 50ml tube, which was carefully dislodged using a 1ml micropipette (cut tip). Cells were washed once again with media followed by centrifugation 1000 rpm in a cooled table-top Eppendorf centrifuge for 7 min at 4°C, after which pellet was resuspended in media. These cells now represent the 120'SUSP time point. For re-adhesion time points, 120'SUSP cells were re-plated in media for 15min (15'FN) or 4h (4hFN) on tissue culture dishes pre-coated with 10µg/ml FN. Adherent cells growing on dishes for 14h (not put through the suspension assay) were lysed to represent stably adherent (ADH) cells. Cells were lysed in RIPA buffer for protein estimation using BCA assay and 20µg total protein used for Western blotting.

### **Surface GM1 labelling**

Cells grown in low serum DMEM for at least 14h were trypsinised (0'SUSP) and held in methyl cellulose suspension for 2h (120'SUSP). Cells at respective time points were labelled with 10µg/ml of CTxB-Alexa 594 in PBS for 15 min on ice. Cells were then washed thrice using cold PBS followed by fixation with 3.5% paraformaldehyde. Cell suspension in leftover ~20ul PBS was mounted on slides with Fluoromount. Imaging was done using Zeiss LSM710

laser confocal microscope, 40X oil objective and identical microscopy settings were used for all samples in that experiment. For image analyses (done using ImageJ, NIH) for quantitation of surface GM1 levels, intensity threshold was set to map the entire cell and a mask was created to measure intensity in that cell. Total integrated density in cells was measured, average integrated density calculated and was represented in arbitrary units in the graphs.

### **Pervanadate treatment**

Cells were plated in 60mm dishes at ~70% confluency and allowed to attach and spread for at least 14h. Cells were then treated with indicated concentration of pervanadate, which was prepared as described below. To prepare 1mM pervanadate, 10 $\mu$ l of 100mM sodium orthovanadate (in MilliQ water) was added to 900 $\mu$ l of 10mM of H<sub>2</sub>O<sub>2</sub> (light-sensitive) and incubated at RT for 30 min. This solution was added to media at required final concentrations of 1 $\mu$ M, 5 $\mu$ M or 10 $\mu$ M. Older spent media was aspirated and pervanadate-containing media added to cells. Cells were incubated at 37°C in the TC incubator for 30 min, after which cells were washed with PBS and lysed in Laemmli's buffer or used for further experiments.

### **RNA isolation**

Total RNA was isolated using the TRIzol method. Cells were harvested in 1ml TRIzol and frozen at -80°C until further processing. TRIzol samples were thawed at room temperature, mixed with 0.2 mL of chloroform per 1 ml of TRIzol, vortexed vigorously and incubated for 15 min at RT. Samples were centrifuged for 15 min at 12,000xg at 4°C. The mixture separates into a lower pink phenol-chloroform phase, an interphase, and a colourless upper aqueous phase. Aqueous phase containing the RNA was collected in a fresh tube, and was roughly half the volume (~0.5 ml). RNA was then precipitated from the aqueous phase by mixing with equal volume (0.5 ml) of isopropyl alcohol. Samples were incubated for 15 min and then centrifuged at 12,000xg for 10 min at 4°C. The RNA precipitate appears as a sticky pellet on the side and bottom of the tube. Supernatant was decanted and the RNA pellet washed using 1ml of 75% molecular biology grade ethanol. RNA pellet was air-dried until no traces of liquid were left back, reconstituted in nuclease-free water and stored at -80°C.

### **cDNA preparation and Quantitative RTPCR**

cDNA was prepared from RNA using iScript cDNA synthesis kit (Biorad) according to the manufacturer's specifications. In brief, a master mix of 5X iScript reaction mix and reverse transcriptase was prepared and added to respective samples of 1 $\mu$ g RNA, and the reaction volume made up to 10 $\mu$ l with NFW. PCR thermal cycler reaction protocol: Priming: 5 min at

25°C → Reverse transcription: 20 min at 46°C → RT inactivation: 1 min at 95°C → Hold at 4°C.

Undiluted cDNA was used to setup a 5µl quantitative PCR (qRT-PCR) reaction with SYBR FAST qPCR master mix (Kapa Biosystems) in a Bio-Rad CFX96 Real Time System using human protein tyrosine phosphatase (PTP) and actin primers.

### **Generation of stable shCav1 SKOV3 clones**

shCav1 oligos were cloned in pLKO.1 using the Addgene protocol. In brief, oligos were annealed before ligation into pLKO.1 cloning vector digested with EcoRI and AgeI. Screening for inserts was done by digesting the cloned products with EcoRI and NcoI. Digested products were run on 1% agarose gels stained using SYBR Safe, and positive clones identified by release of 2 fragments at 2kb and 5kb. Positive clones were verified by sequencing, and transfected in HEK293T cells with 1µg pLKO.1 shCav1, 750ng psPAX2 packaging plasmid and 250ng pMD2.G envelope plasmid using PEI. shCav1-containing lentiviral particles were collected on Day 3 and 4 after transfection, filtered and used to infect SKOV3 cells. Stable cell lines were made from a single cell population selected after transfection of shCav1-pLKO.1 vector using Puromycin.

### **Statistical analysis**

Statistical analysis of data was done using unpaired two-tailed t-test. All analysis was done using Prism Graphpad analysis software. Statistical significance was considered at  $p < 0.05$ .

## SMARTPool and shRNA oligos and Primer sequences

*Table 1: SMARTPool oligos*

Targeted PTP	Catalog no.	Gene Symbol	Gene Accession	Sequence
<b>PTP1B</b>	L-003529-00	PTPN1	NM_002827	GGAGAAAGGUUCGUUAAAA
				CUACCUGGCUGUGAUCGAA
				GCCCAAAGGAGUUACAUUC
				GACCAUAGUCGGAUUAAAC
<b>TCPTP</b>	L-008969-00	PTPN2	NM_080423	GAUGUGAAGUCGUUUUAUA
				GAUGUAAGCCCAUAUGAUC
				AUACAAUGGGAACAGAAUA
				ACAAAGGAGUUACAUCUUA
<b>PTP-Mu</b>	L-006326-00	PTPRM	NM_002845	GGACUUGCCUGGCGACUUU
				GCAAUUUAUUCGAUGGUUA
				GAACGUCCUCGAAGAACUA
				GAGUGAGGCUGCAGACAAU
<b>PTP-PEST</b>	L-008064-00	PTPN12	NM_002835	GGAUUUAAGUUCAGAUCUA
				GUA AUGGCCUGCCGAGAAU
				GGACACUCUUACUUGAAUU
				CGGGAGGUUUACACUAUGA
<b>PRL1</b>	L-006333-00	PTP4A1	NM_003463	GAUUGUUGAUGACUGGUUA
				CCAAUGCGACCUUAAACAA
				GCAAGCAACUUCUGUAUUU
				GAAAGAAGGUUCCAUGUU
<b>PRL2</b>	L-009078-00	PTP4A2	NM_080392	CCUAUGAGAACAUGCGUUU
				AGUAUGGAGUGACGACUUU
				GAAAUACCGACCUAAGAUG
				CCAAUGCUACUCUCAACAA
<b>PTEN</b>	L-003023-00	PTEN	NM_000314	GAUCAGCAUACACAAAUA
				GACUUAGACUUGACCUAUA
				GAUCUUGACCAAUGGCUAA
				CGAUAGCAUUUGCAGUAUA
<b>HDPTP</b>	L-009417-00	PTPN23	NM_015466	GUGCACAGGUGGUAGAUUA
				GCAAACAGCGGAUGAGCAA
				GCAUGAAGGUCUCCUGUAC
				GUAGUGUCCUCCGCAAGUA

**Table 2: RTPCR Primers**

Primer name	Sequence
<b>PTP1B-F</b>	GAGTTCGAGCAGATCGACAAGTC
	TAGGAAGCTTGGCCACTCTACAT
<b>PRL1-A</b>	CCAGCTCCTGTGGAAGTCAC
	TAAGGTCGCATTGGTTGGAT
<b>PTP-PEST-A</b>	CAGAATTCAGACACACCTCCAA
	CCACGTTACATGTCCTTTCTCA
<b>PTP-Mu-B</b>	TCAGTTCCTTTGACCCAGAAAT
	CCAGCTTTGAAACTCTTCCACT
<b>PTEN-H</b>	GTTGGGACTAGGGCTTCAATTT
	GTATGCAGTCTGGGCATATCAA
<b>TCPTP-K</b>	GGGAGTTCGAAGAGTTGGATAC
	AAACTTGGCCACTCTATGAGGA
<b>PRL2-G</b>	ACTTTCCCATCACACTCACAC
	GGACGGTTCATTATGGCAA
<b>HDPTP-N</b>	AAGGTCTCCTGTACCCATTTCC
	GTAGGCTTGAGGGAAGTGCTC
<b>Actin</b>	CTCCTGAGCGCAAGTACTCC
	CCGGACTCGTCATACTCCTG

***Cav1 shRNA oligos***

Sequence 1 (Beardsley *et al*, 2005):

Forward	CCGGAATCTCAATCAGGAAGCTCTTCTCGAGAAGAGCTTCTGATTGAGATTTTTTTG
Reverse	AATTCAAAAAATCTCAATCAGGAAGCTCTTCTCGAGAAGAGCTTCTGATTGAGATT

Sequence 2 (Pellinen *et al*, 2018):

Forward	CCGGGACGTGGTCAAGATTGACTTTCTCGAGAAAGTCAATCTTGACCACGTCTTTTTG
Reverse	AATTCAAAAAGACGTGGTCAAGATTGACTTTCTCGAGAAAGTCAATCTTGACCACGTC

## RESULTS

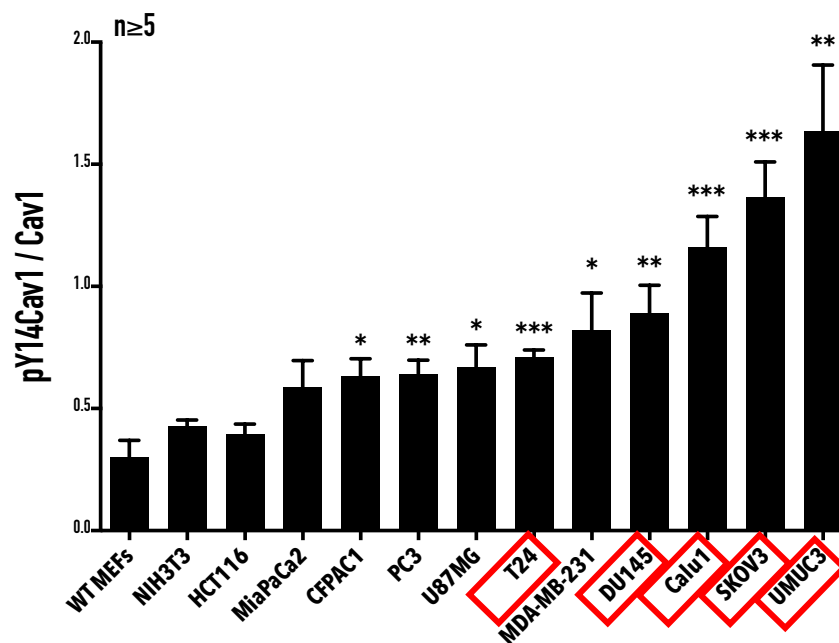
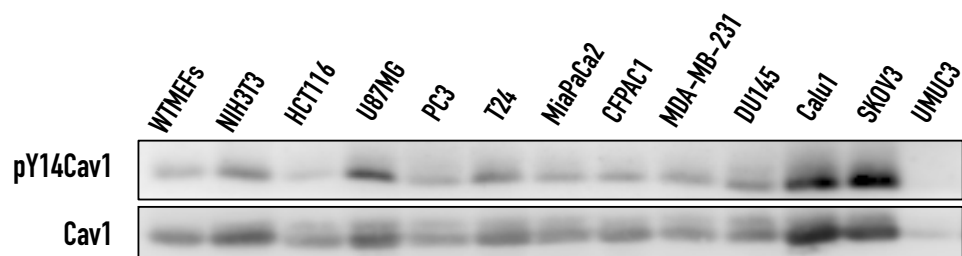
---

### *pY14Cav1 in Cav1-expressing cancers*

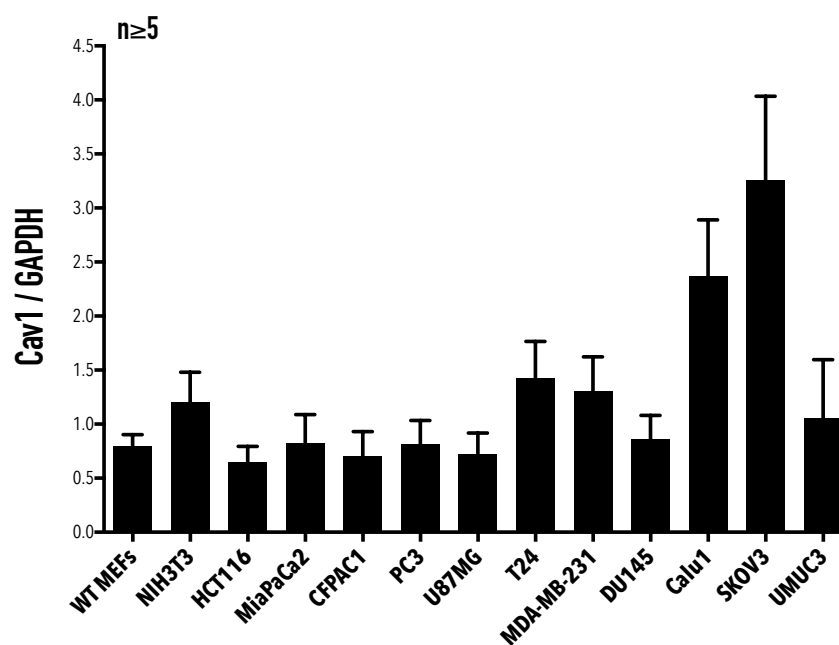
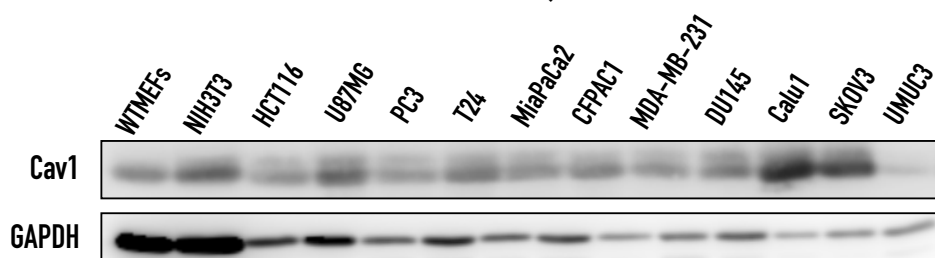
The role of Cav1 in cancers is contentious, and could at least in part be mediated by its Tyr14 phosphorylation, that is seen to regulate the Cav1 function. To this effect, a literature survey was done to identify Cav1-expressing cancer cell lines from the ONCOMINE database (Rhodes *et al*, 2004). ONCOMINE is a cancer microarray database and web-based data-mining platform used for studying differential expression analyses of genes in cancers with respective normal tissues. The criterion applied for selection of cell lines was that they have at least a 2 fold over-expression of Cav1, with p-value 0.001 or lower. Cell lines selected accordingly are listed in the Materials and Methods section. pY14Cav1 expression in these cell lines was compared by Western blotting using the monoclonal pY14Cav1 antibody. We confirmed that these cell lines indeed express Cav1, and compared pY14Cav1 levels to those in WTMEFs and NIH3T3 (Fig. 3.1). Interestingly, pY14Cav1 levels are distinctly different across these cell lines. HCT116, MiaPaCa2, CFPAC1, PC3, U87MG, T24, MDA-MB-231, DU145 have moderate; whereas Calu1, SKOV3 and UMUC3 have significantly higher pY14Cav1 levels compared to those in NIH3T3 (Fig. 3.1A). Total Cav1 levels on the other hand were comparable to NIH3T3 in most cell lines, except in Calu1 and SKOV3 where they seem to be significantly higher (Fig. 3.1B).

**Figure 3.1. Cav1 phosphorylation levels in Cav1-expressing cancer cells.** (A) Western blot analysis of phosphorylated and total Cav1 in cancer cell lines, compared to WTMEFs and NIH3T3 cells, as mentioned. Lysates were protein-estimated and equal amount of protein run on PAGE for comparison. Graph represents densitometry analysis of Western blotting data, from at least five independent experiments, with ratios of band intensities of phosphorylated Cav1 to total Cav1 plotted as mean  $\pm$  SE. Statistical analysis was done using unpaired two-tailed t-test. (B) Western blot analysis of total Cav1 relative to GAPDH loading control from above experiments. Graph represents densitometry analysis of Western blotting data, with ratios of band intensities of total Cav1 to GAPDH plotted as mean  $\pm$  SE.

(A)



(B)



### *Adhesion-dependent regulation of Cav1 phosphorylation in cancers*

We next wanted to test if this phosphorylation was actively regulated by adhesion in these cancer cells, compared to adhesion-dependent regulation in non-transformed fibroblasts. UMUC3, SKOV3, DU145, Calu1 and T24 were chosen to test the same, as these cells have moderate to high pY14Cav1 levels, and are hence likely to show deregulation of pY14Cav1. These cells were held in suspension for 120 min and then re-plated on fibronectin-coated dishes. pY14Cav1 levels show a decrease upon loss of adhesion in UMUC3, Calu1 and T24 cells (Fig. 3.2A, C, E). Interestingly, pY14Cav1 levels in SKOV3 and DU145 do not decrease upon loss of adhesion (Fig. 3.2B, D). FAK activation in all of these cell lines shows adhesion-dependent regulation (Fig. 3.2F-J), similar to that in mouse fibroblasts (Fig. 1.3B, E, H).

Cancer cells often show a deregulation of growth signaling pathways to sustain adhesion-independent signaling. Interestingly, we see adhesion-independent sustenance of Akt activation in SKOV3 cells in our studies (Fig. 3.2L), where pY14Cav1 levels are also adhesion-independent. Whether this sustained activation of growth signaling pathways is dependent on pY14Cav1, remains to be determined. For this purpose, we proposed to knockdown Cav1 using shRNA in SKOV3 cells. Stable, shRNA-mediated Cav1 KD in SKOV3 shows a modest decrease in Cav1 levels in clones tested (Appendix Figure 3, 4). Ongoing experiments evaluating additional clones to identify a Cav1-lacking clone are currently underway. These Cav1 knockdown SKOV3 cells when reconstituted with WT-Cav1, Y14F-Cav1 and Y14D-Cav1 will help address the impact of Cav1 phosphorylation on anchorage-independent signaling and growth.



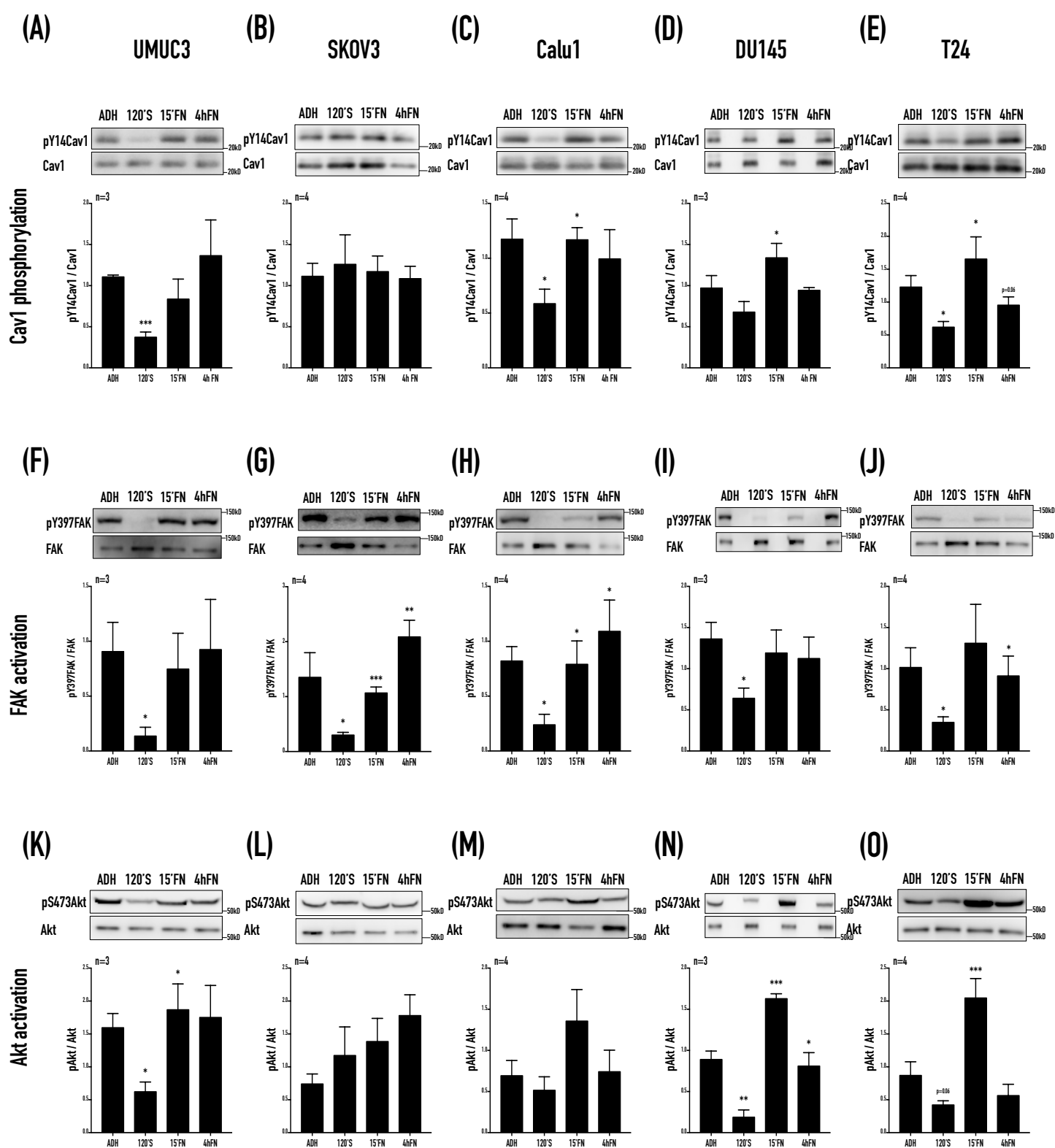


**Figure 3.2. Cav1 phosphorylation and signaling in cancer cells – adhesion-dependence.** Western blot analysis of phosphorylated and total Cav1 (A-E), FAK (F-J) and Akt (K-O) from adherent (ADH), suspended for 120min (120'SUSP), re-adherent for 15min (15'FN) and re-adherent for 4h (4hFN) UMUC3, SKOV3, Calu1, DU145 and T24 cells, as mentioned. Graphs represent densitometry analysis of Western blotting data from 4 independent experiments, with ratios of band intensities of phosphorylated protein to respective total protein plotted as mean  $\pm$  SE. Statistical analysis was done using unpaired two-tailed t-test.

### ***Active regulation of adhesion-dependent Cav1 phosphorylation by protein tyrosine phosphatases (PTPs) in cancer cells***

Cav1 phosphorylation is regulated primarily *via* kinases and phosphatases. Src, the major Cav1 kinase, is known to be frequently overexpressed or hyper-activated in various cancers (Irby & Yeatman, 2000; Ishizawa & Parsons, 2004; Belli *et al*, 2020). Several protein tyrosine phosphatases (PTPs) are found to reside in caveolae (Caselli *et al*, 2002), and some (PTP1B, LMW-PTP, PTPN14) co-immunoprecipitate with Cav1 and dephosphorylate it (Caselli *et al*, 2002, 2007; Díaz-Valdivia *et al*, 2020). PTP1B and PTPN14 bring about a decrease in pY14Cav1 levels to regulate Rho GTPase-mediated migration, invasion and metastasis of cancer cells (Martínez-Meza *et al*, 2019; Díaz-Valdivia *et al*, 2020). PTPs could thus play a role in regulating pY14Cav1 levels and function in cancers.

We hence wanted to ask if endogenous pY14Cav1 levels can be actively stimulated in cancer cells, and whether this would sustain anchorage-dependent signaling. For this, we could either activate Src kinase, or inhibit PTPs. Activating Src, a known proto-oncogene, would affect tumorigenesis on its own, and hence would be counter-productive to study the role of pY14Cav1. Given the reported role of PTPs in regulating Cav1 phosphorylation (Caselli *et al*, 2002), it is likely that they play a role in regulating pY14Cav1-dependent functions in cancers. In addition, not much is known about the role of PTPs in regulating Cav1 phosphorylation and function in cancers. We hence chose to target PTPs to study the role of pY14Cav1 in Cav1-expressing cancer cells.

To first test if PTPs are involved in regulating pY14Cav1 levels in our studies, cells were treated with the general PTP inhibitor pervanadate. At a concentration of 10 $\mu$ M, T24, DU145, Calu1 and SKOV3 all show a robust increase in pY14Cav1 levels, whereas UMUC3 showed a modest increase (Fig. 3.3A-D). These 4 cell lines showing highest increase could hence be good candidates for testing the role of pY14Cav1 in cancers. Interestingly, pervanadate treatment of suspended WTMEFs promotes Cav1 Tyr14 phosphorylation significantly more than in adherent cells. Pervanadate treatment (4 $\mu$ M) causes a ~55% increase in pY14Cav1 in adherent cells (Fig. 3.3E), relative to ~70% increase with much lesser pervanadate (1 $\mu$ M) in suspended cells. Thus pervanadate treatment is able to better recover the in pY14Cav1 levels in suspended cells, even surpassing those in adherent cells (Fig. 3.3E). This suggests a role for PTPs in regulating Cav1 phosphorylation in suspension, and could help evaluate the role of Cav1 phosphorylation in regulating adhesion-dependent signaling by targeting endogenous pY14Cav1.

Given the involvement of PTPs in regulating Cav1 phosphorylation, we shortlisted PTPs to evaluate their role in cancers, based on 1) if they are associated with caveolae, 2) if they interact with Cav1, 3) if they can dephosphorylate pY14Cav1, or 4) if they are regulated by adhesion. Shortlisting of a PTP was done if they fulfilled two out of four of the above criteria, and 8 such PTPs were selected accordingly (Fig. 3.4A). We next checked the expression levels of these PTPs in the 4 cell lines listed above (done by Neha Deshpande). Quantitative RT-PCR showed a characteristic expression pattern for most of the PTPs despite these cancer cells being of different origins (Fig. 3.5B). Expression of PTP1B, PRL1 and PRL2 was seen to be consistently high across cell lines, these 3 PTPs were hence chosen to test for their involvement in regulation of pY14Cav1.

PTP1B, PRL1 and PRL2 were targeted using siRNA-mediated knockdowns (KD) using SMARTPool oligos (Dharmacon) in T24, DU145, Calu1 and SKOV3 cells, and the effect of their knockdown (individually or in combination) on pY14Cav1 levels was compared. While individual PTP KDs show an increase in pY14Cav1 levels (not statistically significant), knockdown of all 3 PTPs (Triple KD) shows a statistically significant almost 4-fold increase in pY14Cav1 levels in T24 cells (Fig. 3.5A). This suggests a joint role for these PTPs in regulating pY14Cav1 in T24 cells. SMARTPool oligos against individual PTPs had minimal non-specific effects as detected by mRNA levels (Fig. 3.5B). It is also worth noting that knockdown of a PTP did not compensate for or affect expression of other PTPs (Fig. 3.5B). Loss of PTP1B and PRL1 in DU145 cells showed a statistically significant ~2.5 fold increase in pY14Cav1 levels, though this was much less than that observed in T24 cells (4-fold) (Fig. 3.5C). Knockdown of PTPs in Calu1 (data not shown) and SKOV3 cells does not affect pY14Cav1 levels (Fig. 3.5E), suggesting their regulation of pY14Cav1 to be distinctly different than in T24 cells. These studies indicate that the relative role of PTPs in regulating Cav1 phosphorylation could be variable across cancers.

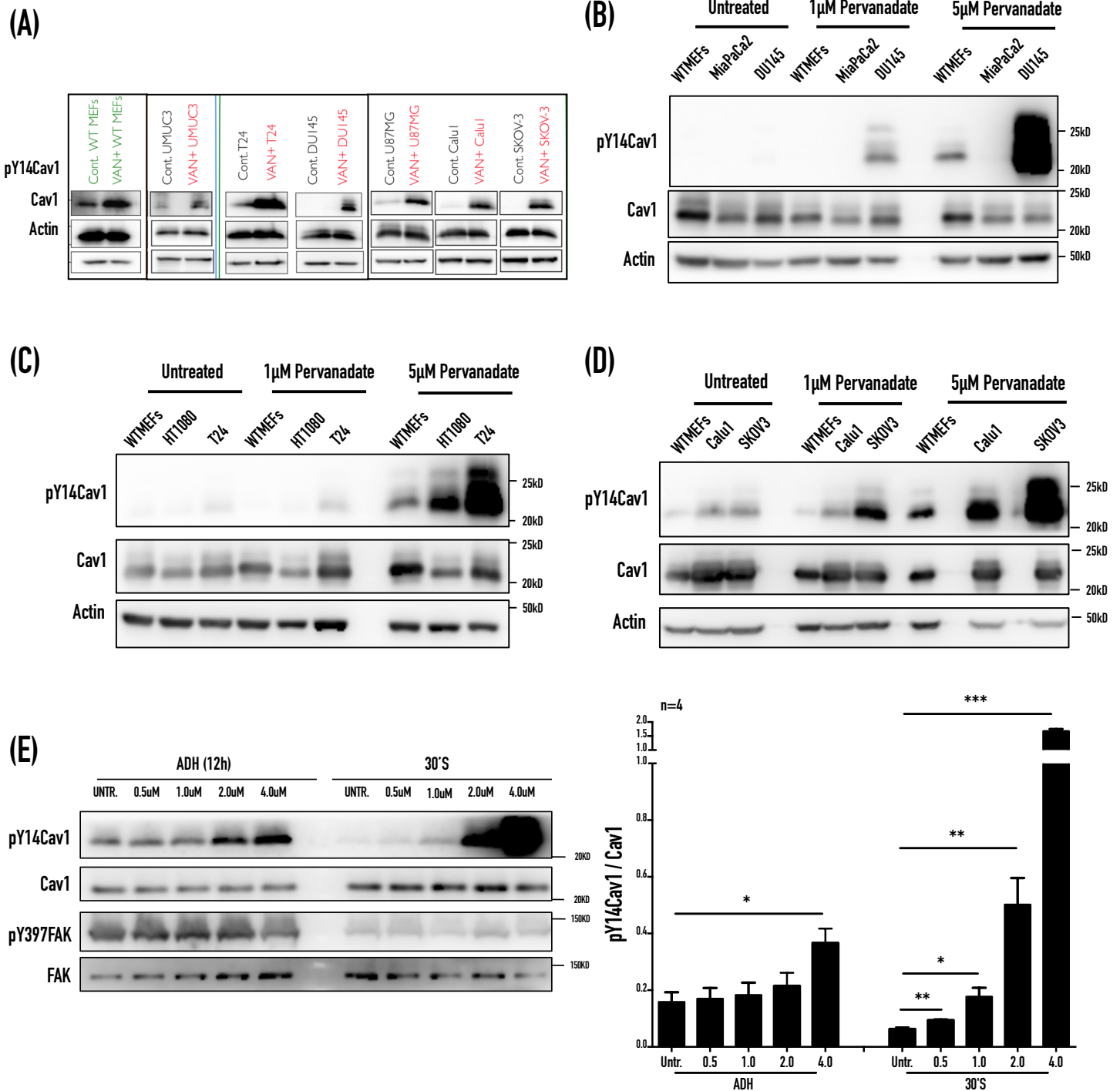
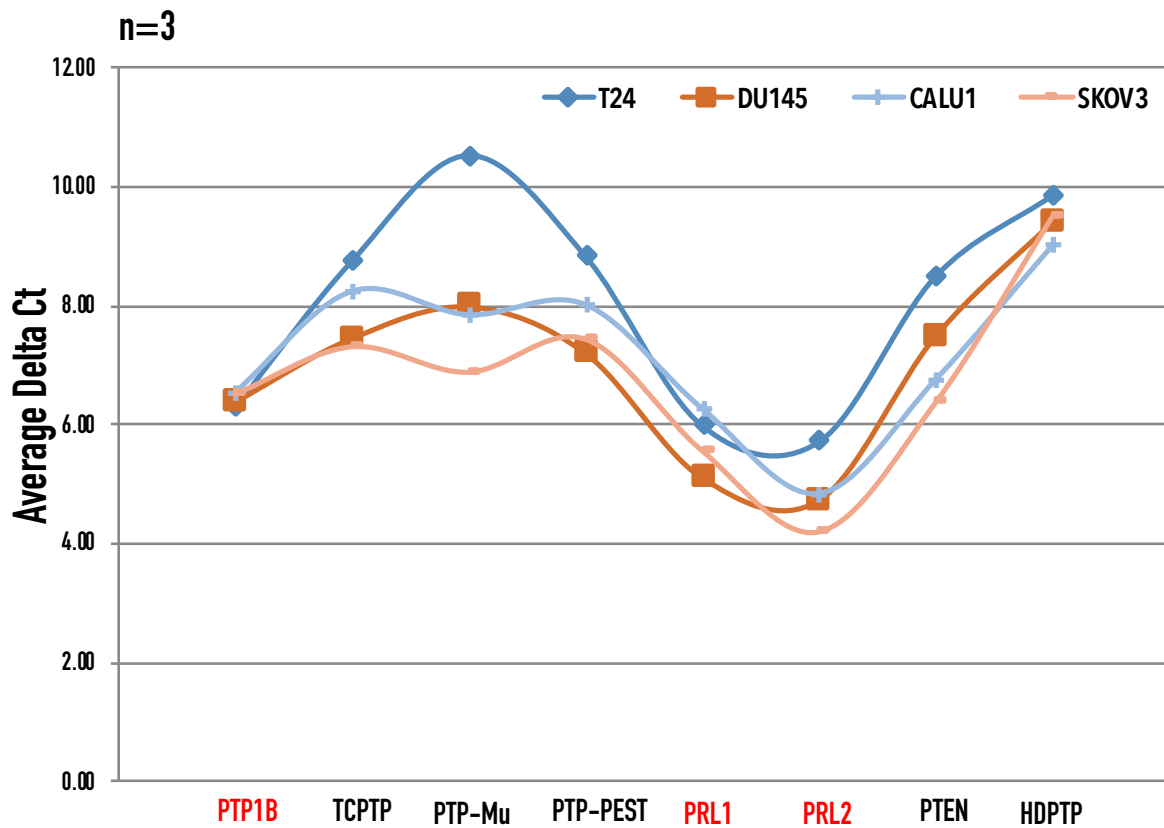


**Figure 3.3. Pervanadate treatment in cancer cells suggests PTP-dependent regulation of Cav1 phosphorylation.** (A) Western blot analysis of phosphorylated and total Cav1 from adherent UMUC3, SKOV3, Calu1, DU145, T24 and U87MG cells treated with pervanadate, as mentioned. (B-D) Western blot analysis of phosphorylated and total Cav1 from cells treated with pervanadate at different concentrations (1μM and 5μM), as mentioned. (E) Western blot analysis of phosphorylated and total Cav1 and FAK from adherent (ADH) and suspended (30'SUSP) WTMEFs treated with different concentrations of pervanadate. Graph on the right represents densitometry analysis of Western blotting data from 4 independent experiments, with ratios of band intensities of phosphorylated to total Cav1 plotted as mean ± SE. Statistical analysis was done using unpaired two-tailed t-test.

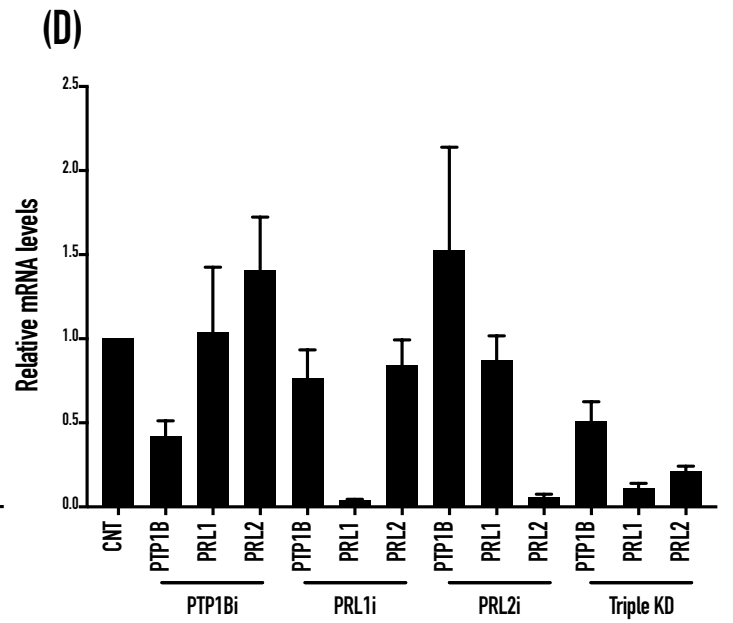
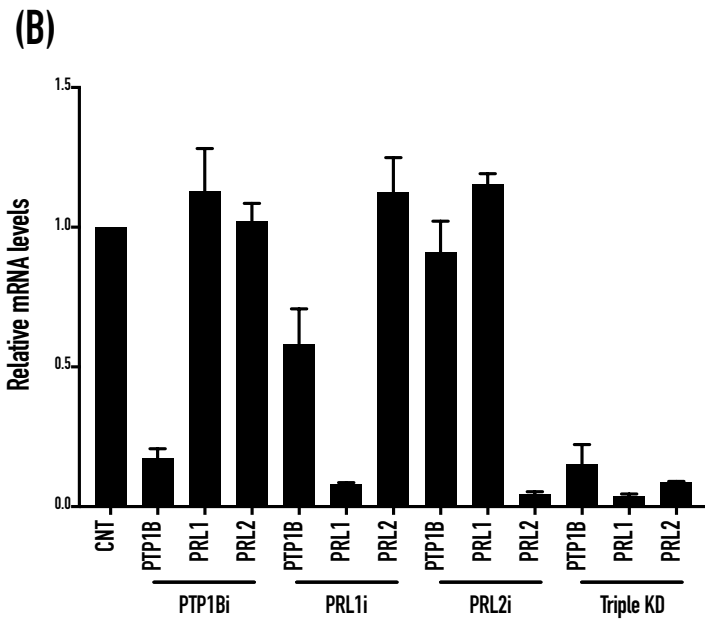
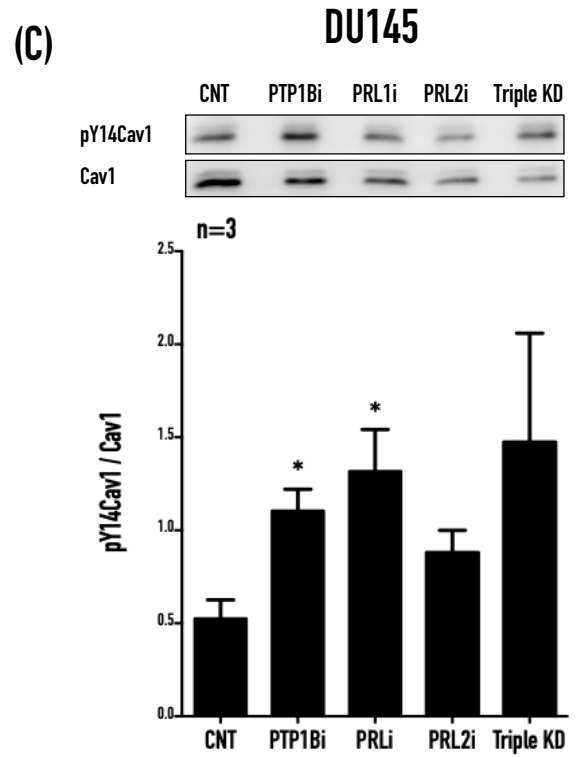
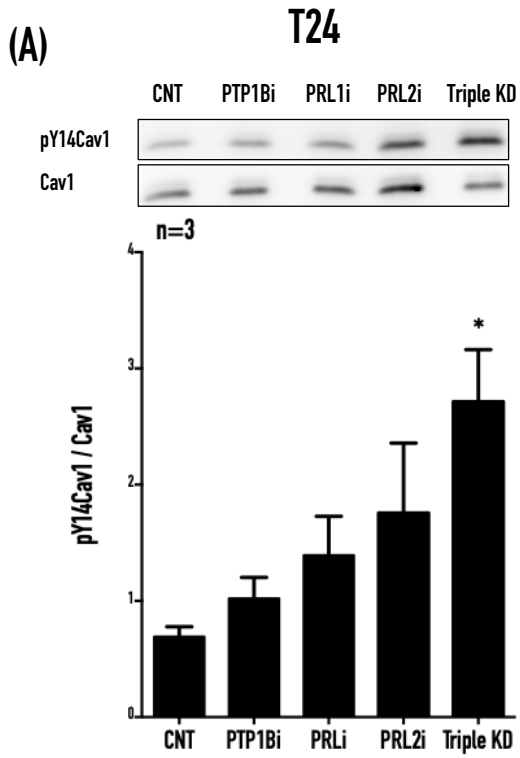
(A)

PTP	Localisation in caveolae	Localisation in rafts	Regulated by adhesion	Expressed in cancers
PTP1B	+	+	+	+
TCPTP	+		+	+
PTP-mu	+		+	+
PTP-PEST			+	+
PRL1			+	+
PRL2			+	+
PTEN		+	+	+
HDPTP			+	+

(B)



**Figure 3.4. Expression profiling of PTPs in Cav1-expressing cancer cells.** (A) List of shortlisted PTP candidates to study their involvement in regulation of pY14Cav1 levels and function. (B) Expression profile of PTPs across various cancer cell lines using quantitative RT-PCR. Graph represents mean  $\pm$  SE of Delta Ct values from three independent experiments. Expression profiling studies done by Neha Deshpande.



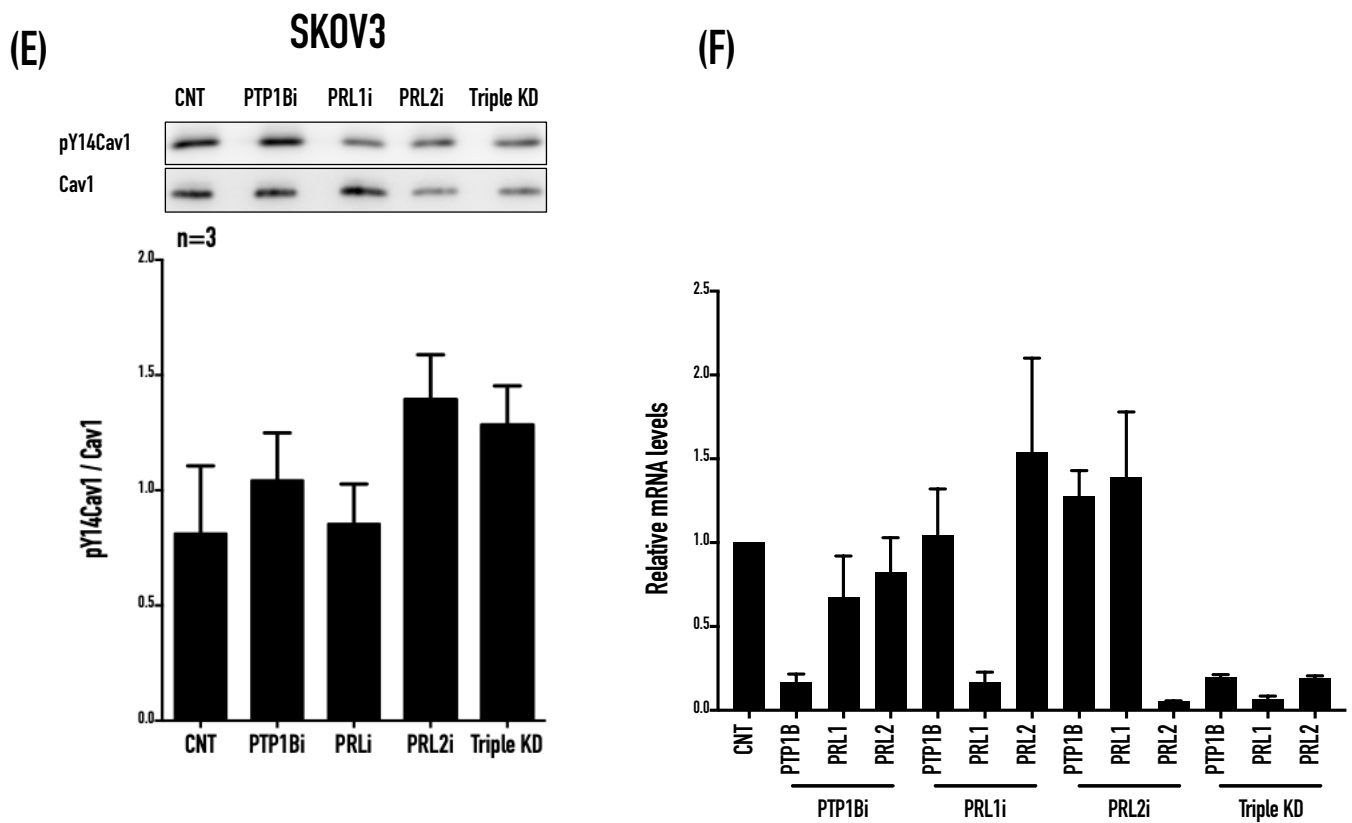


**Figure 3.5. PTPs regulate pY14Cav1 levels in Cav1-expressing cancer cell lines T24 and DU145.** Western blot analysis of phosphorylated and total Cav1 in T24 (A), SKOV3 (C) and DU145 (E) cells lacking PTP1B, PRL1 and PRL2, as mentioned. Graphs represent densitometry analysis of Western blotting data from three independent experiments, with ratios of band intensities of phosphorylated to total Cav1 plotted as mean $\pm$ SE. Statistical analysis was done using unpaired two-tailed t-test. (B, D, F, H) Knockdown efficiency of PTP1B, PRL1 and PRL2 in above cell lines, detected using quantitative RTPCR. Transcript (mRNA) levels of respective PTPs in siRNA-mediated knockdown of PTP1B, PRL1 and PRL2 compared to control (CNT). Delta Delta Ct calculated relative to control was used to determine fold change in gene expression. Graph represents mean  $\pm$  SE of relative gene expression from three independent experiments.

### ***Role of PTP-mediated Cav1 phosphorylation in cancer cells***

Loss of cell-matrix adhesion leads to pY14Cav1-dependent endocytosis of raft microdomains (marked by GM1) through caveolae (Fig. 1.1), to regulate anchorage-dependent signaling and growth in fibroblasts (del Pozo *et al*, 2005). Interestingly, loss of adhesion in DU145 cells did not induce raft microdomain endocytosis (Fig. 3.6; CNT 0'S vs. 120'S). When, however, endogenous pY14Cav1 levels were increased by knockdown of PTP1B or PRL1 (Fig. 3.5C), surface GM1 levels in these cells significantly decreased in suspension (Fig. 3.6; PTP1Bi and PRL1i 0'S vs. 120'S). Pervanadate treatment, also known to increase pY14Cav1 levels (Fig. 3.3B), acts as a positive control and expectedly induced GM1 endocytosis (Fig. 3.6A, B; 1uM Vanadate 0'S vs. 120'S) (del Pozo *et al*, 2005). These results suggest PTP-mediated increase in pY14Cav1 levels to induce adhesion-dependent caveolar endocytosis of raft microdomains in DU145 cells. Ongoing studies aim to determine the effect of pY14Cav1-mediated caveolar endocytosis on anchorage-independent growth and cancer progression.

Loss of adhesion induces endocytosis of raft microdomains in T24 cells (Unpublished data: Archana Pawar and Nagaraj Balasubramanian). PTP-mediated increase in pY14Cav1 is hence likely to regulate functions other than caveolar endocytosis in these cells. It was hence interesting to ask whether loss of PTPs and the resulting high pY14Cav1 levels can be sustained in non-adherent T24 cells, and whether this could sustain *anchorage-independent* signaling. For this, we knocked down the 3 PTPs (Triple KD, that significantly increases pY14Cav1 levels) in these cells to test their effect on pY14Cav1 and anchorage-independent signaling in suspension. We see a significant increase in pY14Cav1 in suspension in Triple KD cells relative to control (Fig. 3.7A). Interestingly, we also see sustained Akt and Erk activation in suspended T24 cells upon Triple PTP KD relative to control (Fig. 3.7B, C). This could in part be mediated by increased pY14Cav1 levels in Triple KD cells, something ongoing studies in the lab aim to understand.



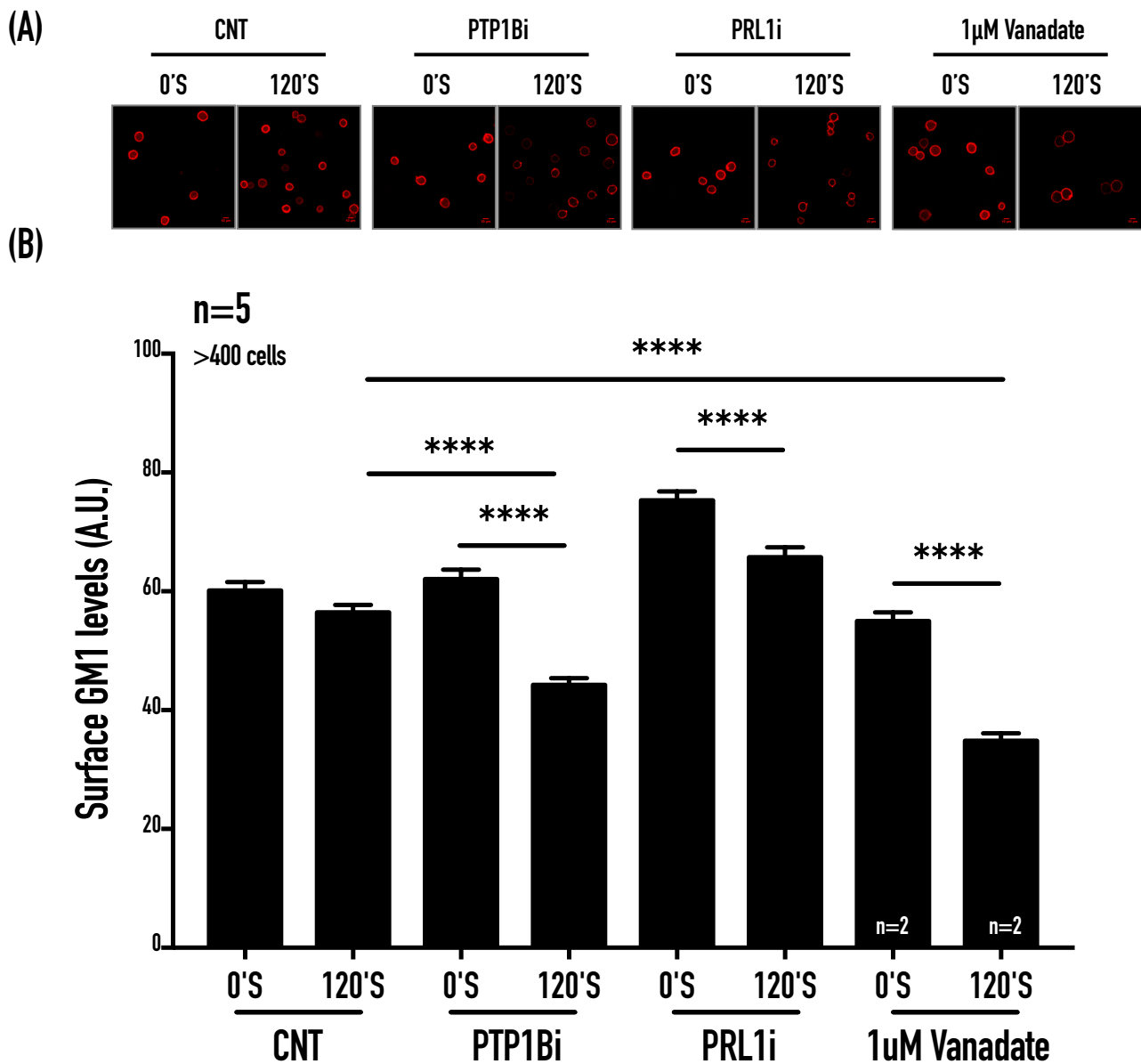


**Figure 3.6. PTP-mediated regulation of Cav1 phosphorylation regulates adhesion-independent GM1 endocytosis in DU145 cells.** A) Cell surface GM1 levels in detached (0'S) and suspended (120'S) DU145 cells lacking PTP1B, PRL1 or PRL2, compared to control (CNT), as mentioned. 1uM pervanadate treated CNT cells act as positive control for GM1 surface levels. (B) Fluorescence intensity of surface GM1 quantitated using integrated density from ImageJ software, plotted as mean  $\pm$  SE from five independent experiments. Statistical analysis was done using unpaired two-tailed t-test.

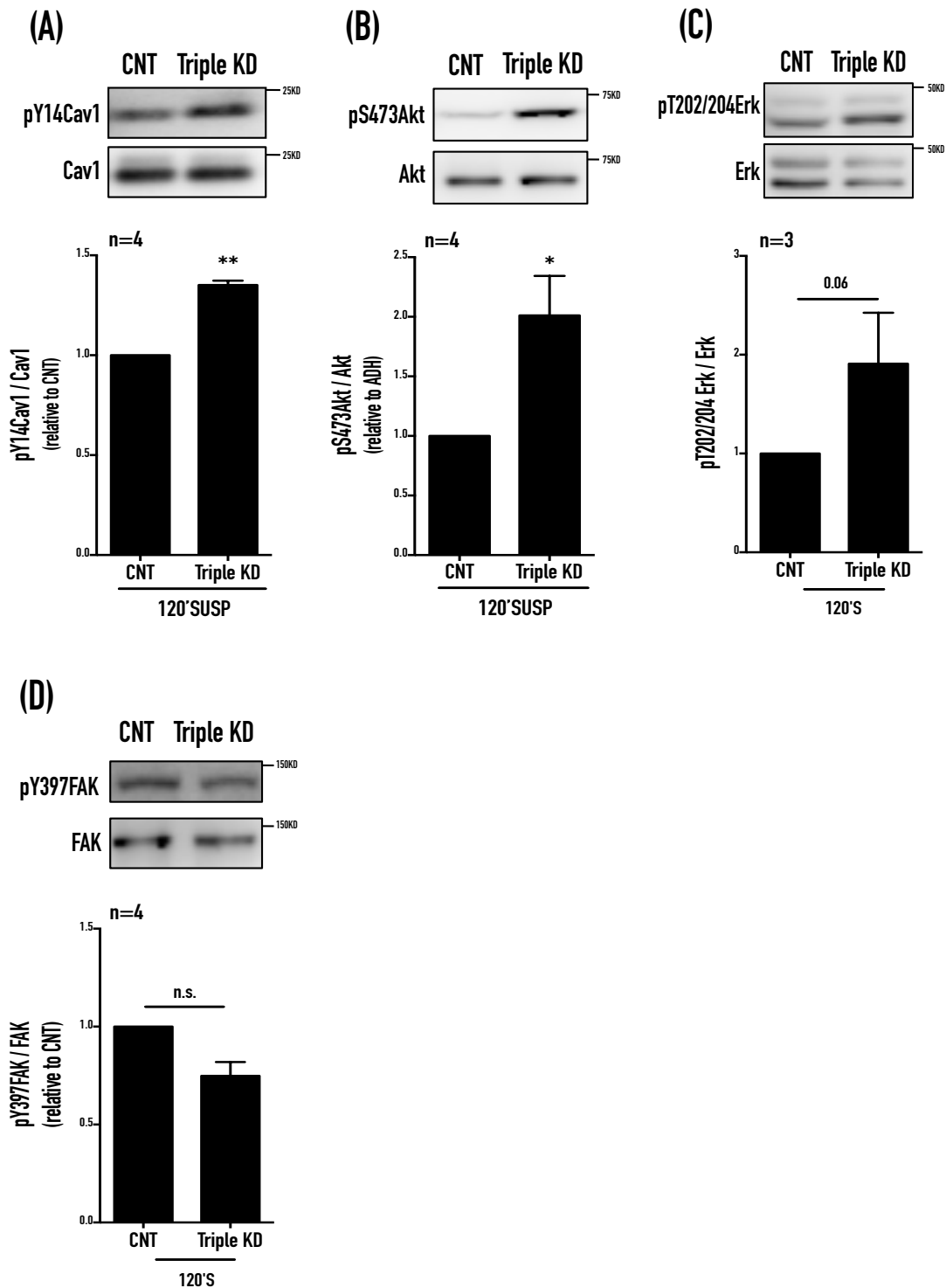


**Figure 3.7. PTP-mediated regulation of Cav1 phosphorylation regulates adhesion-independent Akt and Erk activation in T24 cells.** Western blot analysis of phosphorylated and total Cav1 (A), Akt (B), Erk (C) and FAK (D) in non-adherent (120min suspended) T24 cells lacking all three PTPs - PTP1B, PRL1 and PRL2 (Triple KD). Graphs represent densitometry analysis of Western blotting data from four independent experiments, with ratios of band intensities of phosphorylated to respective total protein plotted as mean  $\pm$  SE. Statistical analysis was done using unpaired two-tailed t-test. Knockdown efficiency of PTP1B, PRL1 and PRL2 in Triple KD T24 cells, detected using quantitative RTPCR was 83%, 93% and 96% respectively. Graphs represents mean  $\pm$  SE of relative gene expression from three independent experiments.

## DISCUSSION

---

The dual role of Cav1 in cancers has been ascribed to its expression at a particular stage or in specific cancer types. Cav1 expression is reported to be reduced in cancers of the lung, colon, ovary, and in glioblastoma (Campos *et al*, 2019). In terms of stage-dependence, Cav1 could function as a tumor suppressor in early stages of the disease, while donning a tumor promoting role in at later stages (Urta *et al*, 2012; Ortiz *et al*, 2016; Nunez-Wehinger *et al*, 2014). Cav1 expression in later stages of some cancers, like prostate, melanoma, breast and thyroid cancers, is known to cause enhanced malignancy, multi-drug resistance and metastasis (Campos *et al*, 2019). Cav1 is absent in normal prostate tissue, but is expressed at high levels and favours metastasis in prostate cancers (Williams *et al*, 2005). These seemingly contradictory roles for Cav1 in cancers could be attributed to and arise from multiple factors, including but not limited to: 1) status of Cav1 Tyr14 phosphorylation, 2) cellular localisation, 3) extracellular cues.

Indeed, Cav1 protein was discovered through a study implicating its phosphorylation to be required for transformation in Rous sarcoma virus-infected fibroblasts (Glenney & Soppet, 1992). We wanted to further explore this role and regulation and hence did a screen for pY14Cav1 levels in Cav1-expressing cancer cell lines, and find a diverse range of pY14Cav1 expression (Fig. 3.1). Anchorage-independent signaling and growth is one of the hallmarks of cancers. Given that pY14Cav1 is regulated by adhesion in fibroblasts (Fig. 1.2, 1.3), we tested this regulation in 5 Cav1-expressing cancer cell lines. Interestingly, 2 cell lines among these, SKOV3 (ovarian cancer cells) and DU145 (prostate) show adhesion-independent regulation of pY14Cav1; whereas T24 (bladder), Calu1 (lung) and UMUC3 (bladder) show adhesion-dependent regulation of pY14Cav1. Basal levels of Cav1 phosphorylation hence do not seem to dictate whether it is regulated by adhesion. We further see an adhesion-dependent correlation between Cav1 phosphorylation and Akt activation in some of these cell lines. Decreased Cav1 phosphorylation correlates with decreased Akt activation in non-adherent T24, Calu1 and UMUC3; whereas sustained Cav1 phosphorylation correlates with sustained Akt activation in non-adherent SKOV3 cells (Fig. 3.2).

Indeed, Cav1 phosphorylation is reported to promote Akt and Erk activation, in turn promoting cell proliferation, migration, and invasion in various cancers including rhabdomyosarcoma (Faggi *et al*, 2014) and metastatic in breast cancer cell line MDA-MB-231 (Yang *et al*, 2016). The mechanism for activation of these pathways could be *via* Cav1-mediated (CSD-dependent) binding and inhibition of serine/threonine protein phosphatases PP1 and PP2A, which in turn leads to increased activation of PDK1, Akt and Erk1/2 and decreased apoptosis, as studied in

prostate cancer cell line LNCaP (Li *et al*, 2003). We also see the adhesion-dependent regulation of pY14Cav1 levels to correlate with Akt activation in T24 and SKOV3 cells our studies (Fig. 3.2).

Targeting of PTPs by siRNA-mediated knockdowns in Cav1-expressing cancer cells allows us to modulate the phosphorylation of endogenous Cav1 (Fig. 3.5), without having to resort to overexpression systems and associated caveats (Pol *et al*, 2020). PTP KDs lead to increased pY14Cav1 levels in adherent and non-adherent T24 cells (Fig. 3.5, 3.7). Increase in Cav1 phosphorylation also concomitantly leads to increased Akt and Erk activation in these cells, (without affecting phosphorylation of an unrelated protein FAK) (Fig. 3.7). This could be mediated by the mechanism suggested above, and help cells sustain anchorage-independent survival and growth. In SKOV3 cells on the other hand, Cav1 phosphorylation is not dependent on PTPs, and could instead be regulated by kinases. At the least, our results suggest the highest expressors PTP1B, PRL1 and PRL2 to not be involved in regulation of pY14Cav1 in these cells. SKOV3 is an ovarian cancer cell line known to express estrogen receptor ER $\alpha$ , its growth enhanced by exposure to estrogen (Rothenberger *et al*, 2018; Chan *et al*, 2014). Cav1 phosphorylation is also known to be regulated by hormonal growth factors (Mastick *et al*, 1995), including estrogen (Kiss *et al*, 2005). It is hence very likely that Cav1 phosphorylation in SKOV3 cells overrides adhesion-dependence due to its incumbent hormonal regulation, a possibility that needs to be explored further.

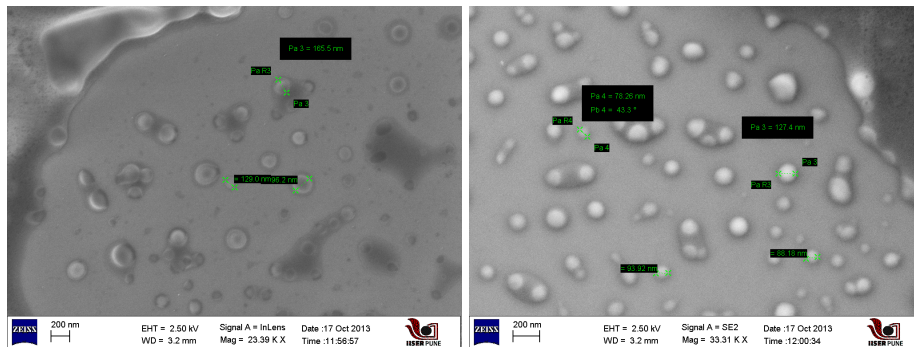
In DU145 cells, pY14Cav1 could regulate caveolar endocytosis (Fig. 3.6). pY14Cav1 has recently been shown to be indispensable for caveolae-dependent endocytosis of the antibody-drug conjugate trastuzumab-emtansine (T-DM1) and resultant cytotoxicity in HER2-positive breast cancer cells (Chandran *et al*, 2020). T-DM1 therapy has shown improved survival in treatment of patients with locally advanced or metastatic HER2-positive breast cancer and HER2-positive lung cancer (von Minckwitz *et al*, 2019; Li *et al*, 2018). Despite the clinical efficacy, one of the limiting factors of T-DM1 therapeutic efficacy is acquired drug-resistance, and conditions like hypoxia that reduce Cav1 phosphorylation could be one of the major reasons for reduced treatment efficacy (Chandran *et al*, 2020). Further studies are needed to understand whether pY14Cav1-mediated regulation of GM1 endocytosis in DU145 cells (Fig. 3.6) could have implications in endocytosis and surface availability of cell surface receptors including HER2, in turn affecting cancer cell survival and progression.

pY14Cav1 localises to both caveolae and focal adhesions (Buwa *et al*, 2020a). This phosphorylation could potentially be regulated in Cav1-expressing cancers to block caveolar

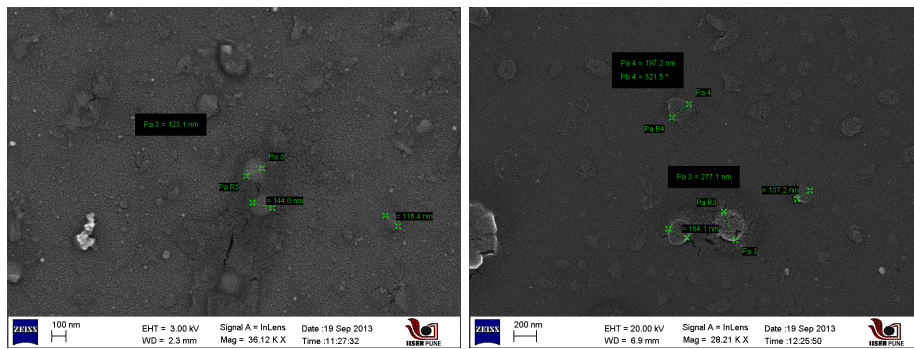
endocytosis (Chandran *et al*, 2020), and/or support focal adhesion-mediated migration and invasion (Joshi *et al*, 2008; Goetz *et al*, 2008a). Some cancer cells like PC-3 (prostate) express Cav1 but lack Cavin1 (Hill *et al*, 2008), and hence cannot form caveolae. Cav1 is upregulated in patient samples with advanced prostate cancers, and could have a tumorigenic role in these cancer cells (Moon *et al*, 2014). Increased Cav1 expression is indeed known to saturate the system, increasing non-caveolar Cav1 and potentially mimicking the *disruption of caveolae*, as seen upon Cavin downregulation or cholesterol sequestration (Parton & Howes, 2010). Moreover, re-expression of Cavin1 in these cells inhibits their anchorage-independent growth, migration and metastasis in mice (Meng *et al*, 2015, 2017; Moon *et al*, 2014). This suggests a tumorigenic role for *non-caveolar* Cav1, which is “neutralised” by Cavin1 expression. On the other hand, caveolar endocytosis, dependent on its phosphorylation, regulates surface availability of receptors like HER2 (Chandran *et al*, 2020). Although these studies implicate pY14Cav1 in mediating drug-resistance in cancer cells, HER2 endocytosis could entail decreased activation (*via* degradation) and shredding of the receptor due to its internalisation (Cheng *et al*, 2020), and could be pY14Cav1-mediated. Regulation of surface receptor levels is likely a role mediated at caveolae, and dependent on *caveolar* pY14Cav1. It is thus likely that the role of Cav1 and pY14Cav1 as a tumour suppressor or promoter could in part be mediated by its *sub-cellular localisation* in *vs* outside of caveolae. It is hence indeed vital to understand the distribution of pY14Cav1 in caveolae relative to non-caveolar sites like FAs in cancers. This aspect could be key to resolving the contentious role of pY14Cav1 and Cav1 in cancers, something ongoing studies in the lab aim to help understand.

# Appendix

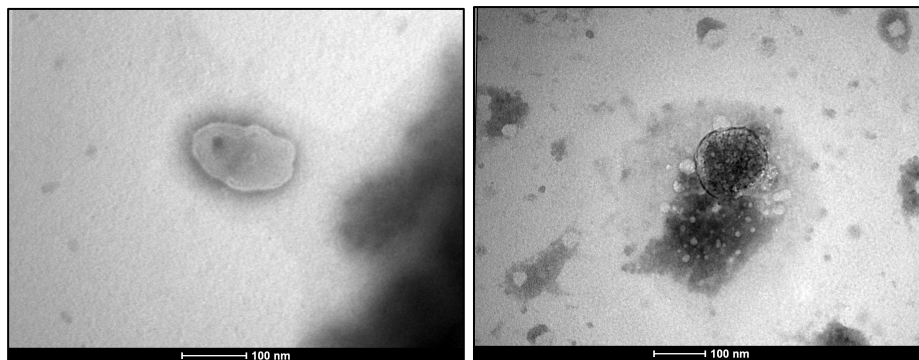
(A)



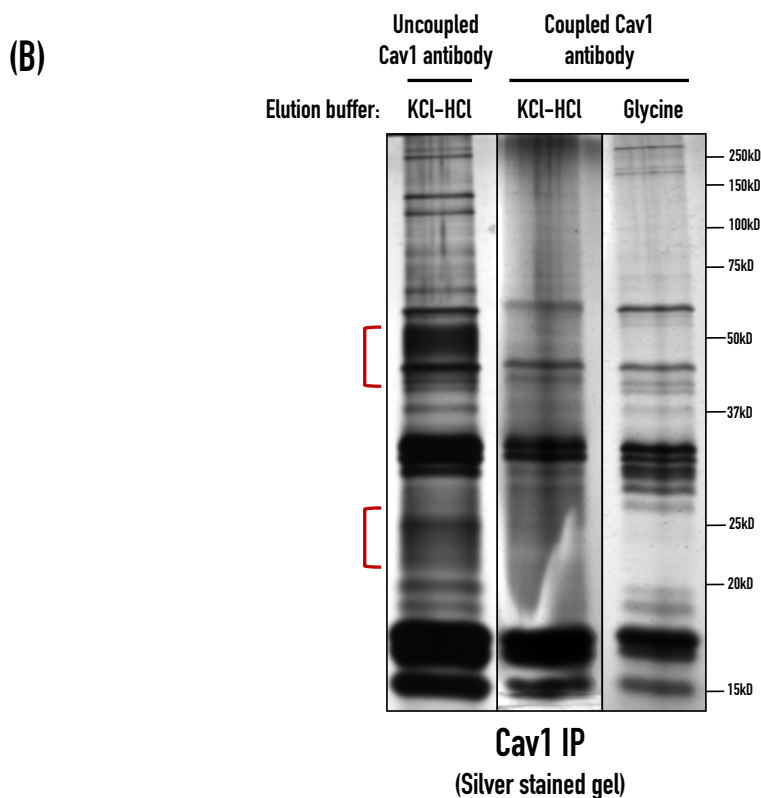
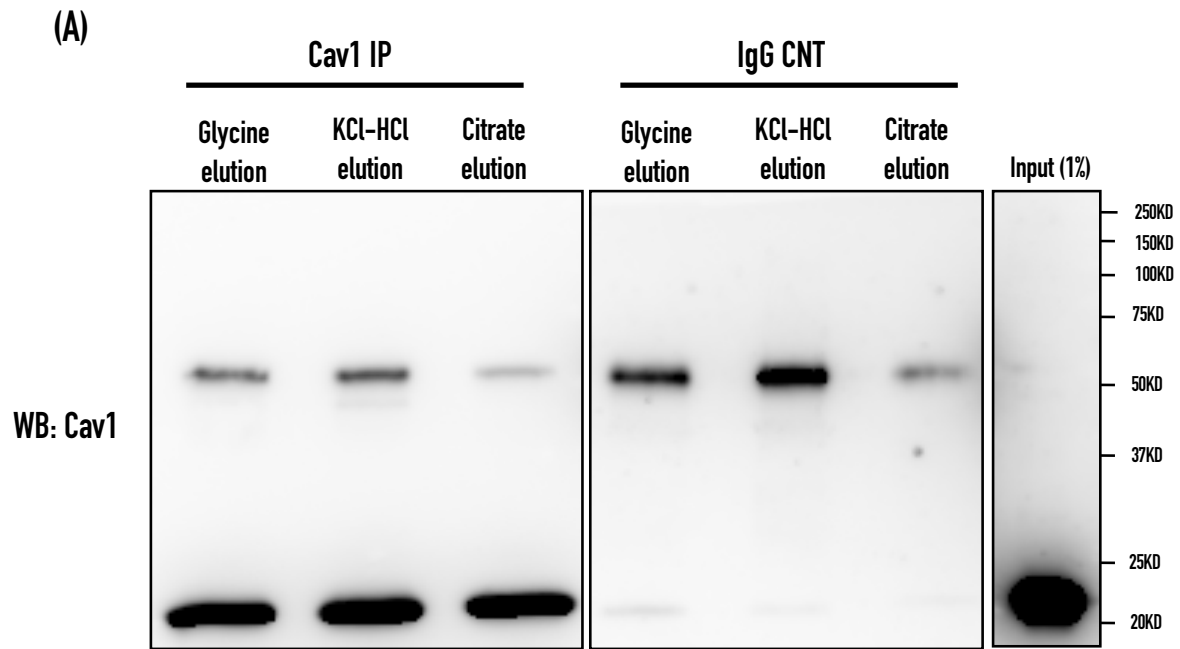
(B)



(C)

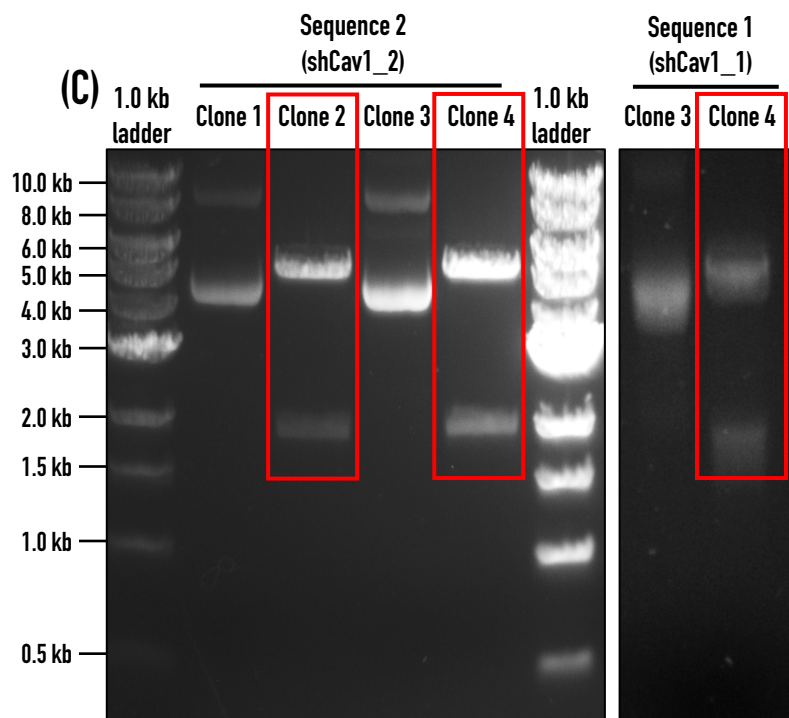
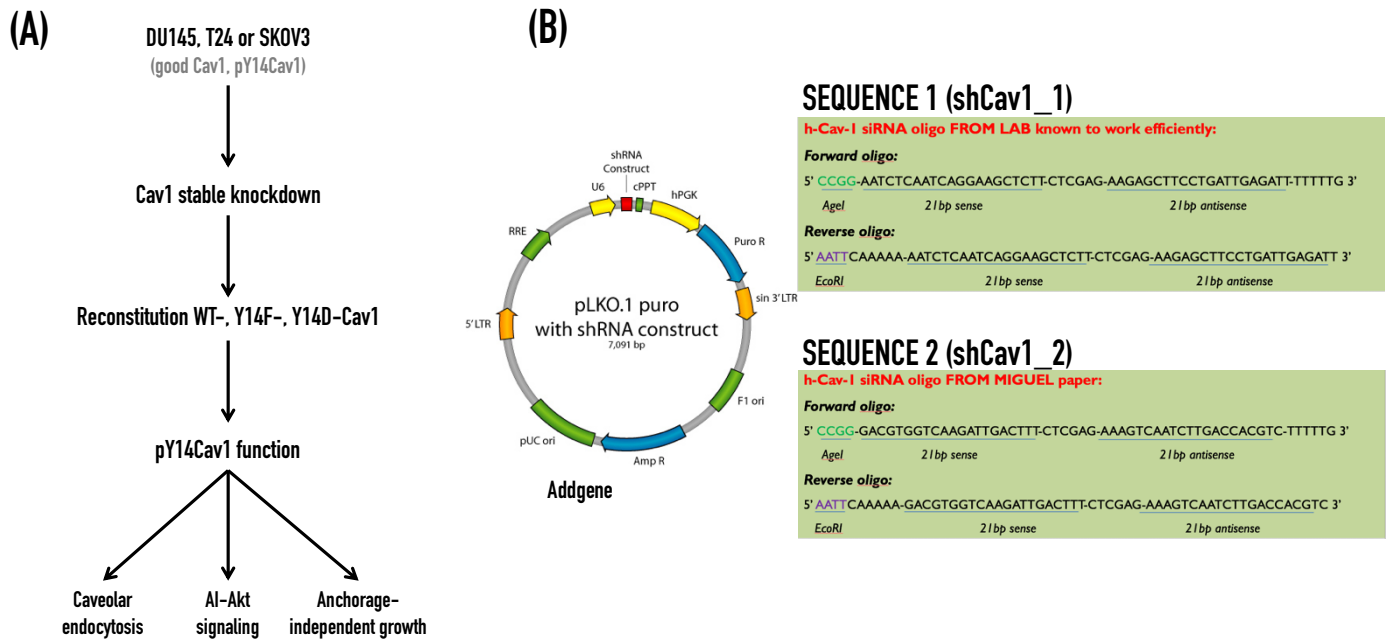


**Appendix Figure 1. Electron Microscopy (FESEM and TEM) of caveolae isolated from WTMEFs.** (A) FESEM of CM2 – CM2 scraped in DPBS, placed on silicon wafers and vacuum-dried, no gold sputter-coating. (B) FESEM of CM2 – CM2 scraped in DPBS, placed on silicon wafers and vacuum-dried followed by 10nm gold sputter-coating. (C) CM2 preps mounted on TEM grids and negative-stained with Phosphotungstic acid. Imaging at 120kV, TEM at NIV. Scale bars are represented in each image.



**Appendix Figure 2. Standardization of Cav1 IP to isolate Cav1-binding proteins from caveolae with minimal background/IgG elution.** (A) Cav1 was immunoprecipitated from PNS obtained from adherent WTMEFs, using Cav1 N20 antibody coupled to Dynabeads (Invitrogen Dynabeads antibody coupling kit), and compared to mouse IgG control on Western blots. Immunoprecipitated protein was eluted using mild elution buffers Glycine, KCl-HCl or Citrate, as indicated. Input represents PNS from WTMEFs used for IP. Results are representative of at least three independent experiments. (B) Cav1 antibody coupled to Dynabeads or uncoupled was used to immunoprecipitate Cav1 as above and subjected to PAGE. Silver staining profiles of Cav1 IP eluates show considerably less elution of IgG in coupled beads compared to uncoupled ones. IgG heavy and light chains (smear bands at ~50kD and ~25kD) eluted in uncoupled IP are marked by red brackets. This method could be used to IP Cav1-binding proteins from isolated caveolae, followed by proteomic analyses of the immune-complexes, to determine proteins differentially recruited to caveolae from adherent *vs* suspended cells.

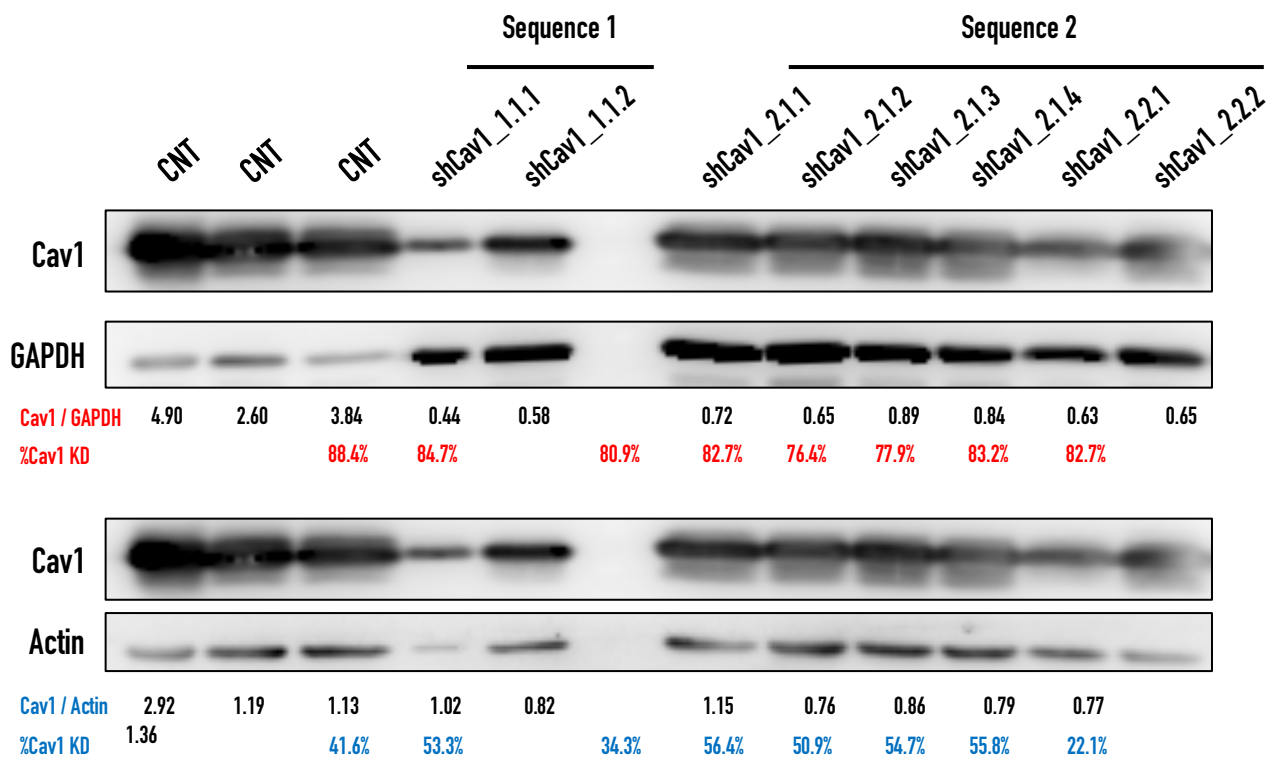




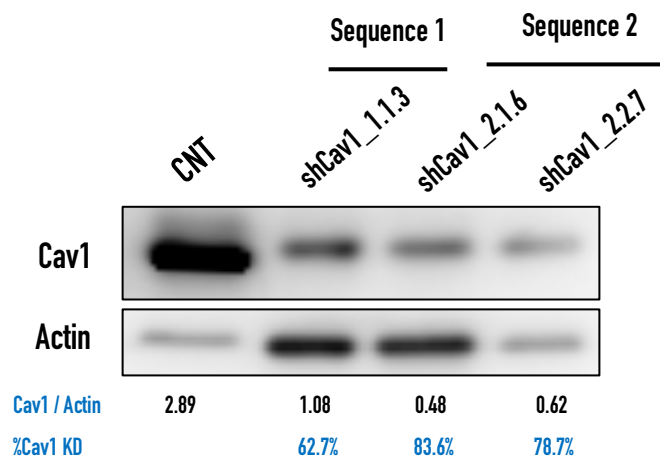
**Appendix Figure 3. Cloning of Cav1 shRNA oligos into stable expression vector pLKO.1.** (A) Strategy outlined for stable Cav1 KD and reconstitution with Cav1 variants in DU145, T24 and SKOV3 cells. (B) Vector map and shRNA oligo sequences (2 oligos) used. (C) shRNA oligos were cloned in the vector backbone using restriction digestion and run on 1% agarose gels. Gel images represent screening of positive clones represented by release of 2kb and 5kb fragments upon digestion with EcoRI and NcoI. Positive clones are represented by red boxes.

(A)

Cav1 KD in puromycin-resistant SKOV3 colonies



(B)



**Appendix Figure 4. shRNA-mediated stable Cav1 knockdown in SKOV3 cells – Screening of positive colonies.** (A), (B) Puromycin-resistant SKOV3 colonies were screened for Cav1 knockdown using Western blotting detection of Cav1. Clone nomenclature: shCav1\_1.1.2: siRNA sequence 1\_bacterial clone 1\_puromycin colony 2.

# References

- Aboulaich N, Vainonen JP, Strålfors P & Vener A V. (2004) Vectorial proteomics reveal targeting, phosphorylation and specific fragmentation of polymerase I and transcript release factor (PTRF) at the surface of caveolae in human adipocytes. *Biochem. J.* **383**: 237–248
- Aoki S, Thomas A, Decaffmeyer M, Brasseur R & Epanand RM (2010) The role of proline in the membrane re-entrant helix of caveolin-1. *J. Biol. Chem.* **285**: 33371–33380
- Apodaca G (2002) Modulation of membrane traffic by mechanical stimuli. *Am. J. Physiol. - Ren. Physiol.*
- Ariotti N & Parton RG (2013) SnapShot: caveolae, caveolins, and cavins. *Cell* **154**: 704-704.e1 Available at: <http://dx.doi.org/10.1016/j.cell.2013.07.009>
- Ariotti N, Rae J, Leneva N, Ferguson C, Loo D, Okano S, Hill MM, Walser P, Collins BM & Parton RG (2015) Molecular characterization of caveolin-induced membrane curvature. *J. Biol. Chem.* **290**: 24875–24890
- Arthur WT & Burridge K (2001) RhoA inactivation by p190RhoGAP regulates cell spreading and migration by promoting membrane protrusion and polarity. *Mol. Biol. Cell* **12**: 2711–2720
- Aung CS, Hill MM, Bastiani M, Parton RG & Parat MO (2011) PTRF-cavin-1 expression decreases the migration of PC3 prostate cancer cells: Role of matrix metalloprotease 9. *Eur. J. Cell Biol.* **90**: 136–142 Available at: <http://dx.doi.org/10.1016/j.ejcb.2010.06.004>
- Baker BM & Chen CS (2012) Deconstructing the third dimension-how 3D culture microenvironments alter cellular cues. *J. Cell Sci.* **125**: 3015–3024
- Balasubramanian N, Meier JA, Scott DW, Norambuena A, White MA & Schwartz MA (2010) RalA-Exocyst Complex Regulates Integrin-Dependent Membrane Raft Exocytosis and Growth Signaling. *Curr. Biol.*
- Bass MD, Williamson RC, Nunan RD, Humphries JD, Byron A, Morgan MR, Martin P & Humphries MJ (2011) A Syndecan-4 Hair Trigger Initiates Wound Healing through Caveolin- and RhoG-Regulated Integrin Endocytosis. *Dev. Cell*
- Bastiani M, Liu L, Hill MM, Jedrychowski MP, Nixon SJ, Lo HP, Abankwa D, Luetterforst R, Fernandez-Rojo M, Breen MR, Gygi SP, Vinten J, Walser PJ, North KN, Hancock JF, Pilch PF & Parton RG (2009) MURC/Cavin-4 and cavin family members form tissue-specific caveolar complexes. *J. Cell Biol.* **185**: 1259–1273

- Beardsley A, Fang K, Mertz H, Castranova V, Friend S & Liu J (2005) Loss of caveolin-1 polarity impedes endothelial cell polarization and directional movement. *J. Biol. Chem.* **280**: 3541–3547
- Belli S, Esposito D, Servetto A, Pesapane A, Formisano L & Bianco R (2020) C-Src and EGFR inhibition in molecular cancer therapy: What else can we improve? *Cancers (Basel)*.
- Boettcher JP, Kirchner M, Churin Y, Kaushansky A, Pompaiah M, Thorn H, Brinkmann V, MacBeath G & Meyer TF (2010) Tyrosine-phosphorylated caveolin-1 blocks bacterial uptake by inducing Vav2-RhoA-mediated cytoskeletal rearrangements. *PLoS Biol.* **8**: 55–56
- Bollu LR, Mazumdar A, Savage MI & Brown PH (2017) Molecular pathways: Targeting protein tyrosine phosphatases in cancer. *Clin. Cancer Res.* **23**: 2136–2142 Available at: <https://pubmed.ncbi.nlm.nih.gov/28087641/> [Accessed March 1, 2021]
- Bonnans C, Chou J & Werb Z (2014) Remodelling the extracellular matrix in development and disease. *Nat. Rev. Mol. Cell Biol.*
- Boscher C & Nabi IR (2013) Galectin-3- and phospho-caveolin-1-dependent outside-in integrin signaling mediates the EGF mitogenic response in mammary cancer cells. *Mol. Biol. Cell* **24**: 2134–2145
- Bourseau-Guilmain E, Menard JA, Lindqvist E, Indira Chandran V, Christianson HC, Cerezo Magaña M, Lidfeldt J, Marko-Varga G, Welinder C & Belting M (2016) Hypoxia regulates global membrane protein endocytosis through caveolin-1 in cancer cells. *Nat. Commun.*
- Boyd NL, Park H, Yi H, Boo YC, Sorescu GP, Sykes M & Jo H (2003) Chronic shear induces caveolae formation and alters ERK and Akt responses in endothelial cells. *Am. J. Physiol. - Hear. Circ. Physiol.* **285**: 1113–1122
- Breen MR, Camps M, Carvalho-Simoes F, Zorzano A & Pilch PF (2012) Cholesterol depletion in adipocytes causes caveolae collapse concomitant with proteosomal degradation of cavin-2 in a switch-like fashion. *PLoS One* **7**: 2–9
- Burgener R, Wolf M, Ganz T & Baggiolini M (1990) Purification and characterization of a major phosphatidylserine-binding phosphoprotein from human platelets. *Biochem. J.* **269**: 729–734
- Buwa N, Kannan N, Kanade S & Balasubramanian N (2020a) Adhesion-dependent Caveolin-

- 1 Tyrosine-14 phosphorylation is regulated by FAK in response to changing matrix stiffness. *FEBS Lett.* **595**: 532–547
- Buwa N, Mazumdar D & Balasubramanian N (2020b) Caveolin1 Tyrosine-14 Phosphorylation: Role in Cellular Responsiveness to Mechanical Cues. *J. Membr. Biol.* **253**: 509–534 Available at: <https://doi.org/10.1007/s00232-020-00143-0>
- Caldieri G, Giacchetti G, Beznoussenko G, Attanasio F, Ayala I & Buccione R (2009) Invadopodia biogenesis is regulated by caveolin-mediated modulation of membrane cholesterol levels. *J. Cell. Mol. Med.*
- Calvo M, Tebar F, Lopez-Iglesias C & Enrich C (2001) Morphologic and functional characterization of caveolae in rat liver hepatocytes. *Hepatology*
- Campos A, Burgos-Ravanel R, González MF, Huilcaman R, González LL & Quest AFG (2019) Cell intrinsic and extrinsic mechanisms of caveolin-1-enhanced metastasis. *Biomolecules* **9**:
- Cao H, Courchesne WE & Mastick CC (2002) A phosphotyrosine-dependent protein interaction screen reveals a role for phosphorylation of caveolin-1 on tyrosine 14. Recruitment of C-terminal Src kinase. *J. Biol. Chem.* **277**: 8771–8774
- Capozza F, Williams TM, Schubert W, McClain S, Bouzahzah B, Sotgia F & Lisanti MP (2003) Absence of caveolin-1 sensitizes mouse skin to carcinogen-induced epidermal hyperplasia and tumor formation. *Am. J. Pathol.*
- Carey SP, Martin KE & Reinhart-King CA (2017) Three-dimensional collagen matrix induces a mechanosensitive invasive epithelial phenotype. *Sci. Rep.* **7**: Available at: </pmc/articles/PMC5301232/> [Accessed February 15, 2021]
- Caselli A, Mazzinghi B, Camici G, Manao G & Ramponi G (2002) Some protein tyrosine phosphatases target in part to lipid rafts and interact with caveolin-1. *Biochem. Biophys. Res. Commun.* **296**: 692–697
- Caselli A, Taddei ML, Bini C, Paoli P, Camici G, Manao G, Cirri P & Ramponi G (2007) Low molecular weight protein tyrosine phosphatase and caveolin-1: Interaction and isoenzyme-dependent regulation. *Biochemistry*
- Chan KKL, Leung THY, Chan DW, Wei N, Lau GTY, Liu SS, Siu MKY & Ngan HYS (2014) Targeting estrogen receptor subtypes (ER $\alpha$  and ER $\beta$ ) with selective ER modulators in ovarian cancer. *J. Endocrinol.* **221**: 325–336 Available at:

<https://pubmed.ncbi.nlm.nih.gov/24819599/> [Accessed February 11, 2021]

- Chandran VI, Ma A-S, Barbachowska M, Cerezo-Maga~ Na M, Orn Nodin B, Joshi B, Koppada N, Saad OM, Gluz O, Isaksson K, Borgquist S, Jirstr€ Om K, Nabi IR, Jernstr€ Om H & Belting M (2020) Hypoxia Attenuates Trastuzumab Uptake and Trastuzumab-Emtansine (T-DM1) Cytotoxicity through Redistribution of Phosphorylated Caveolin-1 A C. *Mol. Cancer Res.* **18**: 644–656 Available at: <http://mcr.aacrjournals.org/>
- Chaudhary N, Gomez GA, Howes MT, Lo HP, McMahon KA, Rae JA, Schieber NL, Hill MM, Gaus K, Yap AS & Parton RG (2014) Endocytic Crosstalk: Cavins, Caveolins, and Caveolae Regulate Clathrin-Independent Endocytosis. *PLoS Biol.* **12**:
- Cheng J, Liang M, Carvalho MF, Tigue N, Faggioni R, Roskos LK & Vainshtein I (2020) Molecular Mechanism of HER2 Rapid Internalization and Redirected Trafficking Induced by Anti-HER2 Biparatopic Antibody. *Antibodies* **9**: 49 Available at: <https://pubmed.ncbi.nlm.nih.gov/32961882/> [Accessed March 12, 2021]
- Cheng JPX, Mendoza-Topaz C, Howard G, Chadwick J, Shvets E, Cowburn AS, Dunmore BJ, Crosby A, Morrell NW & Nichols BJ (2015) Caveolae protect endothelial cells from membrane rupture during increased cardiac output. *J. Cell Biol.* **211**: 53–61
- Cheng ZJ, Singh RD, Holicky EL, Wheatley CL, Marks DL & Pagano RE (2010) Co-regulation of caveolar and Cdc42-dependent fluid phase endocytosis by phosphocaveolin-1. *J. Biol. Chem.* **285**: 15119–15125
- Cox CD, Bae C, Ziegler L, Hartley S, Nikolova-Krstevski V, Rohde PR, Ng CA, Sachs F, Gottlieb PA & Martinac B (2016) Removal of the mechanoprotective influence of the cytoskeleton reveals PIEZO1 is gated by bilayer tension. *Nat. Commun.*
- Díaz-Valdivia NI, Díaz J, Contreras P, Campos A, Rojas-Celis V, Burgos-Ravanal RA, Lobos-González L, Torres VA, Perez VI, Frei B, Leyton L & Quest AFG (2020) The non-receptor tyrosine phosphatase type 14 blocks caveolin-1-enhanced cancer cell metastasis. *Oncogene* **39**: 3693–3709 Available at: <http://dx.doi.org/10.1038/s41388-020-1242-3>
- Diz-Muñoz A, Thurley K, Chintamen S, Altschuler SJ, Wu LF, Fletcher DA & Weiner OD (2016) Membrane Tension Acts Through PLD2 and mTORC2 to Limit Actin Network Assembly During Neutrophil Migration. *PLoS Biol.*
- Drab M, Verkade P, Elger M, Kasper M, Lohn M, Lauterbach B, Menne J, Lindschau C, Mende F, Luft FC, Schedl A, Hailer H & Kurzchalia T V. (2001) Loss of caveolae, vascular

- dysfunction, and pulmonary defects in caveolin-1 gene-disrupted mice. *Science* (80-. ). **293**: 2449–2452
- Dubé N, Bourdeau A, Heinonen KM, Cheng A, Loy AL & Tremblay ML (2005) Genetic ablation of protein tyrosine phosphatase 1B accelerates lymphomagenesis of p53-null mice through the regulation of B-cell development. *Cancer Res.* **65**: 10088–10095 Available at: [www.aacrjournals.org](http://www.aacrjournals.org) [Accessed March 1, 2021]
- Dufort CC, Paszek MJ & Weaver VM (2011) Balancing forces: Architectural control of mechanotransduction. *Nat. Rev. Mol. Cell Biol.*
- Dulhunty AF & Franzini-Armstrong C (1975) The relative contributions of the folds and caveolae to the surface membrane of frog skeletal muscle fibres at different sarcomere lengths. *J. Physiol.*
- Echarri A, Pavón DM, Sánchez S, García-García M, Calvo E, Huerta-López C, Velázquez-Carreras D, Viaris de Lesegno C, Ariotti N, Lázaro-Carrillo A, Strippoli R, De Sancho D, Alegre-Cebollada J, Lamaze C, Parton RG & Del Pozo MA (2019) An Abl-FBP17 mechanosensing system couples local plasma membrane curvature and stress fiber remodeling during mechanoadaptation. *Nat. Commun.* **10**: Available at: <http://dx.doi.org/10.1038/s41467-019-13782-2>
- Epanand RM, Sayer BG & Epanand RF (2005) Caveolin scaffolding region and cholesterol-rich domains in membranes. *J. Mol. Biol.*
- Faggi F, Mitola S, Sorci G, Riuzzi F, Donato R, Codenotti S, Poliani PL, Cominelli M, Vescovi R, Rossi S, Calza S, Colombi M, Penna F, Costelli P, Perini I, Sampaolesi M, Monti E & Fanzani A (2014) Phosphocaveolin-1 enforces tumor growth and chemoresistance in rhabdomyosarcoma.pdf. *PLoS One* Available at: <https://doi.org/10.1371/journal.pone.0084618>
- Fiala GJ & Minguet S (2018) Caveolin-1: The Unnoticed Player in TCR and BCR Signaling. In *Advances in Immunology*
- Fielding PE, Chau P, Liu D, Spencer TA & Fielding CJ (2004) Mechanism of Platelet-Derived Growth Factor-Dependent Caveolin-1 Phosphorylation: Relationship to Sterol Binding and the Role of Serine-80. *Biochemistry*
- Friedland JC, Lee MH & Boettiger D (2009) Mechanically activated integrin switch controls  $\alpha 5\beta 1$  function. *Science* (80-. ).



- Fujita A, Cheng J, Tauchi-Sato K, Takenawa T & Fujimoto T (2009) A distinct pool of phosphatidylinositol 4,5-bisphosphate in caveolae revealed by a nanoscale labeling technique. *Proc. Natl. Acad. Sci. U. S. A.* **106**: 9256–9261
- Gabella G & Blundell D (1978) Effect of stretch and contraction on caveolae of smooth muscle cells. *Cell Tissue Res.*
- Galbiati F, Engelman JA, Volonte D, Zhang XL, Minetti C, Li M, Hou H, Kneitz B, Edelmann W & Lisanti MP (2001) Caveolin-3 Null Mice Show a Loss of Caveolae, Changes in the Microdomain Distribution of the Dystrophin-Glycoprotein Complex, and T-tubule Abnormalities. *J. Biol. Chem.* **276**: 21425–21433
- Gambin Y, Ariotti N, McMahon K-A, Bastiani M, Sierrecki E, Kovtun O, Polinkovsky ME, Magenau A, Jung W, Okano S, Zhou Y, Leneva N, Mureev S, Johnston W, Gaus K, Hancock JF, Collins BM, Alexandrov K & Parton RG (2014) Single-molecule analysis reveals self assembly and nanoscale segregation of two distinct cavin subcomplexes on caveolae. *Elife* **3**: 1–18
- Garver WS, Hossain GS, Winscott MM & Heidenreich RA (1999) The Npc1 mutation causes an altered expression of caveolin-1, annexin II and protein kinases and phosphorylation of caveolin-1 and annexin II in murine livers. *Biochim. Biophys. Acta - Mol. Basis Dis.*
- Gaus K, Le Lay S, Balasubramanian N & Schwartz MA (2006) Integrin-mediated adhesion regulates membrane order. *J. Cell Biol.* **174**: 725–734
- Gauthier NC, Fardin MA, Roca-Cusachs P & Sheetz MP (2011) Temporary increase in plasma membrane tension coordinates the activation of exocytosis and contraction during cell spreading. *Proc. Natl. Acad. Sci. U. S. A.* **108**: 14467–14472
- Gazzerro E, Sotgia F, Bruno C, Lisanti MP & Minetti C (2010) Caveolinopathies: From the biology of caveolin-3 to human diseases. *Eur. J. Hum. Genet.* **18**: 137–145
- Gehler S, Baldassarre M, Lad Y, Leight JL, Wozniak MA, Riching KM, Eliceiri KW, Weaver VM, Calderwood DA & Keely PJ (2009) Filamin A- $\beta$ 1 integrin complex tunes epithelial cell response to matrix tension. *Mol. Biol. Cell*
- Gervásio OL, Phillips WD, Cole L & Allen DG (2011) Caveolae respond to cell stretch and contribute to stretch-induced signaling. *J. Cell Sci.*
- Glenney JR (1989) Tyrosine phosphorylation of a 22-kDa protein is correlated with transformation by Rous sarcoma virus. *J. Biol. Chem.* **264**: 20163–20166

- Glenney JR & Soppet D (1992) Sequence and expression of caveolin, a protein component of caveolae plasma membrane domains phosphorylated on tyrosine in Rous sarcoma virus-transformed fibroblasts. *Proc. Natl. Acad. Sci. U. S. A.* **89**: 10517–10521
- Goetz JG, Joshi B, Lajoie P, Strugnelli SS, Scudamore T, Kojic LD & Nabi IR (2008a) Concerted regulation of focal adhesion dynamics by galectin-3 and tyrosine-phosphorylated caveolin-1. *J. Cell Biol.* **180**: 1261–1275
- Goetz JG, Lajoie P, Wiseman SM & Nabi IR (2008b) Caveolin-1 in tumor progression: The good, the bad and the ugly. *Cancer Metastasis Rev.* **27**: 715–735
- Goetz JG, Minguet S, Navarro-Lérida I, Lazcano JJ, Samaniego R, Calvo E, Tello M, Osteso-Ibáñez T, Pellinen T, Echarri A, Cerezo A, Klein-Szanto AJP, Garcia R, Keely PJ, Sánchez-Mateos P, Cukierman E & Del Pozo MA (2011) Biomechanical remodeling of the microenvironment by stromal caveolin-1 favors tumor invasion and metastasis. *Cell* **146**: 148–163
- Golani G, Ariotti N, Parton RG & Kozlov MM (2019) Membrane Curvature and Tension Control the Formation and Collapse of Caveolar Superstructures. *Dev. Cell* **48**: 523-538.e4 Available at: <https://doi.org/10.1016/j.devcel.2018.12.005>
- Görtzen J, Schierwagen R, Bierwolf J, Klein S, Uschner FE, van der Ven PF, Fürst DO, Strassburg CP, Laleman W, Pollok JM & Trebicka J (2015) Interplay of matrix stiffness and c-SRC in hepatic fibrosis. *Front. Physiol.*
- Gottlieb-Abraham E, Shvartsman DE, Donaldson JC, Ehrlich M, Gutman O, Martin GS & Henis YI (2013) Src-mediated caveolin-1 phosphorylation affects the targeting of active Src to specific membrane sites. *Mol. Biol. Cell*
- Grande-García A, Echarri A, De Rooij J, Alderson NB, Waterman-Storer CM, Valdivielso JM & Del Pozo MA (2007) Caveolin-1 regulates cell polarization and directional migration through Src kinase and Rho GTPases. *J. Cell Biol.* **177**: 683–694
- Gustincich S, Vatta P, Goruppi S, Wolf M, Saccone S, Della Valle G, Baggiolini M & Schneider C (1999) The human serum deprivation response gene (SDPR) maps to 2q32-q33 and codes for a phosphatidylserine-binding protein. *Genomics* **57**: 120–129
- Han B, Tiwari A & Kenworthy AK (2015) Tagging strategies strongly affect the fate of overexpressed caveolin-1. *Traffic*
- Handorf AM, Zhou Y, Halanski MA & Li WJ (2015) Tissue stiffness dictates development,

homeostasis, and disease progression. *Organogenesis*

Hansen CG, Bright NA, Howard G & Nichols BJ (2009) SDPR induces membrane curvature and functions in the formation of caveolae. *Nat. Cell Biol.* **11**: 807–814 Available at: <http://dx.doi.org/10.1038/ncb1887>

Hansen CG, Howard G & Nichols BJ (2011) Pacsin 2 is recruited to caveolae and functions in caveolar biogenesis. *J. Cell Sci.* **124**: 2777–2785

Hansen CG & Nichols BJ (2010) Exploring the caves: Cavins, caveolins and caveolae. *Trends Cell Biol.* **20**: 177–186 Available at: <http://dx.doi.org/10.1016/j.tcb.2010.01.005>

Hanson CA, Drake KR, Baird MA, Han B, Kraft LJ, Davidson MW & Kenworthy AK (2013) Overexpression of Caveolin-1 Is Sufficient to Phenocopy the Behavior of a Disease-Associated Mutant. *Traffic*

Hayer A, Stoeber M, Bissig C & Helenius A (2010) Biogenesis of caveolae: Stepwise assembly of large caveolin and cavin complexes. *Traffic* **11**: 361–382

Heer NC & Martin AC (2017) Tension, contraction and tissue morphogenesis. *Dev.* **144**: 4249–4260

Hetmanski JHR, de Belly H, Busnelli I, Waring T, Nair R V., Sokleva V, Dobre O, Cameron A, Gauthier N, Lamaze C, Swift J, del Campo A, Starborg T, Zech T, Goetz JG, Paluch EK, Schwartz JM & Caswell PT (2019) Membrane Tension Orchestrates Rear Retraction in Matrix-Directed Cell Migration. *Dev. Cell* **51**: 460-475.e10

Hill MM, Bastiani M, Luetterforst R, Kirkham M, Kirkham A, Nixon SJ, Walser P, Abankwa D, Oorschot VMJ, Martin S, Hancock JF & Parton RG (2008) PTRF-Cavin, a Conserved Cytoplasmic Protein Required for Caveola Formation and Function. *Cell* **132**: 113–124

Hill MM, Scherbakov N, Schiefermeier N, Baran JA, Hancock JF, Huber LA, Parton RG & Parat MO (2007) Reassessing the role of phosphocaveolin-1 in cell adhesion and migration. *Traffic* **8**: 1695–1705

Hirama T, Das R, Yang Y, Ferguson C, Won A, Yip CM, Kay JG, Grinstein S, Parton RG & Fairn GD (2017) Phosphatidylserine dictates the assembly and dynamics of caveolae in the plasma membrane. *J. Biol. Chem.* **292**: 14292–14307

Hoekstra E, Das AM, Swets M, Cao W, Van Der Woude JJ, Bruno MJ, Peppelenbosch MP, Kuppen PJK, Ten Hagen TLM & Fuhler GM (2016) Increased PTP1B expression and

- phosphatase activity in colorectal cancer results in a more invasive phenotype and worse patient outcome. *Oncotarget* **7**: 21922–21938 Available at: <https://pubmed.ncbi.nlm.nih.gov/26942883/> [Accessed March 1, 2021]
- Hollander P Den, Rawls K, Tsimelzon A, Shepherd J, Mazumdar A, Hill J, Fuqua SAW, Chang JC, Osborne CK, Hilsenbeck SG, Mills GB & Brown PH (2016) Phosphatase PTP4A3 promotes triple-negative breast cancer growth and predicts poor patient survival. *Cancer Res.* **76**: 1942–1953 Available at: <http://cancerres.aacrjournals.org/> [Accessed March 1, 2021]
- Hoon J, Tan M & Koh C-G (2016) The Regulation of Cellular Responses to Mechanical Cues by Rho GTPases. *Cells*
- Hubert M, Larsson E & Lundmark R (2020a) Keeping in touch with the membrane; Protein- And lipid-mediated confinement of caveolae to the cell surface. *Biochem. Soc. Trans.* **48**: 155–163
- Hubert M, Larsson E, Vegesna NVG, Ahnlund M, Johansson AI, Moodie LW & Lundmark R (2020b) Lipid accumulation controls the balance between surface connection and scission of caveolae. *Elife* **9**: 1–31
- Humphrey JD, Dufresne ER & Schwartz MA (2014) Mechanotransduction and extracellular matrix homeostasis. *Nat. Rev. Mol. Cell Biol.*
- Huveneers S & Danen EHJ (2009) Adhesion signaling - Crosstalk between integrins, Src and Rho. *J. Cell Sci.* **122**: 1059–1069
- Irby RB & Yeatman TJ (2000) Role of Src expression and activation in human cancer. *Oncogene*
- Ishizawar R & Parsons SJ (2004) C-Src and cooperating partners in human cancer. *Cancer Cell*
- Izumi Y, Hirai SI, Tamai Y, Fujise-Matsuoka A, Nishimura Y & Ohno S (1997) A protein kinase C $\delta$ -binding protein SRBC whose expression is induced by serum starvation. *J. Biol. Chem.* **272**: 7381–7389
- Janmey PA, Fletcher DA & Reinhart-King CA (2020) Stiffness Sensing by Cells. *Physiol. Rev.*
- Jansa P, Mason SW, Hoffmann-Rohrer U & Grummt I (1998) Cloning and functional characterization of PTRF, a novel protein which induces dissociation of paused ternary transcription complexes. *EMBO J.* **17**: 2855–2864

- Jo A, Park H, Lee SH, Ahn SH, Kim HJ, Park EM & Choi YH (2014) SHP-2 binds to caveolin-1 and regulates Src activity via competitive inhibition of CSK in response to H<sub>2</sub>O<sub>2</sub> in astrocytes. *PLoS One* **9**:
- Joshi B, Bastiani M, Strugnelli SS, Boscher C, Parton RG & Nabi IR (2012) Phosphocaveolin-1 is a mechanotransducer that induces caveola biogenesis via Egr1 transcriptional regulation. *J. Cell Biol.* **199**: 425–435
- Joshi B, Pawling J, Shankar J, Pacholczyk K, Kim Y, Tran W, Meng F, Abdel Rahman AM, Foster LJ, Leong HS, Dennis JW & Nabi IR (2019) Caveolin-1 Y14 phosphorylation suppresses tumor growth while promoting invasion. *Oncotarget* **10**: 6668–6677
- Joshi B, Strugnelli SS, Goetz JG, Kojic LD, Cox ME, Griffith OL, Chan SK, Jones SJ, Leung SP, Masoudi H, Leung S, Wiseman SM & Nabi IR (2008) Phosphorylated caveolin-1 regulates Rho/ROCK-dependent focal adhesion dynamics and tumor cell migration and invasion. *Cancer Res.* **68**: 8210–8220
- Julien SG, Dubé N, Read M, Penney J, Paquet M, Han Y, Kennedy BP, Muller WJ & Tremblay ML (2007) Protein tyrosine phosphatase 1B deficiency or inhibition delays ErbB2-induced mammary tumorigenesis and protects from lung metastasis. *Nat. Genet.* **39**: 338–346 Available at: <https://pubmed.ncbi.nlm.nih.gov/17259984/> [Accessed March 1, 2021]
- Jung WR, Sierrecki E, Bastiani M, O'Carroll A, Alexandrov K, Rae J, Johnston W, Hunter DJB, Ferguson C, Gambin Y, Ariotti N & Parton RG (2018) Cell-free formation and interactome analysis of caveolae. *J. Cell Biol.* **217**: 2141–2165
- Kabbani AM, Raghunathan K, Lencer WI, Kenworthy AK & Kelly C V. (2020) Structured clustering of the glycosphingolipid GM1 is required for membrane curvature induced by cholera toxin. *Proc. Natl. Acad. Sci. U. S. A.*
- Keely PJ (2011) Mechanisms by which the extracellular matrix and integrin signaling act to regulate the switch between tumor suppression and tumor promotion. *J. Mammary Gland Biol. Neoplasia*
- Khater IM, Liu Q, Chou KC, Hamarneh G & Nabi IR (2019) Super-resolution modularity analysis shows polyhedral caveolin-1 oligomers combine to form scaffolds and caveolae. *Sci. Rep.*
- Kim Y-N, Wiepz GJ, Guadarrama AG & Bertics PJ (2000) Epidermal Growth Factor-stimulated Tyrosine Phosphorylation of Caveolin-1. *J. Biol. Chem.* **275**: 7481–7491

- King SJ & Parsons M (2011) Imaging cells within 3D cell-derived matrix. *Methods Mol. Biol.*
- Kirkham M, Nixon SJ, Howes MT, Abi-Rached L, Wakeham DE, Hanzal-Bayer M, Ferguson C, Hill MM, Fernandez-Rojo M, Brown DA, Hancock JF, Brodsky FM & Parton RG (2008) Evolutionary analysis and molecular dissection of caveola biogenesis. *J. Cell Sci.* **121**: 2075–2086
- Kiss AL, Turi Á, Müllner N, Kovács E, Botos E & Greger A (2005) Oestrogen-mediated tyrosine phosphorylation of caveolin-1 and its effect on the oestrogen receptor localisation: An in vivo study. *Mol. Cell. Endocrinol.* **245**:
- Konkel ME, Samuelson DR, Eucker TP, Shelden EA & O’Loughlin JL (2013) Invasion of epithelial cells by *Campylobacter jejuni* is independent of caveolae. *Cell Commun. Signal.*
- Kosmalska AJ, Casares L, Elosegui-Artola A, Thottacherry JJ, Moreno-Vicente R, González-Tarragó V, Del Pozo MÁ, Mayor S, Arroyo M, Navajas D, Trepát X, Gauthier NC & Roca-Cusachs P (2015) Physical principles of membrane remodelling during cell mechanoadaptation. *Nat. Commun.* **6**:
- Kovtun O, Tillu VA, Ariotti N, Parton RG & Collins BM (2015) Cavin family proteins and the assembly of caveolae. *J. Cell Sci.* **128**: 1269–1278
- Kovtun O, Tillu VA, Jung WR, Leneva N, Ariotti N, Chaudhary N, Mandyam RA, Ferguson C, Morgan GP, Johnston WA, Harrop SJ, Alexandrov K, Parton RG & Collins BM (2014) Structural insights into the organization of the cavin membrane coat complex. *Dev. Cell* **31**: 405–419 Available at: <http://dx.doi.org/10.1016/j.devcel.2014.10.002>
- Krawczyk KK, Mattisson IY, Ekman M, Oskolkov N, Granting R, Kotowska D, Olde B, Hansson O, Albinsson S, Miano JM, Rippe C & Swärd K (2015) Myocardin family members drive formation of caveolae. *PLoS One* **10**: 1–25
- Krishna A & Sengupta D (2019) Interplay between Membrane Curvature and Cholesterol: Role of Palmitoylated Caveolin-1. *Biophys. J.* **116**: 69–78 Available at: <https://doi.org/10.1016/j.bpj.2018.11.3127>
- Kuo JC, Han X, Yates JR & Waterman CM (2011) Isolation of focal adhesion proteins for biochemical and proteomic analysis. *Methods Mol. Biol.* **757**: 297–323
- Labrecque L, Nyalendo C, Langlois S, Durocher Y, Roghi C, Murphy G, Gingras D & Béliveau R (2004) Src-mediated tyrosine phosphorylation of caveolin-1 induces its association with membrane type 1 matrix metalloproteinase. *J. Biol. Chem.* **279**: 52132–52140

- Lampi MC & Reinhart-King CA (2018) Targeting extracellular matrix stiffness to attenuate disease: From molecular mechanisms to clinical trials. *Sci. Transl. Med.*
- Lee H, Volonte D, Galbiati F, Iyengar P, Lublin DM, Bregman DB, Wilson MT, Campos-Gonzalez R, Bouzahzah B, Pestell RG, Scherer PE & Lisanti MP (2000) Constitutive and growth factor-regulated phosphorylation of caveolin-1 occurs at the same site (Tyr-14) in vivo: Identification of a c-Src/Cav-1/Grb7 signaling cassette. *Mol. Endocrinol.* **14**: 1750–1775
- Lee H, Woodman SE, Engelman JA, Volonte D, Galbiati F, Kaufman HL, Lublin DM & Lisanti MP (2001) Palmitoylation of Caveolin-1 at a Single Site (Cys-156) Controls its Coupling to the c-Src Tyrosine Kinase: Targeting of dually acylated molecules (Gpi-linked, transmembrane, or cytoplasmic) to caveolae effectively uncouples c-Src and caveolin-1 (Tyr-14). *J. Biol. Chem.*
- Lee J & Glover KJ (2012) The transmembrane domain of caveolin-1 exhibits a helix-break-helix structure. *Biochim. Biophys. Acta - Biomembr.* **1818**: 1158–1164 Available at: <http://dx.doi.org/10.1016/j.bbmem.2011.12.033>
- Lentini D, Guzzi F, Pimpinelli F, Zaninetti R, Cassetti A, Coco S, Maggi R & Parenti M (2008) Polarization of caveolins and caveolae during migration of immortalized neurons. *J. Neurochem.* **104**: 514–523
- Levental KR, Yu H, Kass L, Lakins JN, Egeblad M, Erler JT, Fong SFT, Csiszar K, Giaccia A, Weninger W, Yamauchi M, Gasser DL & Weaver VM (2009) Matrix Crosslinking Forces Tumor Progression by Enhancing Integrin Signaling. *Cell* **139**: 891–906 Available at: <http://dx.doi.org/10.1016/j.cell.2009.10.027>
- Li BT, Shen R, Buonocore D, Olah ZT, Ni A, Ginsberg MS, Ulaner GA, Offin M, Feldman D, Hembrough T, Cecchi F, Schwartz S, Pavlakis N, Clarke S, Won HH, Brzostowski EB, Riely GJ, Solit DB, Hyman DM, Drilon A, et al (2018) Ado-trastuzumab emtansine for patients with HER2-mutant lung cancers: Results from a phase II basket trial. In *Journal of Clinical Oncology* pp 2532–2537. American Society of Clinical Oncology Available at: <https://ascopubs.org/doi/10.1200/JCO.2018.77.9777> [Accessed February 16, 2021]
- Li L, Okura M & Imamoto A (2002) Focal Adhesions Require Catalytic Activity of Src Family Kinases To Mediate Integrin-Matrix Adhesion. *Mol. Cell. Biol.* **22**: 1203–1217
- Li L, Ren CH, Tahir SA, Ren C & Thompson TC (2003) Caveolin-1 Maintains Activated Akt

- in Prostate Cancer Cells through Scaffolding Domain Binding Site Interactions with and Inhibition of Serine/Threonine Protein Phosphatases PP1 and PP2A. *Mol. Cell. Biol.* **23**: 9389–9404
- Li M, Yang X, Zhang J, Shi H, Hang Q, Huang X, Liu G, Zhu J, He S & Wang H (2013) Effects of EHD2 interference on migration of esophageal squamous cell carcinoma. *Med. Oncol.*
- Lim YW, Lo HP, Ferguson C, Martel N, Giacomotto J, Gomez GA, Yap AS, Hall TE & Parton RG (2017) Caveolae Protect Notochord Cells against Catastrophic Mechanical Failure during Development. *Curr. Biol.* **27**: 1968-1981.e7 Available at: <http://dx.doi.org/10.1016/j.cub.2017.05.067>
- Link AJ & Labaer J (2011) Trichloroacetic acid (TCA) precipitation of proteins. *Cold Spring Harb. Protoc.* **6**: 993–994
- Liu H, Wu Y, Zhu S, Liang W, Wang Z, Wang Y, Lv T, Yao Y, Yuan D & Song Y (2015) PTP1B promotes cell proliferation and metastasis through activating src and ERK1/2 in non-small cell lung cancer. *Cancer Lett.* **359**: 218–225 Available at: <https://pubmed.ncbi.nlm.nih.gov/25617799/> [Accessed March 1, 2021]
- Lo HP, Hall TE & Parton RG (2016) Mechanoprotection by skeletal muscle caveolae. *Bioarchitecture* **6**: 22–27
- López-Colomé AM, Lee-Rivera I, Benavides-Hidalgo R & López E (2017) Paxillin: A crossroad in pathological cell migration. *J. Hematol. Oncol.* **10**: 1–15 Available at: <https://jhoonline.biomedcentral.com/articles/10.1186/s13045-017-0418-y> [Accessed March 5, 2021]
- Ludwig A, Howard G, Mendoza-Topaz C, Deerinck T, Mackey M, Sandin S, Ellisman MH & Nichols BJ (2013) Molecular Composition and Ultrastructure of the Caveolar Coat Complex. *PLoS Biol.* **11**:
- Ludwig A, Nichols BJ & Sandin S (2016) Architecture of the caveolar coat complex. *J. Cell Sci.* **129**: 3077–3083
- Martínez-Meza S, Díaz J, Sandoval-Bórquez A, Valenzuela-Valderrama M, Rojas-Celis ND-VV, Contreras P, Huilcaman R, Ocaranza MP, Chiong M, Leyton L, Lavandero S & Quest AFG (2019) AT2 Receptor Mediated Activation of the Tyrosine Phosphatase PTP1B Blocks Caveolin-1 Enhanced Migration, Invasion and Metastasis of Cancer Cells.



*Cancers (Basel).*: 1–15

- Martino F, Perestrelo AR, Vinarský V, Pagliari S & Forte G (2018) Cellular mechanotransduction: From tension to function. *Front. Physiol.*
- Mastick CC, Brady MJ & Saltiel AR (1995) Insulin stimulates the tyrosine phosphorylation of caveolin. *J. Cell Biol.* **129**: 1523–1531
- Mastick CC & Saltiel AR (1997) Insulin-stimulated tyrosine phosphorylation of caveolin is specific for the differentiated adipocyte phenotype in 3T3-L1 cells. *J. Biol. Chem.* **272**: 20706–20714
- Mastick CC, Sanguinetti AR, Knesek JH, Mastick GS & Newcomb LF (2001) Caveolin-1 and a 29-kDa caveolin-associated protein are phosphorylated on tyrosine in cells expressing a temperature-sensitive v-Abl kinase. *Exp. Cell Res.*
- Matthaeus C, Lahmann I, Kunz S, Jonas W, Melo AA, Lehmann M, Larsson E, Lundmark R, Kern M, Blüher M, Olschowski H, Kompa J, Brügger B, Müller DN, Haucke V, Schürmann A, Birchmeier C & Daumke O (2020) EHD2-mediated restriction of caveolar dynamics regulates cellular fatty acid uptake. *Proc. Natl. Acad. Sci. U. S. A.* **117**: 7471–7481
- McMahon KA, Wu Y, Gambin Y, Sieracki E, Tillu VA, Hall T, Martel N, Okano S, Moradi SV, Ruelcke JE, Ferguson C, Yap AS, Alexandrov K, Hill MM & Parton RG (2019) Identification of intracellular cavin target proteins reveals cavin-PP1alpha interactions regulate apoptosis. *Nat. Commun.* **10**: Available at: <http://dx.doi.org/10.1038/s41467-019-11111-1>
- McMahon KA, Zajicek H, Li WP, Peyton MJ, Minna JD, Hernandez VJ, Luby-Phelps K & Anderson RGW (2009) SRBC/cavin-3 is a caveolin adapter protein that regulates caveolae function. *EMBO J.* **28**: 1001–1015 Available at: <http://dx.doi.org/10.1038/emboj.2009.46>
- Meng F, Joshi B & Nabi IR (2015) Galectin-3 Overrides PTRF / Cavin-1 Reduction of PC3 Prostate Cancer Cell Migration. : 1–15
- Meng F, Saxena S, Liu Y, Joshi B, Wong TH, Shankar J, Foster LJ, Bernatchez P & Nabi IR (2017) The phospho-caveolin-1 scaffolding domain dampens force fluctuations in focal adhesions and promotes cancer cell migration. *Mol. Biol. Cell* **28**: 2190–2201
- Meng H, Tian L, Zhou J, Li Z, Jiao X, Li WW, Plomann M, Xu Z, Lisanti MP, Wang C &

- Pestell RG (2011) PACSIN 2 represses cellular migration through direct association with cyclin D1 but not its alternate splice form cyclin D1b. *Cell Cycle*
- von Minckwitz G, Huang C-S, Mano MS, Loibl S, Mamounas EP, Untch M, Wolmark N, Rastogi P, Schneeweiss A, Redondo A, Fischer HH, Jacot W, Conlin AK, Arce-Salinas C, Wapnir IL, Jackisch C, DiGiovanna MP, Fasching PA, Crown JP, Wülfing P, et al (2019) Trastuzumab Emtansine for Residual Invasive HER2-Positive Breast Cancer. *N. Engl. J. Med.* **380**: 617–628 Available at: <http://www.nejm.org/doi/10.1056/NEJMoa1814017> [Accessed February 16, 2021]
- Mineo C, Ying YS, Chapline C, Jaken S & Anderson RGW (1998) Targeting of protein kinase  $\alpha$  to caveolae. *J. Cell Biol.* **141**: 601–610
- Minetti C, Sotgia F, Bruno C, Scartezzini P, Paolo Broda MB, Masetti E, Mazzocco M, Egeo A, Donati MA, Volonté D, Galbiati F, Cordone G, Bricarelli FD, Lisanti MP & Zara F (1998) Mutations in the caveolin-3 gene cause autosomal dominant limb-girdle muscular dystrophy. *Nat. Genet.* **18**: 365–368 Available at: <https://www.nature.com/articles/ng0498-365#citeas>
- Miron-Mendoza M, Seemann J & Grinnell F (2010) The differential regulation of cell motile activity through matrix stiffness and porosity in three dimensional collagen matrices. *Biomaterials* **31**: 6425–6435 Available at: </pmc/articles/PMC2900504/> [Accessed February 15, 2021]
- Mitra K, Ubarretxena-Belandia I, Taguchi T, Warren G & Engelman DM (2004) Modulation of the bilayer thickness of exocytic pathway membranes by membrane proteins rather than cholesterol. *Proc. Natl. Acad. Sci. U. S. A.*
- Mitra SK & Schlaepfer DD (2006) Integrin-regulated FAK-Src signaling in normal and cancer cells. *Curr. Opin. Cell Biol.*
- Monier S, Parton RG, Vogel F, Behlke J, Henske A & Kurzchalia T V. (1995) VIP21-caveolin, a membrane protein constituent of the caveolar coat, oligomerizes in vivo and in vitro. *Mol. Biol. Cell* **6**: 911–927
- Moon H, Lee CS, Inder KL, Sharma S, Choi E, Black DM, Lê Cao KA, Winterford C, Coward JI, Ling MT, Craik DJ, Parton RG, Russell PJ & Hill MM (2014) PTRF/cavin-1 neutralizes non-caveolar caveolin-1 microdomains in prostate cancer. *Oncogene* **33**: 3561–3570

- Mora R, Bonilha VL, Marmorstein A, Scherer PE, Brown D, Lisanti MP & Rodriguez-Boulan E (1999) Caveolin-2 localizes to the Golgi complex but redistributes to plasma membrane, caveolae, and rafts when co-expressed with caveolin-1. *J. Biol. Chem.* **274**: 25708–25717
- Morén B, Shah C, Howes MT, Schieber NL, McMahon HT, Parton RG, Daumke O & Lundmark R (2012) EHD2 regulates caveolar dynamics via ATP-driven targeting and oligomerization. *Mol. Biol. Cell* **23**: 1316–1329
- Mouritsen OG (2005) Life as a matter of fat
- Mouritsen OG & Bagatolli LA (2015) LIFE – AS A MATTER OF FAT Lipids in a Membrane Biophysics Perspective
- Murata M, Peranen J, Schreinert R, Wielandt F, Kurzchalia T V & Simons KAI (1995) VIP21 / caveolin is a cholesterol-binding protein. **92**: 10339–10343
- Murphy DA & Courtneidge SA (2011) The ‘ins’ and ‘outs’ of podosomes and invadopodia: Characteristics, formation and function. *Nat. Rev. Mol. Cell Biol.*
- Nah J, Yoo SM, Jung S, Jeong E Il, Park M, Kaang BK & Jung YK (2017) Phosphorylated CAV1 activates autophagy through an interaction with BECN1 under oxidative stress. *Cell Death Dis.* **8**: e2822 Available at: <http://dx.doi.org/10.1038/cddis.2017.71>
- Nassar ZD, Hill MM, Parton RG, Francois M & Parat MO (2015) Non-caveolar caveolin-1 expression in prostate cancer cells promotes lymphangiogenesis. *Oncoscience* **2**: 635–645
- Nassoy P & Lamaze C (2012) Stressing caveolae new role in cell mechanics. *Trends Cell Biol.* **22**: 381–389 Available at: <http://dx.doi.org/10.1016/j.tcb.2012.04.007>
- Nethe M, Anthony EC, Fernandez-Borja M, Dee R, Geerts D, Hensbergen PJ, Deelder AM, Schmidt G & Hordijk PL (2010) Focal-adhesion targeting links caveolin-1 to a Rac1-degradation pathway. *J. Cell Sci.* **123**: 1948–1958
- Nethe M & Hordijk PL (2011) A model for phospho-caveolin-1 driven turnover of focal adhesions. *Cell Adhes. Migr.* **5**: 59–64
- Nevins AK & Thurmond DC (2006) Caveolin-1 functions as a novel Cdc42 guanine nucleotide dissociation inhibitor in pancreatic  $\beta$ -cells. *J. Biol. Chem.* **281**: 18961–18972
- Northcott JM, Dean IS, Mouw JK & Weaver VM (2018) Feeling stress: The mechanics of cancer progression and aggression. *Front. Cell Dev. Biol.*
- Nunez-Wehinger S, Ortiz RJ, Diaz N, Diaz J, Lobos-Gonzalez L & Quest AFG (2014)

- Caveolin-1 in Cell Migration and Metastasis. *Curr. Mol. Med.* **14**: 255–274 Available at: <https://pubmed.ncbi.nlm.nih.gov/24467203/> [Accessed February 16, 2021]
- Orlichenko L, Huang B, Krueger E & McNiven MA (2006a) Epithelial growth factor-induced phosphorylation of caveolin 1 at tyrosine 14 stimulates caveolae formation in epithelial cells. *J. Biol. Chem.* **281**: 4570–4579
- Orlichenko L, Huang B, Krueger E & McNiven MA (2006b) Epithelial growth factor-induced phosphorylation of caveolin 1 at tyrosine 14 stimulates caveolae formation in epithelial cells. *J. Biol. Chem.* **281**: 4570–4579
- Örtegren U, Karlsson M, Blazic N, Blomqvist M, Nystrom FH, Gustavsson J, Fredman P & Strålfors P (2004) Lipids and glycosphingolipids in caveolae and surrounding plasma membrane of primary rat adipocytes. *Eur. J. Biochem.* **271**: 2028–2036
- Ortiz R, Díaz J, Díaz N, Lobos-Gonzalez L, Cárdenas A, Contreras P, Díaz MI, Otte E, Cooper-White J, Torres V, Leyton L & Quest AFG (2016) Extracellular matrix-specific Caveolin-1 phosphorylation on tyrosine 14 is linked to augmented melanoma metastasis but not tumorigenesis. *Oncotarget* **7**: 40571–40593
- Pancieria T, Citron A, Di Biagio D, Battilana G, Gandin A, Giulitti S, Forcato M, Bicciato S, Panzetta V, Fusco S, Azzolin L, Totaro A, Dei Tos AP, Fassan M, Vindigni V, Bassetto F, Rosato A, Brusatin G, Cordenonsi M & Piccolo S (2020) Reprogramming normal cells into tumour precursors requires ECM stiffness and oncogene-mediated changes of cell mechanical properties. *Nat. Mater.*
- Parat M-O, Anand-Apte B & Fox PL (2003) Differential Caveolin-1 Polarization in Endothelial Cells during Migration in Two and Three Dimensions. *Mol. Biol. Cell* **14**: 3156–3168
- Park JH, Ryu JM & Han HJ (2011) Involvement of caveolin-1 in fibronectin-induced mouse embryonic stem cell proliferation: Role of FAK, RhoA, PI3K/Akt, and ERK 1/2 pathways. *J. Cell. Physiol.* **226**: 267–275
- Parolini I, Sargiacomo M, Galbiati F, Rizzo G, Grignani F, Engelman JA, Okamoto T, Ikezu T, Scherer PE, Mora R, Rodriguez-Boulan E, Peschle C & Lisanti MP (1999) Expression of caveolin-1 is required for the transport of caveolin-2 to the plasma membrane. Retention of caveolin-2 at the level of the Golgi complex. *J. Biol. Chem.* **274**: 25718–25725

- Parsons JT, Horwitz AR & Schwartz MA (2010) Cell adhesion: Integrating cytoskeletal dynamics and cellular tension. *Nat. Rev. Mol. Cell Biol.*
- Parton RG (2018) Caveolae: Structure, Function, and Relationship to Disease. *Annu. Rev. Cell Dev. Biol.* **34**: 111–136
- Parton RG, Hanzal-Bayer M & Hancock JF (2006) Biogenesis of caveolae: A structural model for caveolin-induced domain formation. *J. Cell Sci.* **119**: 787–796
- Parton RG & Howes MT (2010) Revisiting caveolin trafficking: The end of the caveosome. *J. Cell Biol.*
- Parton RG, McMahon KA & Wu Y (2020a) Caveolae: Formation, dynamics, and function. *Curr. Opin. Cell Biol.* **65**: 8–16 Available at: <https://doi.org/10.1016/j.ceb.2020.02.001>
- Parton RG & Del Pozo MA (2013) Caveolae as plasma membrane sensors, protectors and organizers. *Nat. Rev. Mol. Cell Biol.* **14**: 98–112 Available at: <http://dx.doi.org/10.1038/nrm3512>
- Parton RG, del Pozo MA, Vassilopoulos S, Nabi IR, Le Lay S, Lundmark R, Kenworthy AK, Camus A, Blouin CM, Sessa WC & Lamaze C (2020b) Caveolae: The FAQs. *Traffic* **21**: 181–185
- Parton RG, Tillu VA & Collins BM (2018) Caveolae. *Curr. Biol.* **28**: R402–R405
- Payne-Tobin Jost A & Waters JC (2019) Designing a rigorous microscopy experiment: Validating methods and avoiding bias. *J. Cell Biol.* **218**: 1452–1466
- Pelkmans L & Zerial M (2005) Kinase-regulated quantal assemblies and kiss-and-run recycling of caveolae. *Nature* **436**: 128–133
- Pellinen T, Blom S, Sánchez S, Välimäki K, Mpindi JP, Azegrouz H, Strippoli R, Nieto R, Vitón M, Palacios I, Turkki R, Wang Y, Sánchez-Alvarez M, Nordling S, Bützow A, Mirtti T, Rannikko A, Montoya MC, Kallioniemi O & Del Pozo MA (2018) ITGB1-dependent upregulation of Caveolin-1 switches TGF $\beta$  signalling from tumour-suppressive to oncogenic in prostate cancer. *Sci. Rep.* **8**: Available at: </pmc/articles/PMC5799174/> [Accessed March 15, 2021]
- Pereira PMR, Sharma SK, Carter LM, Edwards KJ, Pourat J, Ragupathi A, Janjigian YY, Durack JC & Lewis JS (2018) Caveolin-1 mediates cellular distribution of HER2 and affects trastuzumab binding and therapeutic efficacy. *Nat. Commun.* **9**: Available at:

<http://dx.doi.org/10.1038/s41467-018-07608-w>

- Pickup MW, Mouw JK & Weaver VM (2014) The extracellular matrix modulates the hallmarks of cancer. *EMBO Rep.*
- Plotnikov S V., Pasapera AM, Sabass B & Waterman CM (2012) Force fluctuations within focal adhesions mediate ECM-rigidity sensing to guide directed cell migration. *Cell* **151**: 1513–1527 Available at: <http://dx.doi.org/10.1016/j.cell.2012.11.034>
- Pol A, Morales-Paytuví F, Bosch M & Parton RG (2020) Non-caveolar caveolins - Duties outside the caves. *J. Cell Sci.* **133**:
- Del Pozo MA, Alderson NB, Kiosses WB, Chiang HH, Anderson RGW & Schwartz MA (2004) Integrins Regulate Rac Targeting by Internalization of Membrane Domains. *Science (80-. )*.
- del Pozo MA, Balasubramanian N, Alderson NB, Kiosses WB, Grande-García A, Anderson RGW & Schwartz MA (2005) Phospho-caveolin-1 mediates integrin-regulated membrane domain internalization. *Nat. Cell Biol.* **7**: 901–908
- Prescott L & Brightman MW (1976) The sarcolemma of Aplysia smooth muscle in freeze-fracture preparations. *Tissue Cell*
- Provenzano PP, Inman DR, Eliceiri KW & Keely PJ (2009) Matrix density-induced mechanoregulation of breast cell phenotype, signaling and gene expression through a FAK-ERK linkage. *Oncogene* **28**: 4326–4343
- Pu W, Qiu J, Nassar ZD, Shaw PN, McMahon KA, Ferguson C, Parton RG, Riggins GJ, Harris JM & Parat MO (2020) A role for caveola-forming proteins caveolin-1 and CAVIN1 in the pro-invasive response of glioblastoma to osmotic and hydrostatic pressure. *J. Cell. Mol. Med.* **24**: 3724–3738
- Radel C, Carlile-Klusacek ME & Rizzo V (2007) Participation of caveolae in  $\beta$ 1 integrin-mediated mechanotransduction. *Biochem. Biophys. Res. Commun.* **358**: 626–631
- Radel C & Rizzo V (2005) Integrin mechanotransduction stimulates caveolin-1 phosphorylation and recruitment of Csk to mediate actin reorganization. *Am. J. Physiol. - Hear. Circ. Physiol.* **288**: 936–945
- Ranade SS, Syeda R & Patapoutian A (2015) Mechanically Activated Ion Channels. *Neuron*
- Rangel L, Bernabé-Rubio M, Fernández-Barrera J, Casares-Arias J, Millán J, Alonso MA &

- Correas I (2019) Caveolin-1 $\alpha$  regulates primary cilium length by controlling RhoA GTPase activity. *Sci. Rep.* **9**: 1–16
- Razani B, Combs TP, Wang XB, Frank PG, Park DS, Russell RG, Li M, Tang B, Jelicks LA, Scherer PE & Lisanti MP (2002a) Caveolin-1-deficient mice are lean, resistant to diet-induced obesity, and show hypertriglyceridemia with adipocyte abnormalities. *J. Biol. Chem.* **277**: 8635–8647
- Razani B, Engelman JA, Wang XB, Schubert W, Zhang XL, Marks CB, Macalusol F, Russell RG, Li M, Pestell RG, Di Vizio D, Hou H, Kneitz B, Lagaud G, Christ GJ, Edelman W & Lisanti MP (2001) Caveolin-1 Null Mice Are Viable but Show Evidence of Hyperproliferative and Vascular Abnormalities. *J. Biol. Chem.* **276**: 38121–38138
- Razani B, Wang XB, Engelman JA, Battista M, Lagaud G, Zhang XL, Kneitz B, Hou H, Christ GJ, Edelman W & Lisanti MP (2002b) Caveolin-2-Deficient Mice Show Evidence of Severe Pulmonary Dysfunction without Disruption of Caveolae. *Mol. Cell. Biol.* **22**: 2329–2344
- Rhodes DR, Yu J, Shanker K, Deshpande N, Varambally R, Ghosh D, Barrette T, Pandey A & Chinnaiyan AM (2004) ONCOMINE: A Cancer Microarray Database and Integrated Data-Mining Platform1. *Neoplasia* **6**: 1–6
- Ridley AJ (2015) Rho GTPase signalling in cell migration. *Curr. Opin. Cell Biol.*
- Riveline D, Zamir E, Balaban NQ, Schwarz US, Ishizaki T, Narumiya S, Kam Z, Geiger B & Bershadsky AD (2001) Focal contacts as mechanosensors: Externally applied local mechanical force induces growth of focal contacts by an mDia1-dependent and ROCK-independent mechanism. *J. Cell Biol.*
- Root KT, Julien JA & Glover KJ (2019) Secondary structure of caveolins: A mini review. *Biochem. Soc. Trans.* **47**: 1489–1498
- Rothenberger NJ, Somasundaram A & Stabile LP (2018) The role of the estrogen pathway in the tumor microenvironment. *Int. J. Mol. Sci.*
- Le Roux AL, Quiroga X, Walani N, Arroyo M & Roca-Cusachs P (2019) The plasma membrane as a mechanochemical transducer. *Philos. Trans. R. Soc. B Biol. Sci.* **374**:
- Rybin VO, Xu X & Steinberg SF (1999) Activated protein kinase C isoforms target to cardiomyocyte caveolae: Stimulation of local protein phosphorylation. *Circ. Res.*

- Sathe M, Muthukrishnan G, Rae J, Disanza A, Thattai M, Scita G, Parton RG & Mayor S (2018) Small GTPases and BAR domain proteins regulate branched actin polymerisation for clathrin and dynamin-independent endocytosis. *Nat. Commun.*
- Schaller MD (2010) Cellular functions of FAK kinases: Insight into molecular mechanisms and novel functions. *J. Cell Sci.*
- Scherer PE, Okamoto T, Chun M, Nishimoto I, Lodish HF & Lisanti MP (1996) Identification, sequence, and expression of caveolin-2 defines a caveolin gene family. *Proc. Natl. Acad. Sci. U. S. A.* **93**: 131–135
- Schiller HB & Fässler R (2013) Mechanosensitivity and compositional dynamics of cell-matrix adhesions. *EMBO Rep.*
- Schlegel A, Arvan P & Lisanti MP (2001) Caveolin-1 binding to endoplasmic reticulum membranes and entry into the regulated secretory pathway are regulated by serine phosphorylation. Protein sorting at the level of the endoplasmic reticulum. *J. Biol. Chem.* **276**: 4398–4408
- Schlunck G, Han H, Wecker T, Kampik D, Meyer-ter-Vehn T & Grehn F (2008) Substrate rigidity modulates cell-matrix interactions and protein expression in human trabecular meshwork cells. *Investig. Ophthalmol. Vis. Sci.* **49**: 262–269
- Schwartz MA (1997) Integrins, oncogenes, and anchorage independence. *J. Cell Biol.*
- Schwartz MA (2010) Integrins and extracellular matrix in mechanotransduction. *Cold Spring Harb. Perspect. Biol.*: 1–13
- Sen S & Kumar S (2009) Cell-matrix de-adhesion dynamics reflect contractile mechanics. *Cell. Mol. Bioeng.* **2**: 218–230
- Senju Y, Rosenbaum E, Shah C, Hamada-Nakahara S, Itoh Y, Yamamoto K, Hanawa-Suetsugu K, Daumke O & Suetsugu S (2015) Phosphorylation of PACSIN2 by protein kinase C triggers the removal of caveolae from the plasma membrane. *J. Cell Sci.* **128**: 2766–2780
- Simón L, Campos A, Leyton L & Quest AFG (2020) Caveolin-1 function at the plasma membrane and in intracellular compartments in cancer. *Cancer Metastasis Rev.*: 435–453
- Singh RD, Marks DL, Holicky EL, Wheatley CL, Kaptzan T, Sato SB, Kobayashi T, Ling K & Pagano RE (2010) Gangliosides and  $\beta 1$ -integrin are required for caveolae and membrane domains. *Traffic* **11**: 348–360



- Singh V, Erady C & Balasubramanian N (2018) Cell-matrix adhesion controls Golgi organization and function through Arf1 activation in anchorage-dependent cells. *J. Cell Sci.*
- Sinha B, Köster D, Ruez R, Gonnord P, Bastiani M, Abankwa D, Stan R V., Butler-Browne G, Védie B, Johannes L, Morone N, Parton RG, Raposo G, Sens P, Lamaze C & Nassoy P (2011) Cells respond to mechanical stress by rapid disassembly of caveolae. *Cell* **144**: 402–413
- Slack-Davis JK, Martin KH, Tilghman RW, Iwanicki M, Ung EJ, Autry C, Luzzio MJ, Cooper B, Kath JC, Roberts WG & Parsons JT (2007) Cellular characterization of a novel focal adhesion kinase inhibitor. *J. Biol. Chem.*
- Smart EJ, Ying Y-S, Mineo C, Anderson RGW & Gilman AG (1995) A detergent-free method for purifying caveolae membrane from tissue culture cells (G proteins/epidermal growth factor receptor/folate receptor). *Cell Biol.* **92**: 10104–10108 Available at: <http://www.pnas.org/content/pnas/92/22/10104.full.pdf>
- Stock K, Estrada MF, Vidic S, Gjerde K, Rudisch A, Santo VE, Barbier M, Blom S, Arundkar SC, Selvam I, Osswald A, Stein Y, Gruenewald S, Brito C, Van Weerden W, Rotter V, Boghaert E, Oren M, Sommergruber W, Chong Y, et al (2016) Capturing tumor complexity in vitro: Comparative analysis of 2D and 3D tumor models for drug discovery. *Sci. Rep.* **6**: 1–15 Available at: [www.nature.com/scientificreports](http://www.nature.com/scientificreports) [Accessed March 22, 2021]
- Stoeber M, Stoeck IK, HéCurrency Signnni C, Bleck CKE, Balistreri G & Helenius A (2012) Oligomers of the ATPase EHD2 confine caveolae to the plasma membrane through association with actin. *EMBO J.* **31**: 2350–2364
- Stutchbury B, Atherton P, Tsang R, Wang DY & Ballestrem C (2017) Distinct focal adhesion protein modules control different aspects of mechanotransduction. *J. Cell Sci.* **130**: 1612–1624
- Suetsugu S, Kurisu S & Takenawa T (2014) Dynamic shaping of cellular membranes by phospholipids and membrane-deforming proteins. *Physiol. Rev.* **94**: 1219–1248
- Tang VW (2020) Collagen, stiffness, and adhesion: The evolutionary basis of vertebrate mechanobiology. *Mol. Biol. Cell* **31**: 1823–1834 Available at: [/pmc/articles/PMC7525820/](https://pubmed.ncbi.nlm.nih.gov/37525820/) [Accessed February 15, 2021]

- Thottacherry JJ, Kosmalska AJ, Kumar A, Vishen AS, Elosegui-Artola A, Pradhan S, Sharma S, Singh PP, Guadamillas MC, Chaudhary N, Vishwakarma R, Trepas X, del Pozo MA, Parton RG, Rao M, Pullarkat P, Roca-Cusachs P & Mayor S (2018) Mechanochemical feedback control of dynamin independent endocytosis modulates membrane tension in adherent cells. *Nat. Commun.* **9**:
- Tomassian T, Humphries LA, Liu SD, Silva O, Brooks DG & Miceli MC (2011) Caveolin-1 Orchestrates TCR Synaptic Polarity, Signal Specificity, and Function in CD8 T Cells. *J. Immunol.* **187**:
- Torgersen ML, Skretting G, Van Deurs B & Sandvig K (2001) Internalization of cholera toxin by different endocytic mechanisms. *J. Cell Sci.*
- Torrino S, Shen W, Blouin CM, Mani SK, de Leseqno CV, Bost P, Grassart A, Köster D, Valades-Cruz CA, Chambon V, Johannes L, Pierobon P, Soumelis V, Coirault C, Vassilopoulos S & Lamaze C (2018) EHD2 is a mechanotransducer connecting caveolae dynamics with gene transcription. *J. Cell Biol.* **217**: 4092–4105
- Urta H, Torres VA, Ortiz RJ, Lobos L, Díaz MI, Díaz N, Härtel S, Leyton L & Quest AFG (2012) Caveolin-1-enhanced motility and focal adhesion turnover require tyrosine-14 but not accumulation to the rear in metastatic cancer cells. *PLoS One* **7**:
- Vidal-Quadras M, Holst MR, Francis MK, Larsson E, Hachimi M, Yau WL, Peränen J, Martín-Belmonte F & Lundmark R (2017) Endocytic turnover of Rab8 controls cell polarization. *J. Cell Sci.*
- Volonté D, Galbiati F, Pestell RG & Lisanti MP (2001) Cellular stress induces the tyrosine phosphorylation of caveolin-1 (Tyr14) via activation of p38 mitogen-activated protein kinase and c-Src kinase. Evidence for caveolae, the actin cytoskeleton, and focal adhesions as mechanical sensors of osmotic stress. *J. Biol. Chem.* **276**: 8094–8103
- Walser PJ, Ariotti N, Howes M, Ferguson C, Webb R, Schwudke D, Leneva N, Cho KJ, Cooper L, Rae J, Floetenmeyer M, Oorschot VMJ, Skoglund U, Simons K, Hancock JF & Parton RG (2012) Constitutive formation of caveolae in a bacterium. *Cell* **150**: 752–763 Available at: <http://dx.doi.org/10.1016/j.cell.2012.06.042>
- Wanaski SP, Ng BK & Glaser M (2003) Caveolin scaffolding region and the membrane binding region of Src form lateral membrane domains. *Biochemistry* **42**: 42–56
- Wang S, Zhang Z, Almenar-Queralt A, Leem J, DerMardirossian C, Roth DM, Patel PM, Patel

- HH & Head BP (2019a) Caveolin-1 phosphorylation is essential for axonal growth of human neurons derived from iPSCs. *Front. Cell. Neurosci.* **13**: 1–13
- Wang W, Lollis EM, Bordeleau F & Reinhart-King CA (2019b) Matrix stiffness regulates vascular integrity through focal adhesion kinase activity. *FASEB J.*
- Way M & Parton RG (1995) M-caveolin, a muscle-specific caveolin-related protein. **376**: 108–112
- Webb DJ, Donais K, Whitmore LA, Thomas SM, Turner CE, Parsons JT & Horwitz AF (2004) FAK-Src signalling through paxillin, ERK and MLCK regulates adhesion disassembly. *Nat. Cell Biol.*
- Wei WC, Lin HH, Shen MR & Tang MJ (2008) Mechanosensing machinery for cells under low substratum rigidity. *Am. J. Physiol. - Cell Physiol.* **295**: 1579–1589
- Wells RG (2008) The role of matrix stiffness in regulating cell behavior. *Hepatology*
- Westhoff MA, Serrels B, Fincham VJ, Frame MC & Carragher NO (2004) Src-Mediated Phosphorylation of Focal Adhesion Kinase Couples Actin and Adhesion Dynamics to Survival Signaling. *Mol. Cell. Biol.*
- White CR & Frangos JA (2007) The shear stress of it all: The cell membrane and mechanochemical transduction. *Philos. Trans. R. Soc. B Biol. Sci.*
- Williams TM (2004) Caveolin-1 in oncogenic transformation, cancer, and metastasis. *AJP Cell Physiol.* **288**: C494–C506
- Williams TM, Hassan GS, Li J, Cohen AW, Medina F, Frank PG, Pestell RG, Vizio D Di, Loda M & Lisanti MP (2005) Caveolin-1 promotes tumor progression in an autochthonous mouse model of prostate cancer: Genetic ablation of Cav-1 delays advanced prostate tumor development in tramp mice. *J. Biol. Chem.* **280**: 25134–25145
- Williamson RC, Cowell CAM, Reville T, Roper JA, Rendall TCS & Bass MD (2015) Coronin-1C protein and caveolin protein provide constitutive and inducible mechanisms of rac1 protein trafficking. *J. Biol. Chem.* **290**: 15437–15449
- Wolfenson H, Iskratsch T & Sheetz MP (2014) Early events in cell spreading as a model for quantitative analysis of biomechanical events. *Biophys. J.*
- Wong TH, Dickson FH, Timmins LR & Nabi IR (2020) Tyrosine phosphorylation of tumor cell caveolin-1: impact on cancer progression. *Cancer Metastasis Rev.*

- Yamaguchi H, Takeo Y, Yoshida S, Kouchi Z, Nakamura Y & Fukami K (2009) Lipid rafts and caveolin-1 are required for invadopodia formation and extracellular matrix degradation by human breast cancer cells. *Cancer Res.*
- Yamaguchi T, Hayashi M, Ida L, Yamamoto M, Lu C, Kajino T, Cheng J, Nakatochi M, Isomura H, Yamazaki M, Suzuki M, Fujimoto T & Takahashi T (2019) ROR1-CAVIN3 interaction required for caveolae-dependent endocytosis and pro-survival signaling in lung adenocarcinoma. *Oncogene* **38**: 5142–5157 Available at: <http://dx.doi.org/10.1038/s41388-019-0785-7>
- Yamaguchi T, Lu C, Ida L, Yanagisawa K, Usukura J, Cheng J, Hotta N, Shimada Y, Isomura H, Suzuki M, Fujimoto T & Takahashi T (2016) ROR1 sustains caveolae and survival signalling as a scaffold of cavin-1 and caveolin-1. *Nat. Commun.* **7**:
- Yang B, Radel C, Hughes D, Kelemen S & Rizzo V (2011) P190 RhoGTPase-activating protein links the  $\beta 1$  integrin/caveolin-1 mechanosignaling complex to RhoA and actin remodeling. *Arterioscler. Thromb. Vasc. Biol.* **31**: 376–383
- Yang G, Xu H, Li Z & Li F (2014) Interactions of caveolin-1 scaffolding and intramembrane regions containing a CRAC motif with cholesterol in lipid bilayers. *Biochim. Biophys. Acta - Biomembr.* **1838**: 2588–2599 Available at: <http://dx.doi.org/10.1016/j.bbamem.2014.06.018>
- Yang H, Guan L, Li S, Jiang Y, Xiong N, Li L, Wu C, Zeng H & Liu Y (2016) Mechanosensitive caveolin-1 activation-induced PI3K/Akt/mTOR signaling pathway promotes breast cancer motility, invadopodia formation and metastasis in vivo. *Oncotarget* **7**: 16227–16247
- Yeh YC, Ling JY, Chen WC, Lin HH & Tang MJ (2017) Mechanotransduction of matrix stiffness in regulation of focal adhesion size and number: Reciprocal regulation of caveolin-1 and  $\beta 1$  integrin. *Sci. Rep.* **7**: 1–14 Available at: <http://dx.doi.org/10.1038/s41598-017-14932-6>
- Yeow I, Howard G, Chadwick J, Mendoza-Topaz C, Hansen CG, Nichols BJ & Shvets E (2017) EHD Proteins Cooperate to Generate Caveolar Clusters and to Maintain Caveolae during Repeated Mechanical Stress. *Curr. Biol.* **27**: 2951-2962.e5 Available at: <https://doi.org/10.1016/j.cub.2017.07.047>
- Zegers MM & Friedl P (2014) Rho GTPases in collective cell migration. *Small GTPases*

- Zhang B, Peng F, Wu D, Ingram AJ, Gao B & Krepinsky JC (2007) Caveolin-1 phosphorylation is required for stretch-induced EGFR and Akt activation in mesangial cells. *Cell. Signal.* **19**: 1690–1700
- Zhang P, Guo A, Possemato A, Wang C, Beard L, Carlin C, Markowitz SD, Polakiewicz RD & Wang Z (2013) Identification and functional characterization of p130Cas as a substrate of protein tyrosine phosphatase nonreceptor 14. *Oncogene* **32**: 2087–2095 Available at: <https://pubmed.ncbi.nlm.nih.gov/22710723/> [Accessed March 1, 2021]
- Zhao Q, Wu K, Geng J, Chi S, Wang Y, Zhi P, Zhang M & Xiao B (2016) Ion Permeation and Mechanotransduction Mechanisms of Mechanosensitive Piezo Channels. *Neuron*
- Zhao YY, Liu Y, Stan RV, Fan L, Gu Y, Dalton N, Chu PH, Peterson K, Ross J & Chien KR (2002) Defects in caveolin-1 cause dilated cardiomyopathy and pulmonary hypertension in knockout mice. *Proc. Natl. Acad. Sci. U. S. A.*
- Zimnicka A, Husain Y, Shajahan A, Toth P & Minshall R (2015) Phosphorylation of Caveolin-1 Tyrosine 14 Leads to Caveolar Coat Destabilization, Membrane Invagination and Endocytosis. *FASEB J.*
- Zimnicka AM, Husain YS, Shajahan AN, Sverdlov M, Chaga O, Chen Z, Toth PT, Klomp J, Karginov A V., Tirupathi C, Malik AB & Minshall RD (2016) Src-dependent phosphorylation of caveolin-1 Tyr-14 promotes swelling and release of caveolae. *Mol. Biol. Cell* **27**: 2090–2106